Influence of Iron Metabolism on Gene Expression in Erythropoietic Protoporphyria

Dissertation

zur

Erlangung der naturwissenschaftlichen Doktorwürde
(Dr. sc. nat.)

vorgelegt der

Mathematisch-naturwissenschaftlichen Fakultät

der

Universität Zürich

von

Jasmin Barman-Aksözen

aus

Deutschland

Promotionskomitee

Prof. Dr. Thomas Lutz (Vorsitz)

Prof. Dr. Elisabeth Minder (Leitung der Dissertation)

Prof. Dr. Kurt Bürki

Prof. Dr. Konrad Basler

Prof. Dr. Xiaoye Schneider-Yin

Dr. Pawel Pelcar

Dr. Paolo Cinelli

Zürich, 2014

Influence of Iron Metabolism on Gene Expression in Erythropoietic Protoporphyria

Jasmin Barman-Aksözen

Dedicated to all schattenspringer

SUMMARY

Erythropoietic protoporphyria (EPP, OMIM 177000) is a hereditary disease characterized by extremely painful photosensitivity. The underlying defect is a partial deficiency of the enzyme ferrochelatase (FECH) which catalyzes the last step of heme biosynthesis, the insertion of ferrous iron into protoporphyrin IX (PPIX). As a result of the enzyme deficiency, a large amount of the phototoxic substance PPIX accumulates in precursors of erythrocytes. In addition, up to 60% of EPP patients show disturbances of iron metabolism, e.g. microcytic, hypochromic anemia, low transferrin saturation and low ferritin. However, administration of iron is observed to worsen the photosensitivity. Genetically, over 97% of EPP patients carry, in addition to a loss of function mutation *in trans*, the identical SNP FECH IVS3-48C which enhances aberrant splicing. Since iron - and heme metabolism as well as splicing are highly regulated we hypothesized that a mechanism exists interconnecting the three processes. An in-depth characterization of *FECH* intron 3 was performed to identify possible sequence features that may be related to the disease causing splice defect or respond directly or indirectly to iron, heme or other products and substrates of heme metabolism. We could show that two homopolymeric tracts in *FECH* intron 3 differ in length between individuals, and that the low expression allele IVS3-48C is associated with longer poly-C tracts. Although homopolymeric tracts are conserved and significantly over-represented in the genome than simply by chance, we could not find a correlation between disease features and the length of these sequences yet. However, we could demonstrate that cultured cells derived from patients and healthy controls show enhanced aberrant splicing of *FECH* intron 3 and a subsequent decrease of the amount of FECH protein under iron depletion. The effect is more pronounced in the more frequent SNP IVS3-48T. In the low expression allele (IVS3-48C), a higher baseline level of aberrant splicing is seen under iron saturated condition, which is less enhanced by iron depletion. The consequence of an IVS3-48C genotype is therefore equivalent to the effect iron depletion exerts on cells from individuals with the more common genotype. The observed effect is mediated by the iron and 2-oxoglutarate-dependent dioxygenase Jmjd6, acting as a link between iron availability and splice regulation. To elucidate systemic aspects of iron metabolism in EPP, we further tested our hypothesis that the rate limiting enzyme of erythroid heme biosynthesis, 5-aminolevulinic acid synthase 2 (ALAS2), is involved in the adverse reaction on iron supplementation observed in patients. ALAS2 mRNA harbors an iron-responsive element (IRE) which prevents translation of the enzyme in case iron is scarce. Since iron is deficient in most EPP patients, the translation of ALAS2 mRNA might be partly repressed. Consequently, administration of iron could lead to an increase in ALAS2 protein due to a de-repression of the translation block and subsequently stimulate synthesis of PPIX, worsening the photosensitivity. In a longitudinal study, a positive correlation between hemoglobin levels and PPIX was seen in the three patients investigated – demonstrating the dependence of both PPIX and heme synthesis on iron availability in EPP. Moreover, by investigating the

expression of ALAS2 in peripheral blood cells of EPP patients, we found a significant increase in ALAS2 protein and mRNA compared to healthy controls, amplifying the proposed effect and supporting the hypothesis of an involvement of ALAS in the etiology of EPP.

SUMMARY FOR LAYPERSONS IN GERMAN

Erythropoietische Protoporphyrie (EPP) ist eine seltene, angeborene Lichtkrankheit bei der schon wenige Minuten an der Sonne oder sogar künstlichem Licht ausreichen, um extreme Schmerzen an allen unbedeckten Hautstellen auszulösen. Da das sichtbare Licht Verursacher der Symptome ist, helfen Sonnencreme und andere Massnahmen zum Schutz vor UV-Strahlung nicht. Hintergrund der EPP ist eine Störung der Herstellung des roten Blutfarbstoffs, bei der Eisen nicht optimal verwertet werden kann. Dadurch kommt es zum einen zu einer Anreicherung von Vorläuferstoffen des roten Blutfarbstoffs, die nicht weiterverarbeitet werden können und sich im Körper anreichern. Diese können mit Licht reagieren und verursachen tief in der Haut liegende Verbrennungen und Schäden an den Blutgefässen. Zum anderen wird vom Körper zu wenig roter Blutfarbstoff hergestellt, was eine Blutarmut hervorruft. Die Ergebnisse von Laboruntersuchungen zur Blutarmut weisen darauf hin, dass dem Körper Eisen fehlt. Paradoxer Weise reagieren viele Betroffene nach der Einnahme von Eisen allerdings mit einer Verschlimmerung der Lichtempfindlichkeit. In der vorliegenden Arbeit wurde untersucht, in welcher Weise Eisen Einfluss auf die Symptome der EPP nehmen kann. Wir konnten feststellen, dass die Einnahme von Eisen die Menge an Vorläufersubstanz nicht verringert, sondern im Gegenteil sogar erhöht, was die gesteigerte Lichtempfindlichkeit erklären würde. Der Grund liegt in einer Besonderheit bei der Herstellung des roten Blutfarbstoffs: Je mehr Eisen im Körper vorhanden ist, desto mehr Vorläuferstoffe werden bereitgestellt, um so viel wie möglich roten Blutfarbstoff herstellen zu können. Bei EPP allerdings kann das Eisen am Ende des Herstellungsweges nicht verwendet werden, so dass der zu viel bereit gestellte Vorläuferstoff ungenutzt bleibt und sich anreichert. Ein interessantes Resultat unserer Untersuchungen war zudem, dass die Produktion der Vorläuferstoffe bei EPP generell angeregt ist, vermutlich wegen des chronischen Mangels an rotem Blutfarbstoffs. Eine Überproduktion an Vorläuferstoff wird durch einen molekularen Schalter verhindert, solange wenig Eisen im Körper vorhanden ist. Wird allerdings Eisen eingenommen, ist diese Blockade gelöst und es kommt zur massenhaften Herstellung von Vorläufersubstanzen – die dann wegen der Eisenverwertungsstörung nicht zu rotem Blutfarbstoff fertiggestellt werden können.

Ein anderes Ergebnis unserer Untersuchungen zeigt allerdings, dass auch zu wenig Eisen einen negativen Effekt bei EPP haben kann: Wir haben herausgefunden, dass Eisen noch an einer anderen Stelle die Menge des hergestellten roten Blutfarbstoffs reguliert. Ist an dieser Stelle zu wenig Eisen vorhanden, wird weniger zelleigene Maschinerie zur Herstellung des roten Blutfarbstoffs bereitgestellt. Dieser Mechanismus ist ein Beispiel dafür, dass Zellen sehr sparsam mit den vorhandenen Ressourcen umgehen. Für Menschen mit EPP bedeuteten unsere Resultate zusammengenommene, dass sowohl zu wenig als auch zu viel Eisen im Körper schaden können. Um das richtige Mass an Eisen für EPP-Patienten zu finden, müssen noch einige Fragen durch die Forschung beantwortet werden.

LIST OF ORIGINAL PUBLICATIONS

The thesis is based on the following publications, indicated as Study I, II and III:

I. **Variations in the length of poly-C and poly-T tracts in intron 3 of the human ferrochelatase gene.**
Barman J, Schneider-Yin X, Mamet R, Schoenfeld N, Minder EI.
Cellular and molecular biology (Noisy-le-Grand, France) 55.2 (2009): 102-110.

II. **Iron availability modulates aberrant splicing of ferrochelatase through the iron-and 2-oxoglutarate dependent dioxygenase Jmjd6 and U2AF^{65}.**
Barman-Aksözen J, Béguin C, Dogar A.M, Schneider-Yin X, Minder EI.
Blood Cells, Molecules, and Diseases 51.3 (2013): 151-161.

III. **In ferrochelatase-deficient protoporphyria patients, ALAS2 expression is enhanced and erythrocytic protoporphyrin-concentration correlates with iron availability.**
Barman-Aksözen J, Minder EI, Schubiger C, Biolcati G, Schneider-Yin X.
Blood Cells, Molecules, and Diseases 54.1 (2015): 71-77.

LIST OF ABBREVIATIONS

A	Adenine
ALAD	Delta-aminolevulinate dehydratase
ADP	Delta-aminolevulinate dehydratase deficiency porphyria
ALA	5-aminolevulinic acid
ALAS1	5-aminolevulinic acid synthase 1
ALAS2	5-aminolevulinic acid synthase 2
AIP	Acute intermittent porphyria
C	Cytidine
CEP	Congenital erythropoietic porphyria
CPOX	Coproporphyrinogen III oxidase
DFO	Deferoxamine
DTM1	Divalent metal transporter 1
EPP	Erythropoietic protoporphyria
FAC	Ferric ammonium citrate
FECH	Ferrochelatase
FTH1	Ferritin heavy chain
FTL	Ferritin light chain
HCP	Hereditary coproporphyria
HGMD	Human gene mutation database
HIF1	Hypoxia inducible factor 1
HMB	Hydroxymethylbilane
HMBS	Hydroxymethylbilane synthase
HO-1	Heme oxygenase-1
HRM	Heme regulatory motifs
IRE	Iron-responsive element
IRP 1	Iron regulatory protein 1
IRP 2	Iron regulatory protein 2

Jmjd6	Jumonji domain-containing protein 6
MC1R	Melanocortin-1-receptor
NMD	Nonsense mediated decay
NMPP	N-methyl protoporphyrin
PBG	Porphobilinogen
PBGD	Porphobilinogen deaminase
PCT	Porphyria cutanea tarda
PLP	Pyridoxal 5-phosphate
PPIX	Protoporphyrin IX
PPOX	Protoporphyrinogen oxidase
PTC	Premature termination codon
PY-tract	Polypyrimidine tract
ROS	Reactive oxygen species
RUST	Regulated unproductive splicing and translation
SNP	Single nucleotide polymorphism
snRNP	Small nuclear ribonucleic particles
T	Thymidin
TfR1	Transferrin receptor-1
UROS	Uroporphyrinogen III synthase
UROD	Uroporphyrinogen decarboxylase
U2AF	U2 snRNP auxiliary factor
VP	Variegate porphyria
XLDPP	X-linked dominant protoporphyria
XLSA	X-linked sideroblastic anemia
Zn-PPIX	Zinc-protoporphyrin
α-MSH	Alpha-melanocyte-stimulating hormone
5`UTR	5’-untranslated region

CONTENTS

I. INTRODUCTION

1. Heme Biosynthesis

Heme is an integral component of many proteins and is therefore essential for every human cell. Around 80 % of the total body heme is produced during erythropoiesis for the synthesis of hemoglobin[1;2]. Another 15 % of heme is required for the synthesis of cytochrome P450 class enzymes in the liver. Furthermore, heme is also necessary for a variety of other hemoproteins such as myoglobin, neuroglobin, cytoglobin, oxidases, hydroxylases, peroxidases like catalase and thyreoperoxidase and the cytochromes necessary for electron transfer in the respiratory chain in mitochondria[3].

The biosynthesis of heme takes place in every nucleated cell, but is differently regulated in erythropoiesis in contrast to ubiquitous synthesis[3]. The pathway consists of eight enzymes that sequentially convert glycine and succinyl-coenzyme A (succinyl-CoA) to heme. The first step occurs in the mitochondrium, where the enzyme 5-aminolevulinate synthase condensates succinyl-CoA and glycine to form 5-aminolevulinic acid (ALA), the exclusive precursor of heme biosynthesis. The enzyme has two isozymes, the housekeeping 5-aminolevulinic acid synthase 1 (ALAS1) and the erythroid 5-aminolevulinic acid synthase 2 (ALAS2), that are encoded by different genes and cannot compensate for each other. The next four biosynthetic steps take place in the cytosol. Two molecules of ALA are condensated by delta-aminolevulinate dehydratase (ALAD) to give rise to the monopyrrol porphobilinogen (PBG). Four molecules of PBG are joined to form the tetrapyrrol hydroxymethylbilane (HMB) by the cytosolic enzyme hydroxymethylbilane synthase (HMBS), also known as porphobilinogen deaminase (PBGD). Subsequently, the linear HMB is closed to form a circular molecule, uroporphyrinogen III by uroporphyrinogen III synthase (UROS). Additionally, the enzyme inverts one of the pyrrols (D-ring). Non-enzymatic cyclisation of HMB may also occur, however the product, uroporphyrinogen I, has no biological function and is excreted in the urine. Uroporphyrinogen III is converted to coproporphyrinogen III by the enzyme uroporphyrinogen III decarboxylase (UROD) which removes the acetic acid side chains of the molecule. The propionate groups of two pyrrols are then decarboxylated by the enzyme coproporphyrinogen III oxidase (CPOX). This reaction takes place in the inter-membrane space of the mitochondrium and results in protoporphyrinogen IX which is then oxidized by the enzyme protoporphyrinogen oxidase (PPOX), located at the outer surface of the inner mitochondria membrane, to form protoporphyrin IX (PPIX). Finally, the enzyme ferrochelatase (FECH) inserts ferrous iron into protoporphyrin IX to form heme. Mutations in each of the biosynthetic enzymes except ALAS1 are associated with the genetic diseases of porphyrias which will be discussed in detail in Chapter III [3-5].

2. Regulation of heme biosynthesis

Excess heme is toxic to the body and excess porphyrinogens spontaneously oxidize to porphyrins that have no biologic function in the mammalian organism but can act as endogenous photosensitizers [3]. The metabolism of heme is therefore tightly regulated in order to meet the requirements of the body but prevent the accumulation of toxic intermediates and products of heme synthesis and catabolism [3;6;7]. The regulation of heme biosynthesis is mainly achieved by the first and rate-limiting enzyme of the pathway, 5-aminolevulinate synthase, which has a housekeeping (ALAS1) and an erythroid-specific (ALAS2) isoform [8;9]. The expression of both enzymes show distinct regulatory features and will be discussed in depth in this chapter. *ALAS1* and *ALAS2* are coded by two separate genes, located on chromosome 3 and X, respectively [10;11]. The rest of the enzymes are encoded by a single gene. If isoforms are present, they are generated by alternative splicing under the control of distinct erythroid-specific and house-keeping promoters [5]. Ferrochelatase (FECH) is the last enzyme of the pathway and inserts ferrous iron into PPIX to form heme. As key enzymes of heme biosynthesis in the disease erythropoietic protoporphyria (EPP), the regulation of ALAS1, ALAS2 and FECH are described in detail in the sections below. Heme degradation is controlled by the enzyme heme oxygenase-1 (HO-1), the rate limiting enzyme of heme catabolism [12]. HO-1 cleaves the porphyrin ring, and subsequently, the pyrrol is degraded to bilirubin, carbon monoxide and free iron, which is reutilized by the body. HO-1 is induced by heme and its derivate hemin [13;14]. Heme synthesis can be limited either by reduced iron availability as the result of nutritional iron deficiency or because of underlying defects of iron acquisition [15]. Alternatively, the synthesis of heme can be impaired by defects in genes necessary for heme biosynthesis leading to one of the forms of inherited porphyrias (see Chapter III and Anderson et al. 2001 [3]). Accumulation of heme precursors may also be a result of intoxication with substances interfering with heme biosynthetic enzymes like lead [16;17], high concentrations of iron [18], viral infections of the liver [19] or xenobiotics like hexachlorobenzene, a toxic ingredient of a fungicide causing an epidemic intoxication in Turkey in the 1950s [20].

2.1. Regulation of ALAS1

ALAS1 is the rate limiting enzyme of the housekeeping heme biosynthesis. The enzyme is a 71 kDa protein of 640 amino acids in length. It is active as a homodimer but requires pyridoxal 5-phosphate (PLP) as cofactor and is located in the mitochondrial matrix [5;21]. The most important site of expression is the liver, where around 15% of the heme biosynthesis takes place. The expression of ALAS1 is controlled by the end-product heme via a negative feedback mechanism. Excess heme binds to three heme regulatory motifs (HRM) present in the amino-terminal end of ALAS1 and prevents the protein from being imported into the mitochondrium [22;23]. Additionally, heme decreases the amount of ALAS1

mRNA in liver cells by suppressing transcription and reducing its half-life [24-26]. Two alternative splice forms exists, a more abundant in which an alternative exon 1A is joined to exon 2 and shows sensitivity to heme, and a less abundant mRNA form containing exon 1B, which renders the protein insensitive to inhibition by heme [26-28]. Heme also has been shown to induce the degradation of ALAS1 enzyme by Lon Peptidase 1 (LONP1) in the mitochondrium [29]. ALAS1 expression is induced by heme deficiency and a plethora of factors and molecular mechanisms extensively reviewed by Thunell (2006) [30]. Xenobiotics, glucose deficiency, fasting, stress and hormonal factors increase ALAS1 expression by several folds, making it the main therapeutic target for the treatment of acute porphyrias (see Chapter III). Acute porphyric crises are treated with glucose or preferably with hemin or heme arginate in order to down regulate the activity of ALAS1 [30].

2.2. Regulation of ALAS2

The gene coding for *ALAS2* is located at position Xp11.21 and consists of 11 exons [10;31]. ALAS2 contains an amino-terminal targeting signal peptide for transport into the mitochondrial matrix, which is cleaved during transport [32]. The enzyme consists of 587 amino acids and the mature enzyme has a molecular weight of 60 kDa. The precursor containing the targeting sequence has a weight of 65 kDa. ALAS2 acts as a homodimer and the activity is PLP dependent; additionally, PLP increases the stability of the enzyme [33;34]. Lathrop (1993) identified heme binding motifs in the amino-terminal end of ALAS2, which seems to have lost its regulatory function[22]. In ALAS1, the same motifs are found which prevents the protein from import into the mitochondrium when heme is bound [22;23].

ALAS2 is only expressed during erythropoiesis and found in erythroid precursor cells in the bone marrow, in reticulocytes and young erythrocytes in the blood. During embryogenesis, ALAS2 is present in fetal liver cell [11]. The transcription of *ALAS2* is regulated by transcription factors binding to sequence elements in the promoter region or to enhancer elements, like GATA1, SP1 and TATA binding protein (TBP) [35-38]. Putative binding sites for the erythroid specific transcription factors GATA1, NF-E2 and EKLF have been identified by Kramer et al. [39], which however do not sufficiently explain the exclusive expression of the enzyme during erythropoiesis. Intron 8 possesses a strong, orientation-dependent sequence element including GATA1 binding sites and CACCC boxes binding GATA1 and SP1 *in vitro*, which enhances erythroid transcription [31]. Han et al. (2006) demonstrated that histone acetyltransferase p300/CBP binds to the *ALAS2* promoter and synergistically enhances ALAS2 mRNA transcription with transcription factor SP1[40]. The expression of ALAS2 is also known to be positively influenced by the presence of heme [41].

Hofer et al. (2003) showed that hypoxia induces ALAS2 mRNA up-regulation, but not by a putative hypoxia inducible factor 1 (HIF1) binding site in the promoter of *ALAS2* [42]. Kaneko et al. (2009) noted that under hypoxic conditions, transforming growth factor-beta1 (TGF-beta1) is over-expressed in

YN-1 human erythroid precursor cells [43]. Exogenous TGF-beta1 signaling enhanced the expression of ALAS2 mRNA. Therefore they concluded that hypoxia mediated TGF-beta1 up-regulation but not HIF1, which in turn induces ALAS2 mRNA expression. On the contrary, Zhang (2011) identified three binding sites for HIF1 downstream of the *ALAS2* gene, which bind HIF1 under hypoxic conditions and increase the expression of ALAS2 mRNA and protein [44]. Hypoxia was described to influence the stability of ALAS2 protein: Abu-Farah (2005) demonstrated that in the human erythroleukemic K562 cell line hypoxic conditions stabilize ALAS2 protein by inhibition of degradation by the proteasome [45].

Hemoglobin biosynthesis and iron metabolism are connected by the regulation of ALAS translation: The 5'-untranslated region (5`UTR) of ALAS2 mRNA contains an iron-responsive element (IRE), that acts as a binding site for iron regulatory protein 1 and 2 (IRP 1 and IRP 2). IRP 1 possesses a [4Fe-4S] iron-sulfur cluster and if iron is present, IRP 1 acts as a cytoslic aconitase that converts citrate to isocitrate [46]. IRP 2 is degraded under iron saturated conditions. Conversely, a low-iron content leads to the binding of IRP 1 or 2 to the IRE which then blocks the translation of ALAS2 mRNA and in turn reduces the amount of active enzyme [7;47;48]. In the absence of iron, less heme precursors are built.

Loss-of-function mutations in *ALAS2* lead to X-linked sideroblastic anemia (XLSA; OMIM 300751), characterized by anemia, iron accumulation and ringed sideroblasts. As learned from XLSA patients, ALAS1 cannot compensate for reduced ALAS2 activity. Carboxy-terminal mutations in ALAS2 lead to disruption of the binding of the beta-subunit of succinyl-CoA synthetase (SUCLA2), which reduces the activity of the enzyme and cause XLSA [49]. A number of modifying genes are known to influence ALAS2 activity: Ye (2010) identified a patient with sideroblastic anemia with a mutation in the glutaredoxin 5 (*GLRX5*) gene, with impairments in iron-sulfur cluster biogenesis and lack of cytolsolic iron and decreased amount of ALAS2 protein, promoted by IRP mediated translational repression [50]. Vice versa, the amount of ALAS2 was shown to be increased in IRP 2 -/- and IRP 2-/- IRP 1 +/- knockout mice [51].

Recently, gain-of-function mutations in *ALAS2* have been detected, leading to X-linked dominant protoporphyria (XLDPP; OMIM 300752). XLDPP is characterized by the accumulation of huge amount of protoporphyrin IX (PPIX) and zinc-protoporphyrin (Zn-PPIX) during erythropoiesis and a phenotypical presentation resembling the symptoms of EPP [52;53]. Gain-of-function mutations in *ALAS2* were also described to worsen the phenotype in one case of congenital erythropoietic porphyria (CEP), were it acts as a modifier gene [54].

2.3. Regulation of FECH

FECH is the last enzyme of the heme biosynthesis pathway [5]. The protein sequence contains a mitochondrial targeting signal peptide of 54 amino acids for mitochondrial import which is cleaved of dur-

ing transport into the inner mitochondrial membrane. The mature protein has a weight of 42 kDa and is supposed to be active as a homodimer [55;56]. Mature FECH possesses a [2Fe-2S] iron-sulfur cluster, which is not present in prokaryotic FECH proteins but is necessary for enzymatic activity in humans (Figure 1) [57-59]. Taketani (2000) and Crooks (2009) suggested a stabilizing function [60;61].

At the transcriptional level, *FECH* is regulated by a 150 bp minimal promoter region containing binding sites for the ubiquitous Sp1 family transcription factors and the erythroid-specific trans-acting factors NF-E2 and GATA1 [62]. During erythropoiesis an additional promoter region of approximately 4 kb is used to up-regulate FECH mRNA synthesis [63;64].

Mutations in the *FECH* gene are associated with erythropoietic protoporphyria (EPP; OMIM 17700), characterized biochemically by the accumulation of the last precursor of heme biosynthesis, protoporphyrin IX [65] and clinically by cutaneous phototoxicity and in some cases, microcytic hypochromic anemia [66-69]. From mouse models of EPP, it is known that the genetic background influences disease severity [70] which indicates modifying genes also play a role in the human phenotype. Knockout of several genes has been shown to interfere with heme biosynthesis and inducing PPIX accumulation. However these mice did show other symptoms in addition to that of EPP. For example, *Irp 2-/-* mice accumulate PPIX and Zn-PPIX, have reduced TfR levels and normal transferrin saturation. They show a microcytic, hypochromic anemia, absence of bone marrow iron stores, and develop neurodegeneration due to axonal degradation [51]. Recently, the disruption of the gene coding for iron transporter protein *Abcb10* in mice was shown to cause anemia with accumulations of both iron and PPIX [71].

Wang et al. (2011)[72] showed that in human EPP and XLDPP patients, an aberrant mitoferrin-1 (SLC25A37) mRNA is detectable, that possesses a premature 477 bp segment of intron 2 with a termination codon and is therefore degraded by nonsense mediated decay (NMD); a surveillance mechanism to remove faulty mRNA [73]. Furthermore, Troadec et al. (2011) showed that mice with targeted disruption of *mitoferrin-1* gene showed anemia and increased hematopoiesis[74]. When the *mitoferrin-1* gene was disrupted in hepatocytes, PPIX accumulated when the mice were fed aminolevulinic acid. Another mouse model with deletion of the ATP-binding cassette drug transporter *breast cancer resistance protein 1/ Abcg2 (Bcrp/Abcg2)* showed elevated levels of PPIX in erythrocytes, indicating that PPIX is a target of Abcg2 and that this transporter may modify disease severity [75;76]. Han et al. (2005) reported that *heme-regulated eIF2alpha inhibitor (Hri)* knockout mice accumulate PPIX in erythrocytes and that disease severity is modified by this protein [77].

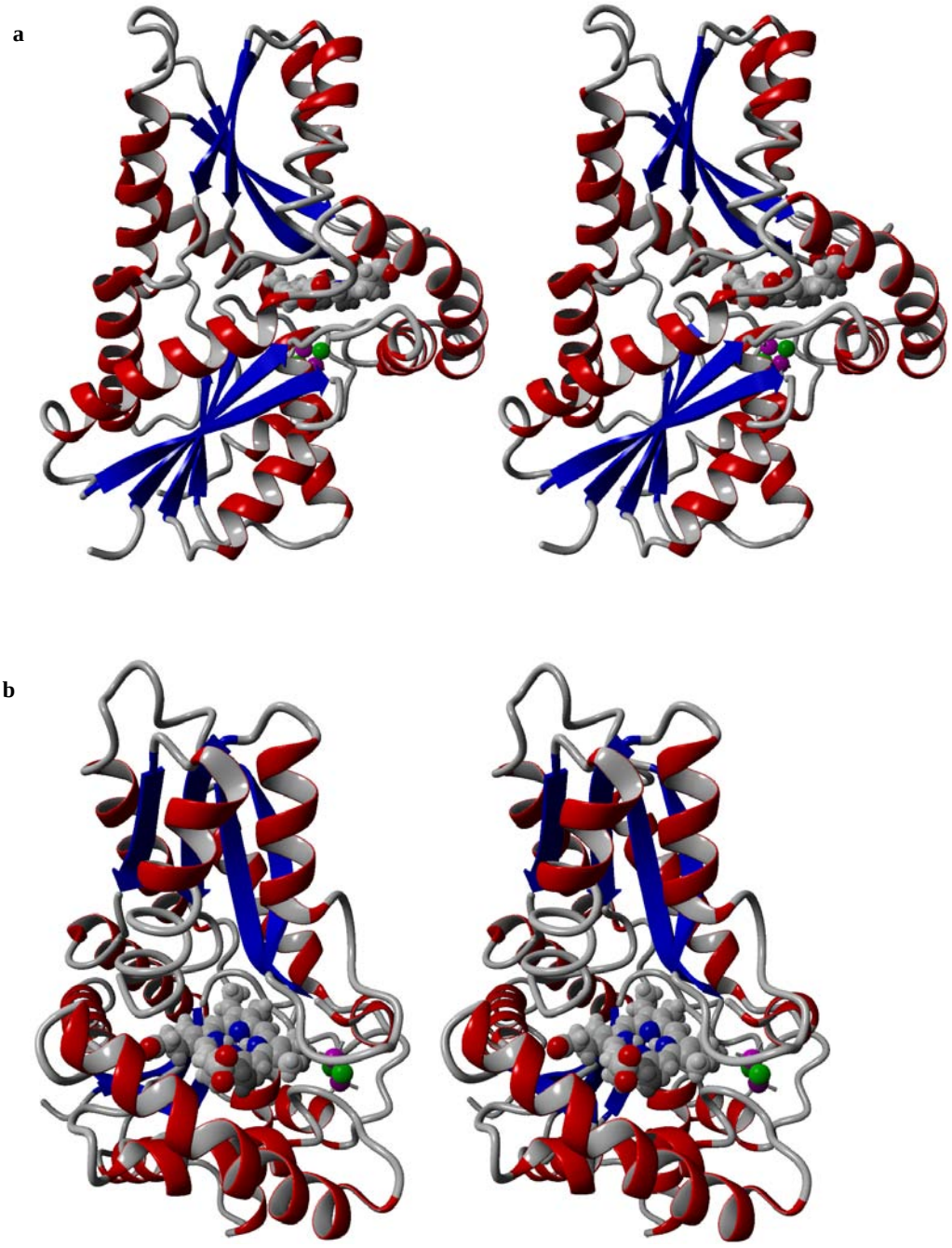

Figure 1
Structure of human ferrochelatase (FECH), stereo view on (a) symmetry axis and (b) active centre with PPIX bound. The iron sulphur cluster is depicted in violet and green. Image based on x-ray structures from Protein Data Base, 2 HRE (http://www.rcsb.org/pdb/explore.do?structureId=2hre). Description of structure by Medlock et al. (2007). The image was generated using YASARA View (www.yasara.org) by Thorsten Schweikardt, with kind permission.

2.4. Iron metabolism and erythroid heme biosynthesis

Iron is an integral part of heme and necessary for life, but toxic when present in excess [78]. The human body contains around 3 - 5 g iron of which 1 - 3 mg has to be substituted daily. Around 70 % of this iron is bound in hemoglobin in the hematopoietic system and 30 % is used in hemoproteins, iron-sulfur cluster containing proteins or stored inside ferritin complexes in the liver, bone marrow and spleen. During uptake from food source in the intestine, ferric iron is reduced to ferrous iron by membrane bound ferrireductases located at the enterocytes and absorbed by divalent metal transporter 1 (DMT1 / SLC11A2 / NRAMP2). Iron is then transported through the cell lumen by an unknown mechanism. It enters the body through ferroportin (SLC40A1), the only known cellular iron exporter. In order to be exported and bound by the iron transporter protein transferrin, iron has to be oxidized to ferric iron by the membrane bound copper dependent oxidase hephaestin. In the circulation, two iron ions are bound and carried by transferrin which binds to transferrin receptor 1 (TFRC / TfR1) on the surface of iron utilizing cells. For cellular iron uptake, the transferrin – transferrin receptor complex is internalized in clathrin-coated vesicle which undergo a pH change (acidification) inducing the release of iron from transferrin In order to be exported by DMT1 into the cytosol, the ferric iron has to be reduced by the metalloreductase STEAP3. Iron is then transported by an unknown mechanism either to the mitochondrium or to the sites of iron-sulfur cluster biogenesis. Since no physiological mechanism to excrete iron exists in the human body, its uptake and metabolism are tightly regulated [7]. The most important regulation of iron homoeostasis is exerted by the peptide hormone hepcidin which is synthesized in the liver. Hepcidin production is enhanced in iron saturated conditions. It binds to ferroportin and induces its degradation, preventing iron uptake by inhibiting it's release from the enterocytes. After approximately three days, the enterocytes are replaced and iron is released from the cells. Enhanced hepcidin levels also prevent iron to be released from body iron stores, reducing the iron contend in circulation [7; 81; 181]. Fine tuning of the iron metabolism of internalized iron is mainly achieved by the iron-responsive element (IRE) / iron regulatory proteins (IRP) system, which links heme biosynthesis and iron availability[79;80]. The untranslated regions (UTR) of the mRNAs of ALAS2 and of a subset of genes involved in iron uptake, transport and storage contain stem loop structures called iron-responsive elements (IRE) that act as binding sites for the iron regulatory protein 1 and 2 (IRP 1 and IRP 2) [81]. IRP 1 possesses a [4Fe-4S] iron-sulfur cluster and if iron is present, it acts as a cytosolic aconitase that converts citrate to isocitrate [46]. IRP 2 is degraded under iron saturated conditions. In contrast, a low cellular iron-content leads to the binding of IRP 1 and IRP 2 to IRE. In mRNAs with an IRE located at the 3`UTR, binding of IRP 1 and IRP 2 stabilizes the mRNA by protecting it against endonuclease cleavage and therefore enhances the expression of the protein. When localized in the 5`UTR, binding of IRP 1 and IRP 2 to the IRE leads to a block of translation and subsequently lower expression. Genes with IRE at 3`UTRs are transferrin receptor-1 (*TfR1*) which is the main receptor for iron uptake into the cell, and the divalent metal transporter 1 (*DTM1*) which is responsible for intesti-

nal iron and other divalent metals absorption as well as for transport within cells in the body. 5`UTR IREs are found in mRNAs of ALAS2, of ferritin heavy chain (FTH1) and ferritin light chain (FTL), both of which are involved in iron storage [82;83] and of ferroportin (*SLC40A1*), the only identified cellular iron exporter [84]. Overall, low cellular iron conditions increase the expression of proteins that are involved in iron uptake and mobilization and decrease proteins that are involved in iron storage and consumption. Additional mRNAs containing IREs have been identified, however their *in vivo* function has to be demonstrated and / or the genes have unknown function in regard of iron metabolism [85]. Mammalian FECH mRNA does not possess an IRE, however the mature enzyme contains a [2Fe-2S] iron-sulfur cluster which is necessary for enzymatic activity in humans [57;58]. Taketani (2000) and Crooks (2010) noted a connection between FECH expression and iron availability, possibly mediated by the stability of this cluster [60;61].

2.5. Splicing in heme biosynthesis

Several of the heme biosynthetic genes are alternatively spliced to give rise to erythroid specific and housekeeping mRNAs. Additionally, alternative splice variants are found with regulatory or unknown function, and a number of diseases-causing splice mutations are described for each gene. In general, protein coding genes are transcribed from DNA into one long, uninterrupted RNA molecule, the precursor-messenger RNA (pre-mRNA). However, most of the sequences transcribed to pre-mRNA do not contain information which is used for protein translation. Splicing is a highly complex, regulated process of joining protein coding sequence elements (exons) of the pre-mRNA together and excluding sequences without protein coding information (introns) to obtain the mature mRNA used for protein translation. The complex splice reaction is extensively reviewed by Maniatis and Tasic (2002) [86]. In short, a stepwise self-assembling multi-protein complex called spliceosome recognizes sequence elements on the pre-mRNA and connects the end of the preceding exon with the beginning of the following exon by a two-step trans-esterification reaction. The splice reaction involves a nucleophilic attack of a specific adenine (A) nucleotide, the branch point, towards the 5`end of the intron, leading to the formation of a lariat shaped intermediate intron structure. In a second step, by connecting both exons, this lariat is removed. The most important spliceosomal proteins are the U1, U2, U4, U5 and U6 small nuclear ribonucleic particles (snRNP) which contain short RNA sequences as catalytic elements or for recognition of their targets. Necessary sequence elements for the splicing of exons are the 3`acceptor site consisting of an AG dinucleotide at the end of each intron, preceded by a polypyrimidine rich sequence (py-tract), a branch point A nucleotide surrounded by a conserved sequence 20-30 bp upstream of an exon and a 5` donor site at the beginning of the intron often consisting of a GU dinucleotide. Besides those core sequence elements, further binding sites for splice regulatory proteins exist which are crucial for the regulation of splicing. The most important additional sequence elements are binding sites for exonic and intronic splice enhancer or silencer proteins which exhibit a synergetic effect by

determining inclusion or exclusion of exons or introns. Alternative splicing of one or more exons is found in over 95% of the roughly 24.000 genes contained in the human genome [87] and accounts for the large variety of proteins found among different cell types, developmental stages or in response to an external signal.

In heme biosynthesis, the genes coding for *ALAD*, *PBGD* and *UROS* contain both erythroid and housekeeping promoters and are alternatively spliced according to their expression in the respective tissue. In erythroid tissue, ALAD mRNA contains the exon 1B instead of 1A [88]. The erythroid splice variant of PBGD mRNA contains exon 2 but not exon 1, as opposed to exon 1 that is present in the housekeeping variant [89-91]. In the erythroid mRNA of UROS, exon 2A is included instead of exon 2B [92]. In addition to tissue specific splicing, alternative splicing giving rise to mRNA variants with known or unknown function or deleterious effects are found in other heme biosynthetic mRNAs. In ALAS1, two alternative splice forms exists, a more abundant one in which an alternative exon 1A is joined to exon 2 which shows sensitivity to heme mediated degradation, and a less abundant mRNA form containing exon 1B which renders the protein insensitive to inhibition by heme [26-28]. In ALAS2, a major splice isoform lacking exon 4 has been identified, accounting for 35-45% of the total transcripts [93]. This splice variant shows a slightly reduced activity; however it possesses the transport signal for mitochondrial import and therefore most likely contributes to the overall ALAS2 activity. In FECH, two major mRNA variants with unknown function exist with a length of 2.5 and 1.6 kb [94] which differ in their polyadenylation sites. For all heme biosynthetic genes, splice mechanism-affecting and disease-causing mutations have been found. Of special interest is the single nucleotide polymorphism IVS3-48C in the *FECH* gene [95] which together with a mutation *in trans*, is disease-causing and is found in over 97 % of overt EPP cases (Chapter IV).

Divalent metal transporter 1 (DMT1, also called natural resistance-associated macrophage protein 2, NRAMP 2 or divalent cation transporter 1, DCT1) is a transmembrane transporter for divalent metals and necessary for intestinal iron absorption and iron transport among different cell types. Its mRNA harbors an IRE in the 3`UTR which is bound by IRP when iron is scarce. The binding stabilizes the mRNA by protecting it against endonuclease degradation and leads to higher expression of the protein and therefore enables enhanced iron uptake [96]. Two major splice forms of *DMT1* exist, one having the 3`UTR IRE, and a second splice form lacking IRE. DMT1 is ubiquitously expressed and the two splice forms show tissue-specific distribution [97]. Hubert and Hentze (2002) later identified an alternative exon 1B, the inclusion or exclusion of which leads to two additional mRNA splice variants [98]. Inclusion of exon 1B encodes an alternative in frame start codon and leads to a 5` prolonged protein with likely regulatory functions in iron metabolism.

3. Porphyrias

Mutations in each gene of the heme biosynthetic enzymes lead to the accumulation of a subset of heme precursors and cause one specific form of genetic diseases named porphyria (Figure 2) [3;99]. Exceptions are the housekeeping *ALAS1*, in which no disease-causing mutations are described, possibly because loss-of-functions of this enzyme are not compatible with eukaryotic life. In *ALAS2*, loss-of-function mutations lead to X-linked sideroblastic anemia (XLSA; OMIM 300751) due to the inability to synthesize sufficient quantities of aminolevulinic acid (ALA) for heme synthesis. Based on their major side of excessive synthesis and accumulation of heme precursors, porphyrias can be grouped into hepatic and erythropoietic forms. However, because of different management schemes, clinicians might prefer a classification into acute and non-acute forms (Figure 3) [100]. Acute porphyrias are characterized by potentially life-threatening acute neurovisceral attacks and extreme abdominal pain without morphological anomalies of the tissue. Additional symptoms occur like nausea, headache, pain in the back and extremities, muscle weakness, vomiting, sweating, dysuria, constipation, tachycardia, hypertension and psychosis. The attacks are triggered by certain “unsafe” drugs which are metabolized by P450 cytochromes in the liver, by alcohol, hormones, stress and fasting [30]. During acute attacks, high amounts of ALA and porphobilinogen (PBG) are excreted in the urine which is the most useful diagnostic marker of a symptomatic acute porphyria. Four acute porphyrias caused by mutations in heme biosynthetic genes exist: Acute intermittent porphyria (AIP) with a dominant mutation in the *HMBS* gene, variegate porphyria (VP) with a dominant mutation in the gene coding for the enzyme *PPOX*, hereditary coproporphyria (HCP) with a dominant mutation in the gene for *CPOX* and the extremely rare recessive delta-aminolevulinate dehydratase deficiency porphyria (ADP), in which ALA but not PBG is excreted. Besides the acute attacks, PV and HCP show sunlight sensitivity in form of bulbous lesions and scarring. Non-acute porphyrias are characterized by sun and light sensitivity without abdominal pain. Porphyria cutanea tarda (PCT) is a hepatic, non-acute porphyria and shows bulbous lesions and skin fragility and the diagnostic relevant accumulation of isocoproporphyrin in the stool. The hereditary form which occurs in roughly 30% of the PCT patients is caused by heterozygous mutations in the gene for *UROD*. For a symptomatic manifestation, usually additional triggers, like iron accumulation in the liver due to an underlying hemochromatosis, alcohol abuse or environmental factors are required. Besides the genetic form, sporadic PCT may occur, triggered by environmental factors and genetic predisposition but with a normal *UROD* gene. Erythropoietic porphyrias are characterized by phototoxic reactions after sun and artificial light exposure associated with extreme pain and bulbous lesions. Congenital erythropoietic porphyria (CEP) is caused by recessive mutations in the *UROS* gene or its promoter region which cause uroporphyrin I and coproporphyrin I to accumulate in urine, blood and coproporphyrin I in the stool. In this disease light exposure leads besides extreme pain, to severe skin injuries and to the loss of tissue and digits due to secondary infections. Due

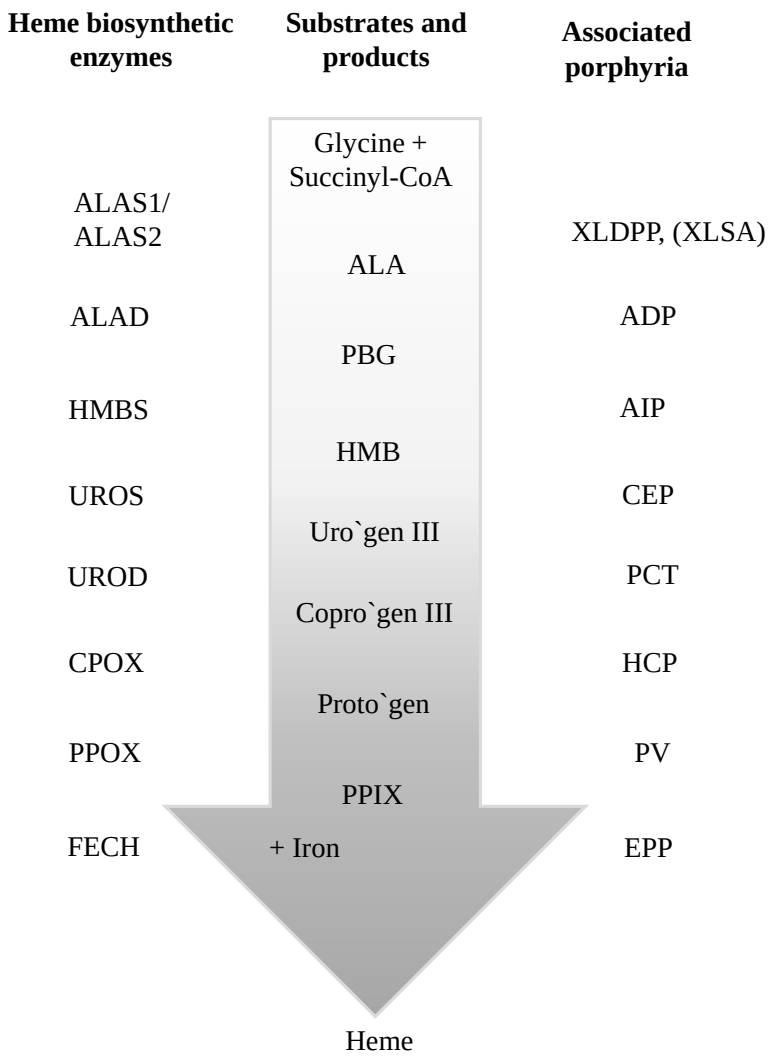

Figure 2

Heme biosynthetic enzymes, substrates and products and associated porphyrias. Mutations in each gene of the heme biosynthetic enzymes lead to the accumulation of a subset of heme precursors and cause one specific form of genetic diseases named porphyria. Exceptions are the housekeeping ALAS1, in which no disease-causing mutations are described, possibly because loss-of-functions of this enzyme are not compatible with eukaryotic life. Heme biosynthetic enzymes: ALAS1 5-aminolevulinic acid synthase 1, ALAS2 5-aminolevulinic acid synthase 2, ALAD Delta-aminolevulinate dehydratase, HMBS Hydroxymethylbilane synthase, UROS Uroporphyrinogen III synthase, UROD Uroporphyrinogen III decarboxylase, CPOX Coproporphyrinogen oxidase, PPOX Protoporphyrinogen oxidase, FECH Ferrochelatase. Substrates and products: ALA 5-aminolevulinic acid, PBG Porphobilinogen, HMB Hydroxymethylbilane, PPIX, Uro`gen III Uroporphyrinogen III, Copro`gen III Coproporphyrinogen IIII, Proto`gen Protoporphyrinogen, Protoporphyrin IX Porphyrias: XLDPP X-linked dominant protoporphyria, XLSA X-linked sideroblastic anemia, ADP Delta-aminolevulinate dehydratase deficiency porphyria, AIP Acute intermittent porphyria, CEP Congenital erythropoietic porphyria, PCT Porphyria cutanea tarda HCP Hereditary coproporphyria, VP Variegate porphyria, EPP Erythropoietic protoporphyria

to deposition of porphyrins, teeth may acquire a reddish coloration. Newborns with CEP can be identified by brownish-red urine, they often show jaundice and must not be treated by visible blue light irradiation to destroy bilirubin which in CEP causes severe burns. X-linked dominant protoporphyria (XLDPP) and erythropoietic protoporphyria (EPP) accumulate free PPIX in their erythrocytes and show an indistinguishable clinical presentation with painful phototoxic reactions after light exposure, usually without acute visible changes of affected skin areas. After prolonged light exposure time reddening, burns and persistent swelling of the skin may occur. XLDPP is caused by gain-of-function mutations in the first and rate limiting enzyme, *ALAS2*, whereas EPP is caused by mutations in *FECH*, the last enzyme of the pathway [52;101].

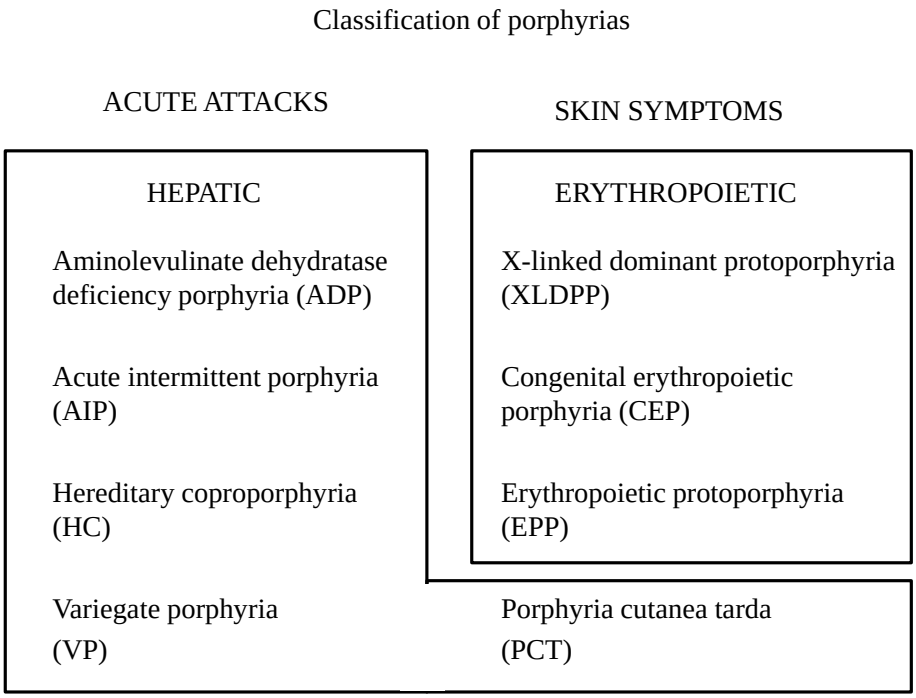

Figure 3
Classification of porphyrias according to their symptoms and main site of heme precursor overproduction

4. Erythropoietic Protoporphyria

4.1. Inheritance of EPP

4.1.1. Mutations of *FECH*

The *ferrochelatase* (*FECH*) gene has a size of about 45 kb, is located on chromosome 18q21.3 and contains 11 exons [102]. At present, 189 loss-of-function mutations are described in the human gene mutation database (HGMD), including missense and nonsense, splicing and regulation mutations, small deletions, insertions and indels, complex rearrangements and gross deletions affecting e.g. the promoter region or the entire gene.

Only a few families with an autosomal recessive inheritance of EPP have been reported [103-109]. The usual inheritance of EPP is however not dominant, but shows a more complex pattern [110], since not all FECH mutation carriers of a family develop symptoms. The inheritance of EPP is therefore described as autosomal dominant with incomplete penetrance [3] or by some authors as pseudodominant [111]. Recently it could be revealed, that the overt disease is dependent on the co-inheritance of a low expression allele *in trans* to a loss-of-function mutation of *FECH*. Rarely, de novo mutations are described and late onset cases connected to myeloproliferative disorders with somatic *FECH* mutations are observed [112-118].

4.1.2. Low expression allele

In a thorough study by Went and Klasen (1984) including 200 patients from 91 Dutch families with EPP, they put forward the hypothesis of a 3-allele system of inheritance[119]. Gouya et al. (1996) identified a decrease in FECH activity co-inherited with an overt disease, strengthening the evidence of a low expression allele compatible with the 3-allele hypothesis[120]. Henrikson et al. (1996) and Schneider-Yin et al. (2000) investigated the haplotype of the possible low expression allele and sequenced polymorphisms with strong linkage disequilibrium of the *FECH* gene [121;122]. They identified the polymorphisms -251G located in the promoter region and IVS1-23T to be associated with the low expression allele, whereas -251A/IVS1-23C to be present in the control group and the allele carrying the FECH mutation. Gouya et al. (2002) could show that the common single nucleotide polymorphism (SNP) of FECH intron 3 IVS3-48C/T co-segregates with the low expression allele [95]. In a minigene assay, they revealed that the SNP influences splicing of *FECH* (Figure 4): Intron 3 of the FECH pre-mRNA can be either spliced correctly or alternatively at the aberrant splice acceptor site IVS3-63, located 63 bp upstream from the correct splice site. The aberrant splicing results in a mature mRNA which contains additional 63 bp of intronic sequence. Due to the presence of a premature termination

codon (PTC) within this insertion, the aberrant splice product is subjected to nonsense mediated decay (NMD) and does not serve as a template for protein synthesis. In the mini-gene assay, Gouya et al. (2002) found that IVS3-48C/T determines the relative amount of normal and aberrant splice products [95]. If a T is present at the −48 position (IVS3-48T), only 10 to 20 % of the FECH pre-mRNA is aberrantly spliced. In an IVS3-48C genotype, however, the amount of aberrant splice product is increased to 30–40% of the total transcripts. The IVS3-48C SNP carrying allele is therefore denominated as "low expression allele".

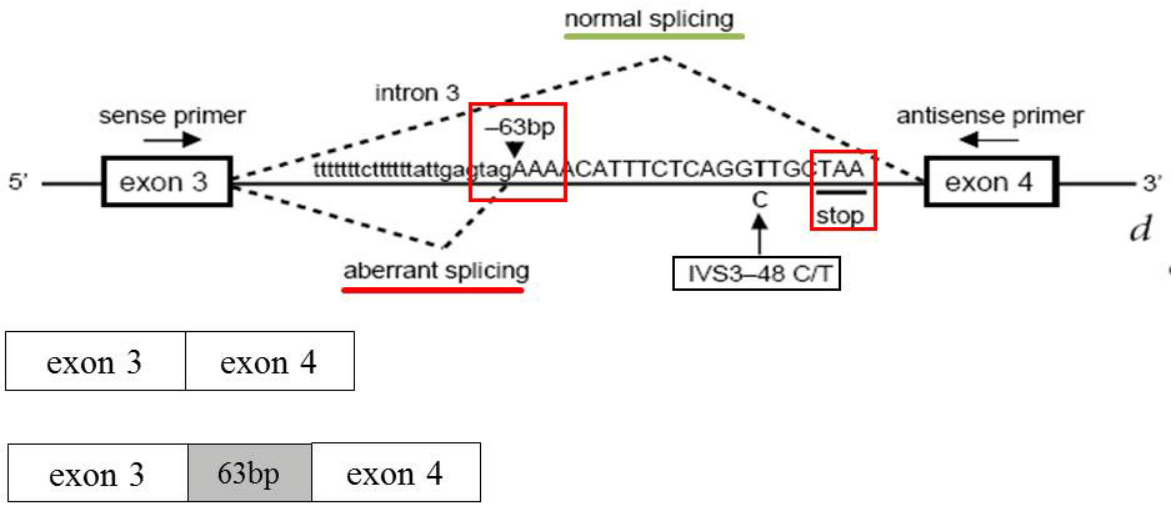

Figure 4
FECH intron 3 low expression due to partial aberrant splicing (modified from Gouya et al., 2002). Aberrant splicing causes a 63bp inclusion of intronic sequence, which carries a premature stop codon leading to degradation of the aberrant mRNA by nonsense mediated decay. Aberrant splicing is enhanced by the SNP IVS3-48C.

Although reducing the amount of FECH produced, the IVS3-48C allele does not lead to an EPP phenotype – even in homozygous individuals (Figure 5). Only when the low expression allele is inherited *in trans* to a *FECH* loss-of-function mutation carrying allele and thus reducing the overall activity of FECH enzyme under a certain threshold level, the phenotype of EPP develops. Carriers of one FECH mutation are asymptomatic, whereas zygotes with a double null allele mutation do not develop, since a complete block of heme biosynthesis is not compatible with eukaryotic life.

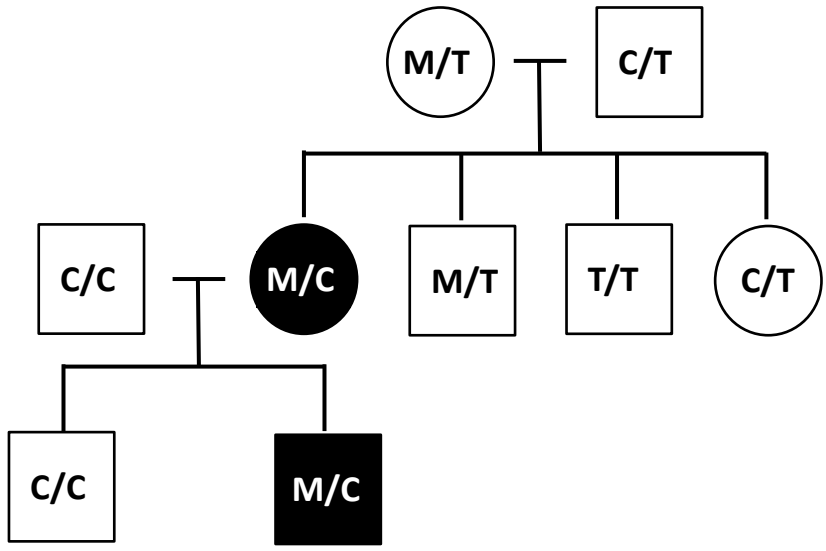

Figure 5
Inheritance of erythropoietic protoporphyria (EPP): The inheritance is described as autosomal dominant with incomplete penetrance. Individuals with one FECH loss-of-function mutation (M) in *trans* to the frequent allele FECH IVS3-48T (T) are asymptomatic carriers of the mutation. When the low expression allele FECH IVS3-48C (C) is inherited in trans to a FECH mutation carrying allele (M), it reduces the overall activity of FECH enzyme under a certain threshold level and the phenotype of EPP develops. The low expression allele (C) does not lead to an EPP phenotype, even in homozygous individuals (C/C). Zygotes with two loss-of-function mutation of FECH do not develop, since a complete block of heme biosynthesis is not compatible with eukaryotic life. Only a few recessive cases are described.

4.1.3. Prevalence of the low expression allele and epidemiology

The prevalence of EPP is dependent on the frequency of IVS3-48C in a population. The distribution of IVS3-48C/T differs among populations which suggest a positive selection pressure for this SNP in some population [123]. In the European population, IVS3-48T is the more frequent genotype whereas 7% to 13% of the population carries the IVS3-48C genotype [124-127]. The highest frequency of IVS3-48C is found in Asia, with Japan having 43% of its population carrying the SNP. In the French African immigrant populations, between <1% (West African origin) and 2.7 % (North African origin) of the population carry the low expression allele and accordingly only one EPP case has been reported in a man of black African origin [123;128]. By haplotype analysis, the first occurrence of the mutation leading to the low expression allele was estimated to date back 60.000 years ago [123]. The prevalence of EPP is estimated to be 1:58.000 in Slovenia [129;130], 1:75.000 in the Netherlands [119], 1:79.000 in Northern Ireland [131], 1:143.000 in the UK [132], 1:152.000 in South Africa [133], 1:155'000 in Switzerland[67] and 1:180.000 in Sweden [69]. However, as the disease is often underdiagnosed for different reasons, the true prevalence of EPP is expected to be higher in many countries [69;99].

4.2. Clinical features

4.2.1. Photosensitivity

During development in the bone marrow, erythrocytes of EPP patients accumulate large amounts of free protoporphyrin (PPIX) which leaks into the blood during circulation where it attaches to the membranes of endothelial cells lining the blood vessels [134-136]. Due to its ability to absorb visible light from sunlight and artificial light sources, PPIX is responsible for the main clinical symptom of EPP, extremely painful cutaneous photosensitivity [3]. The symptoms are caused by sunlight and artificial light sources like intense halogen light bulbs and surgery light [137-139]. The phototoxic reactions can trigger a cascade of symptoms, starting from discomfort to severe pain up to second degree burns which can be fatal in case of a surgery without appropriate light protection [140-142]. Symptoms usually start within minutes after contact of uncovered skin and tissue to light and comprise of a prickling, stinging and itching sensation. Upon prolonged exposure times to light, a burning feeling and severe to unbearable neuropathic pain develops [67;132]. Although clearly caused by light, EPP related symptoms are enhanced by different environmental conditions such as, cold wind, humidity and air temperature, time of the day and physical contact – an effect not understood at the moment but well documented in the literature [69;132;143;144]. Typically, no acute visible changes are observed on the affected skin areas, only occasionally immediate reddening of the skin, blisters or bulbous lesions may develop in some individuals. After extreme irradiation events, with a delay of hours swelling, reddening and sunburn resembling signs may develop in some patients (Figure 6), whereas in others no visible changes are seen despite excruciating pain [122;145;146]. Severe pain can persist several days up to two weeks. Additionally, a painful sensitivity to even weak light sources, heat, cold, wind, body heat and physical contact can persist which typically makes sleep impossible for several nights. Once a painful irradiation event happened, the onset of symptom during a subsequent sun exposure starts earlier, an observation described as “priming effect” [132;147]. The individual sensitivity to the sun and artificial light correlates with PPIX values, varies among patients and is influenced by many factors: The amount of PPIX differs strongly among patients with a significantly higher mean value in male patients [69;132] and the amount of PPIX within one patient may vary, influenced by factors like season [65] and liver health [148]. One case of increased light sensitivity and elevated PPIX levels was described in Grave’s disease hyperthyroidism which improved after treatment [149]. An improvement of symptoms is also frequently observed in pregnancy [69;150-153]. Permanent visible changes of the skin comprise of a slight lichenification

Figure 6
Visible symptoms after prolonged sun exposure in patients with erythropoietic protoporphyria (EPP). a) & b) Swellings in the face the day after sun exposure. c) habitus of an affected child during acute symptoms. d) severe erythema on the hand with sparing of the areas protected by rings the day after sun exposure. e) burns, erythema and scarring of the face several days after sun exposure. f) abatement of severe burns and swellings one week after last sun exposure, damage of the skin due to secondary infections related to scratching because of itching sensation and to cooling with water and subsequent dry skin. Photos by Arun Barman (a-c), Selbsthilfe EPP e.V. (d), Swiss society for porphyria (e), and Kinderklinik Mannheim (f), with kind permission.

above the basal knuckles. In a minority of patients hyperkeratotic lesions on the face occur, especially on the nose, and deep wrinkles may develop around the mouth and eyes [122;132].

The phototoxic reaction is caused by the physical properties of PPIX which is a planar, heterocyclic and highly conjugated circular molecule (Figure 7). Isolated PPIX has an absorbance maximum at 405-410 nm in the visible blue range (Soret band) and minor absorption peaks at wavelengths between 500 nm and 650 nm (Q-bands). Additional minor absorption bands are present in the near UV-A and the IR spectrum [154]. As red light penetrates the skin deeper than blue light and might therefore particularly reach the capillaries in the dermis, it is not conclusively clarified which wavelength is the main trigger for the symptoms in EPP patients [155;156]. In acidic solution PPIX can emit the absorbed energy as fluorescence when excited with a blue light LED (Figure 7). In red blood cells of EPP patients when excited with wavelengths around 410 nm, a red fluorescence can be seen under a fluorescence microscope [157;158]. In tissues, two types of photoreactions with the surrounding cellular structures are assumed. After absorption of the energy of photons with an adequate energy contends, PPIX is transformed from its ground state to a short lived excited singlet state and then to an exited triplet state. The energy of this triplet state can be transferred directly to surrounding cell structures (photoreaction type I): An electron or proton is transferred most likely to the lipids of the cell membrane and/or peptides which turn into radicals. By interaction with cellular oxygen, reactive oxygen species (ROS) are produced. Alternatively, the energy of the excited triplet state can be directly transferred from PPIX to oxygen (photoreaction type II), whereby exited singlet oxygen is produced [159]. Singlet oxygen is further converted into ROS such as O2•, H2O2 and •OH which damage lipids and proteins of the cell. Considering the amount of PPIX present under physiological conditions in cells, type II is assumed to be the most prevalent type of photoreaction occurring in EPP [160].

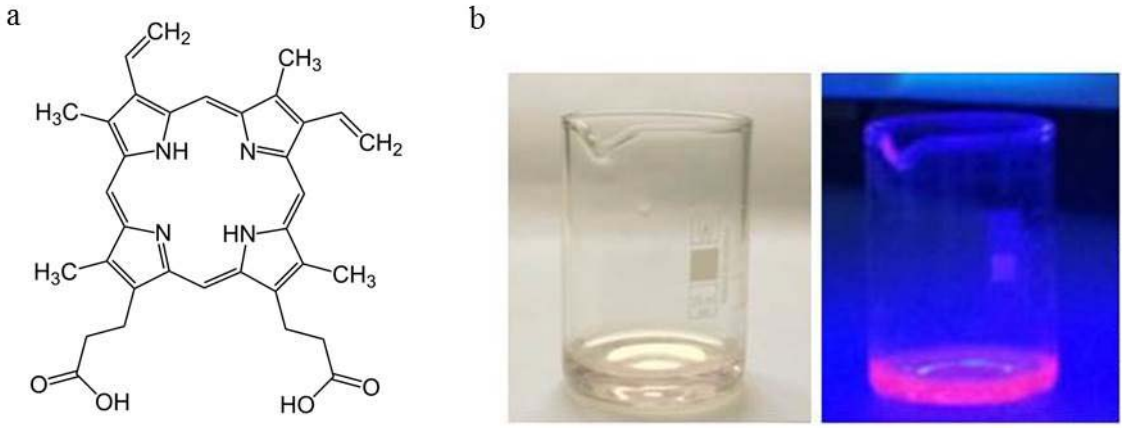

Figure 7
a) Protoporphyrin IX (PPIX) is a planar, heterocyclic and highly conjugated circular molecule. Wikicommons licence, author: Jü. b) Fluorescenece of protoporphyrin IX (PPIX) in 1.5 M HCl upon excitation with visible blue light (LED), image by the author.

4.2.2. Palmar keratoderma in homoallelic recessive patient

A special phenotypic feature found exclusively in homoallelic recessive patient is palmar keratoderma [108;109;161;162]. The reasons for this additional clinical presentation have to be elucidated.

4.2.3. Vitamin D and bone density

Because of the avoidance of sunlight exposure, less vitamin D precursor is converted into its biological active 25-hydroxyvitamin D form in the skin of EPP sufferers. Vitamin D deficiency is inversely correlated to the amount of PPIX, severity of symptoms and time to onset of symptoms [163;164]. Concomitantly, one study by Allo et al. (2013) showed an overall low to insufficient bone mineral density in EPP patients[165].

4.2.4. Cholestatic liver disease and gallstones

Due to its hydrophobic character, PPIX is cleared from the body only through the liver, where it is secreted via the bile. In the bile, gallstones composed of PPIX might form even in young age [145;166]. The excess amount of PPIX exerts damage on the liver cells, as concluded by permanently increased liver transaminases and histological abnormalities in the liver tissue observed in most EPP patients. In 5-10 % of patients, sudden rapidly progressing liver damage and subsequently liver failure occurs. Triggers for liver failure in EPP can be viral infections of the liver or sudden massive damage such as excessive alcohol consumption [167]; however the exact aetiology is not understood at the moment and might contain a component of genetic predisposition. Brown discoloration of the tissue and maltese-cross formed PPIX crystals are found in cells of affected livers. In severe liver involvement transplantation of a donor organ is necessary, in some cases liver and bone marrow transplants were used to protect the donor organ from further damage by the newly formed PPIX [141;148;168-170].

4.2.5. Iron metabolism

20-60% of EPP patients show low serum iron concentration and hematologic abnormalities which resemble those of iron deficiency i.e., low serum concentrations of iron, decreased transferrin saturation and abnormal hematologic indices including low hemoglobin, hematocrit, MCV and MCH and microcytic and hypochromic anemia. Also iron storage can be decreased as assessed by low serum ferritin [66-68;171]. However, iron supplementation was found to be beneficial in some cases only while be counterproductive in terms of worsening the skin symptoms in others – a paradox not explained so far [172-174], own observation. In an animal model of EPP, a disturbance in iron metabolism rather than a deficiency of iron was observed [175]. In humans, no increase in soluble transferrin receptor was found in a cohort of EPP patients [68]. Soluble transferrin receptor is an iron receptor which is present on the sur-

face of developing erythrocytes. It is shed from the surface of the cells during development of the erythrocyte and therefore can be detected in serum. Iron deficiency leads to an increased expression of transferrin receptors which enhances the amount of soluble transferrin receptor detectable in the serum [176]. Delaby therefore concluded that iron is not the limiting factor of erythropoiesis in EPP.

4.2.6. Delay of diagnosis and psychosocial impact

As a hereditary disease, EPP related symptoms usually start in early childhood. The extremely painful events experienced by the patients together with the prompt appearance of it after short sun exposure times leads to an understanding of the cause – consequence relation by the sufferers already at young age. Patients therefore develop strategies to minimize sun exposure times from early childhood on. However, avoiding sunlight includes peculiar behavior e.g. wearing protective long cloth during sunny days or having to change to the shadow side of the street. Once symptoms started, the patient may show unusual measures in order to reduce the pain, e.g. cooling the affected areas of the skin with wet cloth. This behavioral adaption can isolate patients from their peers [177]. A major complicating difficulty is the absence of immediate visible changes of the skin despite severe pain which leads to the underestimation of the severity of the symptoms by the social environment and physicians [145;146]. Due to the absence of objective clinical signs, especially young patients often face allegations of being maligners or hyperactive. Therefore, in the attempt to be accepted as a normal member of society and their social groups, patients try not to openly show their discomfort. As a consequence, dissimulation becomes a deep rooted behavioral adaption in the majority of EPP patients which may lead to the underestimation of the severity of the pain experienced. However, if visible signs occur, they are often mislabeled as “sun allergy”, although not comprising a valid diagnosis. As EPP is a rare disorder, most physicians and dermatologists are not aware of its existence, however even in case of EPP is considered as differential diagnosis, many textbook descriptions of the disease are misleading or wrong. Frequently, only UV radiation is mentioned as provoking phototoxic reactions, although evidence such as the use of visible light sources in photodynamic therapy with PPIX and the lack of efficacy of sun screens and other protection measures against UV radiation clearly demonstrate that protection against visible light is the most important measure in preventing EPP symptoms [178]. In many textbooks, the description of EPP is confused with other forms of porphyria like CEP, e.g. mentioning of red teeth, and sometimes it is written that males only are affected by EPP. All the above mentioned reasons lead to the delay of diagnoses by decades, despite the childhood being the most difficult time in the life of EPP patients [69;122;179].

However, even with a correct diagnosis, many patients complain about not being taken seriously by health care professionals, e.g. insufficient photo protection during surgeries or when treatment decisions are taken without consulting the patients experience with their own disease like the administra-

tion of intravenous iron after which many patients observed a worsening of their photosensitivity. In addition, the need to visit a specialist for the disease is often denied by the familial physician which leads to insufficient and wrong knowledge transfer to the patients with consequences like neglecting the monitoring of liver function and iron metabolism, missing of new treatment possibilities or wrong advice, e.g. the often mentioned wrong causality between sun exposure and liver damage. The management of patients with EPP by general physicians sometimes also leads to highly questionable outcomes like the attempt of a physician to perform liver biopsy without any medical need in a newly diagnosed eight year old female EPP patient (Minder, personal communication). Patients therefore face unnecessary risks if not treated by specialists. Also, the mentioning of an assumed connection of porphyrias to the origin of the vampire myth is considered as inappropriate and insulting by many patients (own observation). Already proved wrongly, this hypothesis is still described in nearly every textbook for medical students [180;181].

4.3. Treatment options

4.3.1. Amelioration of acute phototoxic reactions

Since analgetics are insufficient to relieve the pain caused by light in EPP [160], avoidance of further exposure is the most important measure once acute phototoxic reactions developed. Temporal pain relieve is achieved by cooling the affected skin areas with cold water, air-flow or by pressing the skin on cool surfaces. Cooling however only is effective for short time periods and does subsequently increase the sensitivity to heat. Treatment with moderate heat in form of e.g. warm water has been described by patients to improve the condition and shortens the time until pain resolves (own observation).

4.3.2. Photoprotection

Since in EPP visible light causes phototoxic reactions of exposed skin areas and tissue, UV protection measures are not sufficient to prevent symptoms – which can be depicted by the fact that EPP symptoms also start when the patients remain behind window glass which effectively filters most UV radiation [178]. Therefore, complete light avoidance would be the most effective prevention of symptoms such as physical barriers, like thick, dense cloth, shade providing items like huts, gloves or umbrellas or make-up preventing light penetration into the skin. However, such devices are only partly effective, i.e. because of hands and face are not completely covered.

Different drugs to reduce phototoxic reactions have been tested since the 1970s. The carotenoids beta-carotene and canthaxantin were believed to reduce oxidative stress in the skin as seen in plants by scavenging radical oxygen species (ROS). Canthaxantin was later found to induce crystal formation in

the eye when taken in high doses and was therefore withdrawn as treatment option for EPP [182]. However, results with beta-carotene were unsatisfactory with regard to photo protection[183]. In addition, a recent study by Virtamo (2013) showed that high doses of beta-carotene as recommended for the treatment of EPP increase the risk for lung cancer, although in smokers only[184]. Other substances with antioxidative properties used in single studies on a limited number of participants were cysteine, N-acetyl-cysteine (NAC) and vitamin C [185-187]. UVB exposure was used to increase melanin density and dihydroxyacetone/ Lawson (henna) was employed for coloring the skin, both were approaches to induce a physical barrier preventing light from penetrating the skin. However, in a systematic metastudy, Minder (2009) showed that none of the tested therapies did significantly protect against EPP related phototoxicity[183]. Importantly, this lack of efficacy is in concordance with self-reports of patients when asked outside of the study setups e.g. free from expectations of the respective PIs. Solely UVB-treatment did show a protective effect, however the increased risk for skin cancer by UV exposure makes this option not applicable in young patients and for long term use in this lifelong condition [188;189].

In 2006, a Swiss clinical phase II trial tested a new approach with the synthetic alpha-melanocyte-stimulating hormone (α-MSH) analogue afamelanotide ([Nle4, D-Phe7]-α-MSH, SCENESSE®)[190]. Afamelanotide is a linear peptide of 13 amino acids in length which does not cross the blood-brain barrier. It binds to melanocortin-1-receptor (MC1R) on melanocytes of the skin and induces melanin synthesis and subsequently skin tanning by the same mechanism as the natural hormone. The amino acid sequence of afamelanotide is modified from the natural occurring sequence at position four, where methionine is exchanged by norleucine and at position seven, where an l-phenylanaline is replaced by d-phenylalanine. The modifications confer higher binding capacity to the receptor and a higher resistance to decay mechanisms. Since the half-life of α-MSH is in the range of minutes, the more stable and potent analogue afamelanotide is used in an implant formulation. Besides the tanning effect, α-MSH and afamelanotide have strong anti-inflammatory properties. Up to date, more than 350 EPP patients worldwide were included in multicentre clinical phase III trials, all showing efficacy of the treatment which is well tolerated without major side effects. Afamelanotide (SCENESSE®, Clinuvel Pharmaceuticals Ltd.) has been submitted to the European Medicinal Agency (EMA) for marked authorization and has been assigned the orphan drug status. At present, it is available for the treatment of EPP patients in Italy and Switzerland under special legislation for severe and incapacitating orphan diseases without treatment options.

4.3.3. Photoprotection during surgeries

Intense artificial light sources like surgery lamps can cause severe to lethal injuries during surgical intervention [191]. Especially in liver involvement, higher PPIX concentrations are accumulated in the

body and exacerbate the phototoxicity. Protective yellow filters should be used during surgeries to prevent or limit phototoxic injuries [192].

4.3.4. Vitamin D supplementation

Serum vitamin 25(OH)D levels should be monitored and supplemented in case of a deficiency. Since a normal, well-balanced diet usually contains enough calcium and other trace elements, preferably vitamin D supplementation without calcium should be used. Otherwise, addition of calcium without deficiency may compete with the incorporation of phosphate which is necessary for the building of a healthy bone architecture [193].

4.3.5. Transplantation in cholestatic liver disease

Photoprotection does only symptomatically treat EPP and, since by such a treatment the amount of the liver toxic agent PPIX is not reduced, does not confer protection against liver injury. In case of liver involvement, a transplantation of a donor organ has to be conducted to stop the otherwise fatal progression of liver damage. A curative treatment for EPP can be achieved by transplanting the liver and bone marrow from a donor [194;195]. The high risks associated with such a holistic intervention make it only applicable in severe and otherwise terminal liver failure caused by excess PPIX with the risk of damage to the donor liver caused by constantly high PPIX production during erythropoiesis [170;196]. Approaches like red cell blood exchange were unsuccessfully used in an attempt to diminish liver damage by reducing the amount of PPIX present in the blood [197] and dialysis with albumin only showed marginal effects [198;199]. Also treatment with oral cholestyramine which discontinues the enterohepatic circulation of bile acids and is used in the attempt to increase bilary PPIX excretion, has been shown to be not effective in a small study with 3 patients with uncomplicated liver [200]. One attempt to reduce liver damage by N-acetyl cysteine has to be investigated in a larger trial [201].

4.3.6. Gene therapy

A curative approach to treat EPP would be gene therapy, the correction of the mutated DNA of own body cells. Despite successful tests in a mouse model for EPP [202], the technique is not yet mature enough for human trials and connected to a number of concerns which have to be considered first. Recently, splice modulating oligonucleotides have been described which target the low expression allele in EPP and correct aberrant splicing to form additional mRNA and subsequently FECH protein [203]. However, a proof of concept in a humanized mouse model and a technique how to target erythropoietic precursors in the bone marrow in a sensitive developmental stage of porphyrin accumulation will remain a challenge for this interesting therapeutic approach.

II. AIMS OF THE STUDIES:

Erythropoietic protoporphyria (EPP) is associated with a change in serum iron parameters and a microcytic, hypochromic anemia both indicating iron deficiency. However, clinical experience showed that iron supplementation aggravated the symptoms of EPP, an up-to-now unexplained phenomenon. On the other hand, over 97% of EPP patients carry the splice modulating SNP IVS3-48C/T which enhances aberrant splicing of intron 3. Since iron, heme metabolism as well as splicing are highly regulated processes, an assumed connection among them builds the working hypothesis of this thesis.

All three studies selected for this thesis therefore focus on aspects of regulatory mechanisms and expression of genes related to EPP and heme synthesis, possibly influenced by iron availability. We specifically wanted to perform studies concerning the following issues:

1. An in-depth characterization of *FECH* intron 3 to reveal whether additional sequence features exist that may be related to the disease causing splice defect
2. Whether the alternative splicing of *FECH* intron 3 has a regulatory function, especially
    a. Whether any of the substrates or products of the FECH reaction iron, protoporphyrin IX, heme or zinc-protoporphyrin IX influence the splice side choice of *FECH* intron 3
    b. Which splice factors are involved in the alternative splicing and its supposed regulation
    c. Whether the polymorphism *FECH* IVS3-48 which influences the ratio of the splice side choice also has an influence on the supposed regulatory process
3. Possible reasons for the observed exacerbation of symptoms after iron supplementation, especially to test our hypothesis that ALAS2 is involved in the pathophysiology of EPP

III. RESULTS

STUDY I

Variations in the length of poly-C and poly-T tracts in intron 3 of the human ferrochelatase gene

The third intron of human ferrochelatase (*FECH*) gene contains two homopolymeric tracts, a stretch of cytidines (poly-C) and thymidins (poly-T) which are located approximately 900 bp upstream from the known splice modulating SNP IVS3-48C/T. According to the NCBI database, the length of the tracts is 11 cytidines and 24 thymidins. Since we previously sequenced intron 3 of volunteers and found differences to the reference sequence, we analyzed the length of those tracts in 23 healthy controls homozygous for the T-variant of IVS3-48T/T, 14 healthy heterozygous controls (C/T), 7 unrelated EPP mutation carriers (M/T; M stands for *FECH* mutation) and 10 unrelated EPP patients (M/C). The length of the poly-C tracts in the study cohort varied from 10 to 16, and that of the poly-T tracts from 22 to 24. Statistical analysis showed, that the low-expressed FECH allele (IVS3-48C) is associated with longer poly-C tracts (poly-C12, -C13 and -C15) and poly-T22. In addition, the segregation of poly-C and poly-T tracts was studied in two Israeli EPP families. Instabilities, as seen by both insertion and deletion of one nucleotide between two generations, were observed in the poly-T tract. A possible function of the observed variations in the length of homopolymeric sequence in introns has to be elucidated.

STUDY II

Iron availability modulates aberrant splicing of ferrochelatase through the iron- and 2-oxoglutarate dependent dioxygenase Jmjd6 and U2AF^{65}

In Study II, we tested whether the FECH substrate iron or the products heme or zinc-protoporphyrin IX (Zn-PPIX) exhibits a modulating function on the splice side choice of *FECH* intron 3 *in vitro*. We used the erythroleukemic K562 and lymphoblastoid cell lines previously generated in our laboratory from healthy and EPP affected volunteers with different genotypes regarding the splice modulating SNP (IVS3-48T/T; C/C and M/C). While addition of iron, heme and Zn-PPIX had no influence on the splice ratio, treatment with chelators to reduce iron availability altered the choice of the splice site: depletion of iron with the chelators deferoxamine (DFO) or 1,2-dimethyl-3-hydroxy-4-pyridone (deferiprone) resulted in a decrease of the correct spliced FECH mRNA and, concomitantly, an increase of the aberrant splice product in the erythroleukemic K562 cell line. The amount of FECH protein was measured under normal conditions and under DFO treatment which was found to be decreased, too. The effects were shown to be prevented by neutralizing the chelator DFO with equimolar amounts of iron (ferric ammonium citrate, FAC) and were reversed upon treatment with iron 24 h after treatment with the chelator. Interestingly, the strongest effect was detected in the erythroleukemic K562 and lymphoblastoid cell lines both homozygous for IVS3-48T, where the aberrant splice product increased to 56% and 50% of total FECH mRNA, respectively. Iron deficiency had less effect on the FECH splice ratio in the investigated lymphoblastoid cell line homozygous for the SNP IVS3-48C and a cell line with the EPP-genotype (M/C).

To elucidate the mechanism of the splice alteration modulated by iron availability, we tested whether the dioxygenase Jumonji domain-containing protein 6 (Jmjd6) is involved in the FECH splice reaction: Jmjd6 is an iron (II) - and 2-oxoglutarate-dependent dioxygenase recently described to interact with the splice factor U2AF^{65} by lysyl-hydroxylation. U2AF (U2 snRNP auxiliary factor) is an essential splicing factor composed of two subunits. The large subunit of 65-kDa (U2AF^{65}) binds to the polypyrimidine tract (PY-tract) upstream from the 3′ splice site and promotes U2 snRNP binding to the pre-mRNA. The small subunit U2AF^{35} is important for the splicing of introns that contain short or weak PY-tracts. However, the recognition of a weak 3′ binding site requires the interaction between the two subunits. The correct splice site of FECH intron 3 is indeed very weak and proceeded mostly by short sequences of 3 or less cytosines or thymines (Cs/Ts), whereas the aberrant splice acceptor site contains a strong polypyrimidine stretch of 15 Cs/Ts. By consecutively applying different inhibitors we were able to demonstrate an involvement of the splice factor U2AF^{65} and Jmjd6 in the splice site choice of *FECH* intron 3 by iron availability.

Inhibition of Jmjd6 activity can be achieved by iron deprivation with either iron chelators such as DFO or deferiprone, by competitive inhibition of iron binding with $CoCl_2$, by competitive inhibition of 2-oxoglutarate binding with DMOG, and by suppression of transcription with specific siRNA against Jmjd6. Inhibition of $U2AF^{65}$ can be achieved by siRNA. Upon inhibition of either Jmjd6 or $U2AF^{65}$, the splice ratio shifts toward the aberrant product, leading to fewer amounts of both FECH mRNA and protein.

STUDY III

In ferrochelatase-deficient protoporphyria patients, ALAS2 expression is enhanced and erythrocytic protoporphyrin-concentration correlates with iron availability

Patients with erythropoietic protoporphyria (EPP) often show signs of iron deficiency, in addition to the symptom of photosensitivity which is caused by the accumulation of the second substrate of this enzyme, protoporphyrin IX (PPIX). However, iron supplementation frequently leads to exacerbation of phototoxicity. By analyzing hematological laboratory data from three EPP patients over a prolonged time span, we found low hemoglobin (HGB) correlated with a reduced PPIX concentration in erythrocytes whereas higher amounts of HGB were associated with higher PPIX concentrations. To explain our finding, we performed further analyses among a cohort of EPP patients which revealed increases in the amount of both mRNA and protein of the erythroid-specific isoenzyme 5-aminolevulinic acid synthase (ALAS2) in peripheral blood samples. The amount of ALAS2 mRNA in EPP patients was determined to be 782.7 arbitrary units (a.u.; interquartile range: 329.0 – 948.7 a.u., n=15) and that of healthy controls 194.8 a.u. (90.9 - 360.0 a.u., n=20). ALAS2 protein in EPP patients was found to be two-fold increased compared to healthy subjects. To verify our finding, we performed in vitro experiments to inhibit FECH with N-methyl protoporphyrin (NMPP), a known inhibitor of FECH activity, in the erythroleukemic K562 cell line and were able to measure a two-fold increase in ALAS2 mRNA subsequently. The results of this study brought new insights into the pathogenesis of EPP, i.e. the primary deficiency in FECH leads to a secondary increase in the expression of ALAS2 which is the first and rate-limiting enzyme in the erythroid heme biosynthetic pathway. A higher activity of ALAS2 combined with a lower activity of FECH contributes to the accumulation of PPIX in EPP. The translation of ALAS2 is regulated by IRE-binding proteins (IRP) 1 and 2 which bind at an iron-responsive element (IRE) present in the 5`UTR region of ALAS2 mRNA which blocks translation if iron is scarce. The frequently observed iron deficiency among EPP patients could therefore act protective against an unlimited PPIX production by restricting ALAS2 over-expression.

IV. DISCUSSION

In over 90% of EPP cases, the underlying genetic defect consists of the splice modulating SNP IVS3-48C (low expression allele) *in trans* to a mutation of the *FECH* allele [95;107]. The splicing reaction is complex and not entirely understood and is influenced by a plethora of sequence and protein factors. In **Study I**, we therefore investigated sequence features of *FECH* intron 3, a poly-C and a poly-T homopolymeric tract located approximately 900 bp upstream of the splice site. Stretches rich in T and C nucleotides (polypyrimidine tracts) are binding sites for splice factors when preceding splice acceptor sites, and deletions in homopolymeric poly-T tracts are reported to result in aberrant splicing in cancer related genes such as *ATM* and *MRE 11* [204;205]. A poly (C)–binding protein 1 (PCBP1) exists which seem to function as a cytosolic iron chaperone. It binds ferritin and increases the amount of iron bound by ferritin when expressed in yeast cells. Disruption of PCBP1 expression in human cells leads to an increase in cytosolic iron and a decrease in ferritin iron [206]. In general, homopolymeric tracts are significantly over-represented and more widely spread in the genome than simply by chance, indicating a function [207;208]. In our study, we demonstrated an association of the low expression allele IVS3-48C with longer poly-C tracts (poly-C12, -C13 and -C15) and poly-T22. In the poly-T tract, a difference of only one nucleotide between the two alleles has been observed in the study subjects. Additionally, in segregation studies of two Israeli families, single nucleotide deletions and insertion in the poly-T tract were observed. However, possible functions of the poly-C and poly-T tracts in the *FECH* gene remain to be studied.

One of the hitherto not sufficiently understood phenomena of EPP is the adverse reaction on iron supplementation in many individuals affected by EPP. Although 20-60% of EPP patients show low serum iron concentration and hematologic abnormalities which resemble those of iron deficiency, i.e. microcytic and hypochromic anemia [66], iron supplementation was found to be beneficial in some cases only [209;210], while to be counterproductive in terms of worsening the skin symptoms in others [172-174], own observation. Additionally, the fate of iron in the organism of an EPP patient is not understood at the moment [66;68]. The biosynthesis of heme is tightly regulated since its intermediary porphyrins as well as the end product heme are toxic to the organism if present in excess (reviewed in references [3;6;211]). A regulatory function of alternative splicing with a PTC, termed regulated unproductive splicing and translation (RUST), has been described in a number of genes [212]. Our guess that iron itself or the products of FECH reaction, either PPIX or Zn-PPIX might negatively influence the splice site choice of *FECH* intron 3 was confirmed, but in a way not foreseen by us (**Study II**): The worsening of the symptoms under iron therapy would suggest, that iron or FECH reaction products in a kind of feedback inhibition negatively affect the FECH protein or its activity. However, we could not find an effect of enhanced cellular iron content, but found that the deficiency of iron causes the correctly spliced mRNA to decrease and the aberrantly spliced mRNA to increase. Concomitantly, the amount of FECH

protein decreased. A common splice factor, $U2AF^{65}$, which is modified by the iron dependent dioxygenase Jmjd6 [213] was studied in detail and could be identified as a link between iron metabolism and splicing of FECH. In iron deficiency, Jmjd6 activity is inhibited and less $U2AF^{65}$ can be modified. Subsequently, the recognition of the correct splice site is no longer supported. The splice ratio shifts toward the aberrant product, leading to fewer amounts of both FECH mRNA and protein - which is reasonable since in the absence of substrate the enzyme is dispensable.

Interestingly, the observed effect is strongest in the two cell lines without the low expression allele but the common genotype IVS3-48T/T. In cell lines bearing the low expression allele (IVS3-48C/C and M/C (EPP)), the baseline amount of aberrantly spliced FECH mRNA is higher. However, under iron depletion, the increase in aberrantly and decrease in correctly spliced FECH mRNA is less pronounced. Assuming that the described effect of iron deprivation on splicing in the T/T genotype has a regulatory feature, the observed loss in sensitivity in the IVS3-48C background constitutes a loss of potential for regulation. Taking both together, the increase in aberrant splicing under baseline condition and the less pronounced increase in aberrant splicing compared to the T/T genotype under iron deprivation indicate that even if enough iron is available, the C/C genotype is less sensitive to iron deficiency.

Based on the clinical observation, that iron supplementation can lead to aggravation of EPP symptoms, we hypothesized in **Study III** that ALAS2 is involved in the etiology of EPP: ALAS2 is the first and rate-limiting enzyme of erythroid heme biosynthesis. The mRNA of ALAS2 harbors a structural element, the iron response element (IRE), which upon binding of the iron response protein (IRP) prevents translation of the mRNA if iron is scarce - but enables protein synthesis if iron is available. Surprisingly, we found ALAS2 mRNA to be enhanced in peripheral blood samples of EPP patients compared to healthy controls. Since also ALAS2 protein was increased, the IRE-IRP system seems to only partially exert a block of ALAS2 translation in EPP. Therefore, one may speculate that an enhanced ALAS2 activity contributes to the excess amount of PPIX accumulating in EPP. Furthermore, iron supplementation could lead to a de-repression of the IRE block which would further increase the amount of ALAS2 enzyme and explain the worsening of the EPP symptoms under iron therapy.

Out of ethical considerations, no study to provoke an enhancement of PPIX due to higher amount of ALAS2 after iron supplementation can be conducted. However, we analyzed the data of three EPP patients from our clinic who received iron therapy because of low hemoglobin levels and pronounced anemia with fatigue and fainting. Two of the patients displayed markedly increased levels of soluble transferrin receptor which is seen as the most reliable marker for iron deficiency in EPP. Since both patients responded with an increase in hemoglobin after iron administration, we interpret hemoglobin as a measure for the amount of iron available for erythropoiesis. A positive correlation between the amount of hemoglobin and PPIX was found in all three patients, indicating that iron stimulates PPIX production. This observation is explicable by the interpretation that iron stimulates ALAS2 expression

which results in higher PPIX values. Therefore, possible benefits of an iron supplementation therapy in EPP patients should be carefully weighed against an increased PPIX burden, especially in regard of liver damage caused by increased PPIX blood concentrations.

V. CONCLUSION

The presented studies show that

1. The alternative splicing observed in *FECH* intron 3 (IVS3-48T) is a regulatory feature which links iron availability to amount of enzyme. This regulatory sequence element is conserved in primates, which adds evidence to the hypothesis that the splice alteration is part of a regulatory mechanism described as Regulated Unproductive Splicing and Translation (RUST).

2. The splice-modifying and disease-causing *FECH* SNP IVS3-48C exhibits a de-regulation in regard to the splice regulation in such that it displays higher levels of aberrant splicing under iron-saturated conditions and less inducibility of aberrant splicing in iron depletion compared to the IVS3-48T genotype.

3. ALAS2, the first and rate limiting enzyme of erythroid heme biosynthesis, is enhanced in EPP at the mRNA and protein level. Although considered a monogenetic disease, the aetiology of EPP is therefore more complex and includes possible feedback regulation which might lead to new treatment options.

4. Further evidence and a proposition for an underlying mechanism could be added to the observation, that iron therapy in EPP patients may be accompanied by adverse effects. Higher PPIX levels were measured when more iron was available for hemoglobin synthesis. Since in EPP patients the ALAS2 mRNA was found to be enhanced, iron supplementation could lead to an increase in ALAS2 protein translation due to a de-repression of the IRE-IRP mediated translation block and therefore a stimulated synthesis of PPIX.

VI. OUTLOOK

Out of two reasons, it is of great importance to identify good parameters to distinguish EPP patients in need of extra iron versus patients with a low hemoglobin but stable iron metabolism: Both iron deficiency and iron overload are harmful to the body, however the fate of iron in EPP patients is not understood at the moment – a block of resorption might account for the low iron values as well as an iron loss by unknown mechanism or its deposition in the liver or other organs. Secondly, since our studies showed a mechanism to explain exacerbated light sensitivity under iron supplementation by an enhanced ALAS2 expression, iron can trigger PPIX production and subsequently liver damage by PPIX.

In my view, iron in EPP has to be seen as not only a simple substrate of FECH reaction, but as a factor exhibiting a regulatory function on many levels of metabolic regulation. In erythroid heme synthesis, iron plays a regulatory role at the first and rate-limiting enzyme by the regulation by the IRE/ IRP – system. Additionally, we demonstrated a role of iron in splice regulation of intron 3 of FECH. Iron exhibits its regulatory role as a substrate of the iron-dependent dioxygenase Jmjd6. Since Jmjd6 modifies the common splice factor $U2AF^{65}$, an effect on the splicing of other genes was demonstrated by others as well [213;214]. It will be fascinating to search for a conclusive hypothesis to connect the genes regulated by this mechanism with a response of the body to different metabolic conditions.

A better understanding of the splicing of *FECH* intron 3 and the necessary and / or significant sequence features could enable a therapy based on splice modification – an approach which could be used in over 97% of all EPP patients due to the shared sequence of the low expression allele. However, targeting the hematopoietic cells in the bone marrow with a possibly effective substance might turn out to be a big challenge.

Another treatment option could be the down regulation of ALAS2, the first and rate-limiting enzyme of heme biosynthesis which was demonstrated by us to be enhanced in EPP. A first step would be to measure ALAS2 mRNA, protein and activity in EPP mouse models to elucidate the mechanism of the enhancement and enable to test possible treatments.

VII. REFERENCES

Reference List

1. Samuel D, Boboc B, Bernuau J *et al*. Liver transplantation for protoporphyria. Evidence for the predominant role of the erythropoietic tissue in protoporphyrin overproduction. *Gastroenterology* 1988; **95**: 816-9.

2. Bloomer JR, Hill HD, Kools AM *et al*. Heme synthesis in protoporphyria. *Curr Probl Dermatol* 1991; **20**: 135-47.

3. Anderson K, Sassa S, Bishop DF *et al*. Disorders of heme biosynthesis: X-linked sideroblastic anemia and the porphyrias. In: *The Metabolic and Molecular Basis of Inherited Disease* (Scriver,CR, Beaugrand,M, Sly,WS et al, eds), 8 edn. New York: McGraw-Hill, 2001: 2991-3062.

4. Sassa S. Modern diagnosis and management of the porphyrias. *Br J Haematol* 2006; **135**: 281-92.

5. Ajioka RS, Phillips JD, Kushner JP. Biosynthesis of heme in mammals. *Biochim Biophys Acta* 2006; **1763**: 723-36.

6. Kohgo Y, Ikuta K, Ohtake T *et al*. Body iron metabolism and pathophysiology of iron overload. *Int J Hematol* 2008; **88**: 7-15.

7. Ponka P. Tissue-specific regulation of iron metabolism and heme synthesis: distinct control mechanisms in erythroid cells. *Blood* 1997; **89**: 1-25.

8. Ferreira GC. Erythroid 5-aminolevulinate synthase and X-linked sideroblastic anemia. *J Fla Med Assoc* 1993; **80**: 481-3.

9. Bottomley SS, May BK, Cox TC *et al*. Molecular defects of erythroid 5-aminolevulinate synthase in X-linked sideroblastic anemia. *J Bioenerg Biomembr* 1995; **27**: 161-8.

10. Astrin KH, Bishop DF. Assignment of human erythroid delta-aminolevulinate synthase (ALAS2) to the X-chromosome. *Cytogenet Cell Genet* 1989; **51**: 953-4.

11. Bishop DF, Henderson AS, Astrin KH. Human delta-aminolevulinate synthase: assignment of the housekeeping gene to 3p21 and the erythroid-specific gene to the X chromosome. *Genomics* 1990; **7**: 207-14.

12. Abraham NG, Kappas A. Pharmacological and clinical aspects of heme oxygenase. *Pharmacol Rev* 2008; **60**: 79-127.

13. Boyle JJ, Johns M, Lo J *et al*. Heme induces heme oxygenase 1 via Nrf2: role in the homeostatic macrophage response to intraplaque hemorrhage. *Arterioscler Thromb Vasc Biol* 2011; **31**: 2685-91.

14. Bonkovsky HL, Guo JT, Hou W *et al*. Porphyrin and heme metabolism and the porphyrias. *Compr Physiol* 2013; **3**: 365-401.

15. UNICEF, World Health Organization. *Iron deficiency anaemia: assessment, prevention, and control: a guide for programme managers*. WHo, 2001.

16. Lamola AA, Yamane T. Zinc protoporphyrin in the erythrocytes of patients with lead intoxication and iron deficiency anemia. *Science* 1974; **186**: 936-8.

17. Piomelli S, Lamola AA, Poh-Fitzpatrick MF *et al*. Erythropoietic protoporphyria and lead intoxication: the molecular basis for difference in cutaneous photosensitivity. I. Different rates of disappearance of protoporphyrin from the erythrocytes, both in vivo and in vitro. *J Clin Invest* 1975; **56**: 1519-27.

18. Kushner JP, Steinmuller DP, Lee GR. The role of iron in the pathogenesis of porphyria cutanea tarda. II. Inhibition of uroporphyrinogen decarboxylase. *J Clin Invest* 1975; **56**: 661-7.

19. Fargion S, Piperno A, Cappellini MD *et al*. Hepatitis C virus and porphyria cutanea tarda: evidence of a strong association. *Hepatology* 1992; **16**: 1322-6.

20. Can C, Nigogosyan G. Acquired toxic porphyria cutanea tarda due to hexachlorobenzene. Report of 348 cases caused by this fungicide. *JAMA* 1963; **183**: 88-91.

21. Hunter GA, Ferreira GC. 5-aminolevulinate synthase: catalysis of the first step of heme biosynthesis. *Cell Mol Biol (Noisy -le-grand)* 2009; **55**: 102-10.

22. Lathrop JT, Timko MP. Regulation by heme of mitochondrial protein transport through a conserved amino acid motif. *Science* 1993; **259**: 522-5.

23. Munakata H, Sun JY, Yoshida K *et al*. Role of the heme regulatory motif in the heme-mediated inhibition of mitochondrial import of 5-aminolevulinate synthase. *J Biochem* 2004; **136**: 233-8.

24. Hamilton JW, Bement WJ, Sinclair PR *et al*. Heme regulates hepatic 5-aminolevulinate synthase mRNA expression by decreasing mRNA half-life and not by altering its rate of transcription. *Arch Biochem Biophys* 1991; **289**: 387-92.

25. Drew PD, Ades IZ. Regulation of the stability of chicken embryo liver delta-aminolevulinate synthase mRNA by hemin. *Biochem Biophys Res Commun* 1989; **162**: 102-7.

26. Cable EE, Miller TG, Isom HC. Regulation of heme metabolism in rat hepatocytes and hepatocyte cell lines: delta-aminolevulinic acid synthase and heme oxygenase are regulated by different heme-dependent mechanisms. *Arch Biochem Biophys* 2000; **384**: 280-95.

27. Roberts AG, Elder GH. Alternative splicing and tissue-specific transcription of human and rodent ubiquitous 5-aminolevulinate synthase (ALAS1) genes. *Biochim Biophys Acta* 2001; **1518**: 95-105.

28. Roberts AG, Redding SJ, Llewellyn DH. An alternatively-spliced exon in the 5'-UTR of human ALAS1 mRNA inhibits translation and renders it resistant to haem-mediated decay. *FEBS Lett* 2005; **579**: 1061-6.

29. Tian Q, Li T, Hou W *et al*. Lon peptidase 1 (LONP1)-dependent breakdown of mitochondrial 5-aminolevulinic acid synthase protein by heme in human liver cells. *J Biol Chem* 2011; **286**: 26424-30.

30. Thunell S. (Far) Outside the box: genomic approach to acute porphyria. *Physiol Res* 2006; **55 Suppl 2**: S43-S66.

31. Surinya KH, Cox TC, May BK. Identification and characterization of a conserved erythroid-specific enhancer located in intron 8 of the human 5-aminolevulinate synthase 2 gene. *J Biol Chem* 1998; **273**: 16798-809.

32. Palmieri F, Pierri CL. Structure and function of mitochondrial carriers - role of the transmembrane helix P and G residues in the gating and transport mechanism. *FEBS Lett* 2010; **584**: 1931-9.

33. May A, Bishop DF. The molecular biology and pyridoxine responsiveness of X-linked sideroblastic anaemia. *Haematologica* 1998; **83**: 56-70.

34. Hunter GA, Ferreira GC. Molecular enzymology of 5-aminolevulinate synthase, the gatekeeper of heme biosynthesis. *Biochim Biophys Acta* 2011; **1814**: 1467-73.

35. Surinya KH, Cox TC, May BK. Transcriptional regulation of the human erythroid 5-aminolevulinate synthase gene. Identification of promoter elements and role of regulatory proteins. *J Biol Chem* 1997; **272**: 26585-94.

36. Han L, Zhong Y, Huang B *et al*. Sodium butyrate activates erythroid-specific 5-aminolevulinate synthase gene through Sp1 elements at its promoter. *Blood Cells Mol Dis* 2008; **41**: 148-53.

37. Campagna DR, de Bie CI, Schmitz-Abe K *et al*. X-linked sideroblastic anemia due to ALAS2 intron 1 enhancer element GATA-binding site mutations. *Am J Hematol* 2014; **89**: 315-9.

38. Kaneko K, Furuyama K, Fujiwara T *et al*. Identification of a novel erythroid-specific enhancer for the ALAS2 gene and its loss-of-function mutation which is associated with congenital sideroblastic anemia. *Haematologica* 2014; **99**: 252-61.

39. Kramer MF, Gunaratne P, Ferreira GC. Transcriptional regulation of the murine erythroid-specific 5-aminolevulinate synthase gene. *Gene* 2000; **247**: 153-66.

40. Han L, Lu J, Pan L *et al*. Histone acetyltransferase p300 regulates the transcription of human erythroid-specific 5-aminolevulinate synthase gene. *Biochem Biophys Res Commun* 2006; **348**: 799-806.

41. Sadlon TJ, Dell'Oso T, Surinya KH *et al*. Regulation of erythroid 5-aminolevulinate synthase expression during erythropoiesis. *Int J Biochem Cell Biol* 1999; **31**: 1153-67.

42. Hofer T, Wenger RH, Kramer MF *et al*. Hypoxic up-regulation of erythroid 5-aminolevulinate synthase. *Blood* 2003; **101**: 348-50.

43. Kaneko K, Furuyama K, Aburatani H *et al*. Hypoxia induces erythroid-specific 5-aminolevulinate synthase expression in human erythroid cells through transforming growth factor-beta signaling. *FEBS J* 2009; **276**: 1370-82.

44. Zhang FL, Shen GM, Liu XL *et al*. Hypoxic induction of human erythroid-specific delta-aminolevulinate synthase mediated by hypoxia-inducible factor 1. *Biochemistry* 2011; **50**: 1194-202.

45. Abu-Farha M, Niles J, Willmore WG. Erythroid-specific 5-aminolevulinate synthase protein is stabilized by low oxygen and proteasomal inhibition. *Biochem Cell Biol* 2005; **83**: 620-30.

46. Eisenstein RS. Iron regulatory proteins and the molecular control of mammalian iron metabolism. *Annu Rev Nutr* 2000; **20**: 627-62.

47. Melefors O, Goossen B, Johansson HE *et al*. Translational control of 5-aminolevulinate synthase mRNA by iron-responsive elements in erythroid cells. *J Biol Chem* 1993; **268**: 5974-8.

48. Bhasker CR, Burgiel G, Neupert B *et al*. The putative iron-responsive element in the human erythroid 5-aminolevulinate synthase mRNA mediates translational control. *J Biol Chem* 1993; **268**: 12699-705.

49. Bishop DF, Tchaikovskii V, Hoffbrand AV *et al*. X-linked sideroblastic anemia due to carboxyl-terminal ALAS2 mutations that cause loss of binding to the beta-subunit of succinyl-CoA synthetase (SUCLA2). *J Biol Chem* 2012; **287**: 28943-55.

50. Ye H, Jeong SY, Ghosh MC *et al*. Glutaredoxin 5 deficiency causes sideroblastic anemia by specifically impairing heme biosynthesis and depleting cytosolic iron in human erythroblasts. *J Clin Invest* 2010; **120**: 1749-61.

51. Cooperman SS, Meyron-Holtz EG, Olivierre-Wilson H *et al*. Microcytic anemia, erythropoietic protoporphyria, and neurodegeneration in mice with targeted deletion of iron-regulatory protein 2. *Blood* 2005; **106**: 1084-91.

52. Whatley SD, Ducamp S, Gouya L *et al*. C-terminal deletions in the ALAS2 gene lead to gain of function and cause X-linked dominant protoporphyria without anemia or iron overload. *Am J Hum Genet* 2008; **83**: 408-14.

53. Kadirvel S, Furuyama K, Harigae H *et al*. The carboxyl-terminal region of erythroid-specific 5-aminolevulinate synthase acts as an intrinsic modifier for its catalytic activity and protein stability. *Exp Hematol* 2012; **40**: 477-86.

54. To-Figueras J, Ducamp S, Clayton J *et al*. ALAS2 acts as a modifier gene in patients with congenital erythropoietic porphyria. *Blood* 2011; **118**: 1443-51.

55. Ferreira GC, Franco R, Lloyd SG *et al*. Structure and function of ferrochelatase. *J Bioenerg Biomembr* 1995; **27**: 221-9.

56. Wu CK, Dailey HA, Rose JP *et al*. The 2.0 A structure of human ferrochelatase, the terminal enzyme of heme biosynthesis. *Nat Struct Biol* 2001; **8**: 156-60.

57. Dailey HA, Finnegan MG, Johnson MK. Human ferrochelatase is an iron-sulfur protein. *Biochemistry* 1994; **33**: 403-7.

58. Schneider-Yin X, Gouya L, Dorsey M *et al*. Mutations in the iron-sulfur cluster ligands of the human ferrochelatase lead to erythropoietic protoporphyria. *Blood* 2000; **96**: 1545-9.

59. Medlock A, Swartz L, Dailey TA *et al*. Substrate interactions with human ferrochelatase. *Proc Natl Acad Sci U S A* 2007; **104**: 1789-93.

60. Taketani S, Adachi Y, Nakahashi Y. Regulation of the expression of human ferrochelatase by intracellular iron levels. *Eur J Biochem* 2000; **267**: 4685-92.

61. Crooks DR, Ghosh MC, Haller RG *et al*. Posttranslational stability of the heme biosynthetic enzyme ferrochelatase is dependent on iron availability and intact iron-sulfur cluster assembly machinery. *Blood* 2010; **115**: 860-9.

62. Tugores A, Magness ST, Brenner DA. A single promoter directs both housekeeping and erythroid preferential expression of the human ferrochelatase gene. *J Biol Chem* 1994; **269**: 30789-97.

63. Magness ST, Tugores A, Diala ES *et al*. Analysis of the human ferrochelatase promoter in transgenic mice. *Blood* 1998; **92**: 320-8.

64. Magness ST, Tugores A, Brenner DA. Analysis of ferrochelatase expression during hematopoietic development of embryonic stem cells. *Blood* 2000; **95**: 3568-77.

65. Magnus IA, JARRETT A, PRANKERD TA *et al*. Erythropoietic protoporphyria. A new porphyria syndrome with solar urticaria due to protoporphyrinaemia. *Lancet* 1961; **2**: 448-51.

66. Holme SA, Worwood M, Anstey AV *et al*. Erythropoiesis and iron metabolism in dominant erythropoietic protoporphyria. *Blood* 2007; **110**: 4108-10.

67. Schneider-Yin X, Harms J, Minder EI. Porphyria in Switzerland, 15 years experience. *Swiss Med Wkly* 2009; **139**: 198-206.

68. Delaby C, Lyoumi S, Ducamp S *et al*. Excessive erythrocyte PPIX influences the hematologic status and iron metabolism in patients with dominant erythropoietic protoporphyria. *Cell Mol Biol (Noisy -le-grand)* 2009; **55**: 45-52.

69. Wahlin S, Floderus Y, Stal P *et al*. Erythropoietic protoporphyria in Sweden: demographic, clinical, biochemical and genetic characteristics. *J Intern Med* 2011; **269**: 278-88.

70. Abitbol M, Bernex F, Puy H *et al*. A mouse model provides evidence that genetic background modulates anemia and liver injury in erythropoietic protoporphyria. *Am J Physiol Gastrointest Liver Physiol* 2005; **288**: G1208-G1216.

71. Yamamoto M, Arimura H, Fukushige T *et al*. Abcb10 role in heme biosynthesis in vivo: Abcb10 knockout in mice causes anemia with protoporphyrin IX and iron accumulation. *Mol Cell Biol* 2014; **34**: 1077-84.

72. Wang Y, Langer NB, Shaw GC *et al*. Abnormal mitoferrin-1 expression in patients with erythropoietic protoporphyria. *Exp Hematol* 2011; **39**: 784-94.

73. Holbrook JA, Neu-Yilik G, Hentze MW *et al*. Nonsense-mediated decay approaches the clinic. *Nat Genet* 2004; **36**: 801-8.

74. Troadec MB, Warner D, Wallace J *et al*. Targeted deletion of the mouse Mitoferrin1 gene: from anemia to protoporphyria. *Blood* 2011; **117**: 5494-502.

75. Jonker JW, Buitelaar M, Wagenaar E *et al*. The breast cancer resistance protein protects against a major chlorophyll-derived dietary phototoxin and protoporphyria. *Proc Natl Acad Sci U S A* 2002; **99**: 15649-54.

76. Zhou S, Zong Y, Ney PA *et al*. Increased expression of the Abcg2 transporter during erythroid maturation plays a role in decreasing cellular protoporphyrin IX levels. *Blood* 2005; **105**: 2571-6.

77. Han AP, Fleming MD, Chen JJ. Heme-regulated eIF2alpha kinase modifies the phenotypic severity of murine models of erythropoietic protoporphyria and beta-thalassemia. *J Clin Invest* 2005; **115**: 1562-70.

78. Eaton JW, Qian M. Molecular bases of cellular iron toxicity. *Free Radic Biol Med* 2002; **32**: 833-40.

79. Rouault TA. The role of iron regulatory proteins in mammalian iron homeostasis and disease. *Nat Chem Biol* 2006; **2**: 406-14.

80. Muckenthaler MU, Galy B, Hentze MW. Systemic iron homeostasis and the iron-responsive element/iron-regulatory protein (IRE/IRP) regulatory network. *Annu Rev Nutr* 2008; **28**: 197-213.

81. Anderson CP, Shen M, Eisenstein RS *et al*. Mammalian iron metabolism and its control by iron regulatory proteins. *Biochim Biophys Acta* 2012; **1823**: 1468-83.

82. Leibold EA, Munro HN. Cytoplasmic protein binds in vitro to a highly conserved sequence in the 5' untranslated region of ferritin heavy- and light-subunit mRNAs. *Proc Natl Acad Sci U S A* 1988; **85**: 2171-5.

83. Harrison PM, Arosio P. The ferritins: molecular properties, iron storage function and cellular regulation. *Biochim Biophys Acta* 1996; **1275**: 161-203.

84. Sangokoya C, Doss JF, Chi JT. Iron-responsive miR-485-3p regulates cellular iron homeostasis by targeting ferroportin. *PLoS Genet* 2013; **9**: e1003408.

85. Sanchez M, Galy B, Schwanhaeusser B *et al*. Iron regulatory protein-1 and -2: transcriptome-wide definition of binding mRNAs and shaping of the cellular proteome by iron regulatory proteins. *Blood* 2011; **118**: e168-e179.

86. Maniatis T, Tasic B. Alternative pre-mRNA splicing and proteome expansion in metazoans. *Nature* 2002; **418**: 236-43.

87. Pan Q, Shai O, Lee LJ *et al*. Deep surveying of alternative splicing complexity in the human transcriptome by high-throughput sequencing. *Nat Genet* 2008; **40**: 1413-5.

88. Kaya AH, Plewinska M, Wong DM *et al*. Human delta-aminolevulinate dehydratase (ALAD) gene: structure and alternative splicing of the erythroid and housekeeping mRNAs. *Genomics* 1994; **19**: 242-8.

89. Grandchamp B, de Verneuil H, Beaumont C *et al*. Tissue-specific expression of porphobilinogen deaminase. Two isoenzymes from a single gene. *Eur J Biochem* 1987; **162**: 105-10.

90. Chretien S, Dubart A, Beaupain D *et al*. Alternative transcription and splicing of the human porphobilinogen deaminase gene result either in tissue-specific or in housekeeping expression. *Proc Natl Acad Sci U S A* 1988; **85**: 6-10.

91. Mignotte V, Eleouet JF, Raich N *et al*. Cis- and trans-acting elements involved in the regulation of the erythroid promoter of the human porphobilinogen deaminase gene. *Proc Natl Acad Sci U S A* 1989; **86**: 6548-52.

92. Aizencang G, Solis C, Bishop DF *et al*. Human uroporphyrinogen-III synthase: genomic organization, alternative promoters, and erythroid-specific expression. *Genomics* 2000; **70**: 223-31.

93. Cox TC, Sadlon TJ, Schwarz QP *et al*. The major splice variant of human 5-aminolevulinate synthase-2 contributes significantly to erythroid heme biosynthesis. *Int J Biochem Cell Biol* 2004; **36**: 281-95.

94. Nakahashi Y, Taketani S, Okuda M *et al*. Molecular cloning and sequence analysis of cDNA encoding human ferrochelatase. *Biochem Biophys Res Commun* 1990; **173**: 748-55.

95. Gouya L, Puy H, Robreau AM *et al*. The penetrance of dominant erythropoietic protoporphyria is modulated by expression of wildtype FECH. *Nat Genet* 2002; **30**: 27-8.

96. Gunshin H, Allerson CR, Polycarpou-Schwarz M *et al*. Iron-dependent regulation of the divalent metal ion transporter. *FEBS Lett* 2001; **509**: 309-16.

97. Lee PL, Gelbart T, West C *et al*. The human Nramp2 gene: characterization of the gene structure, alternative splicing, promoter region and polymorphisms. *Blood Cells Mol Dis* 1998; **24**: 199-215.

98. Hubert N, Hentze MW. Previously uncharacterized isoforms of divalent metal transporter (DMT)-1: implications for regulation and cellular function. *Proc Natl Acad Sci U S A* 2002; **99**: 12345-50.

99. Puy H, Gouya L, Deybach JC. Porphyrias. *Lancet* 2010; **375**: 924-37.

100. Balwani M, Desnick RJ. The porphyrias: advances in diagnosis and treatment. *Hematology Am Soc Hematol Educ Program* 2012; **2012**: 19-27.

101. Ducamp S, Schneider-Yin X, de RF *et al*. Molecular and functional analysis of the C-terminal region of human erythroid-specific 5-aminolevulinic synthase associated with X-linked dominant protoporphyria (XLDPP). *Hum Mol Genet* 2013; **22**: 1280-8.

102. Taketani S, Inazawa J, Nakahashi Y *et al*. Structure of the human ferrochelatase gene. Exon/intron gene organization and location of the gene to chromosome 18. *Eur J Biochem* 1992; **205**: 217-22.

103. Deybach JC, Da S, V, Pasquier Y *et al*. Ferrochelatae in human erythropoietic protoporphyria: the first case of a homozygou form of the enzyme deficiency. In: *Porphyrins and porphyrias* (Nordmann,Y, ed), Vol. 134. INSERM/John Libbey, 1986: 163-73.

104. Lamoril J, Boulechfar S, de Verneuil H *et al*. Human erythropoietic protoporphyria: two point mutations in the ferrochelatase gene. *Biochem Biophys Res Commun* 1991; **181**: 594-9.

105. Todd DJ. Erythropoietic protoporphyria. *Br J Dermatol* 1994; **131**: 751-66.

106. Sarkany RP, Cox TM. Autosomal recessive erythropoietic protoporphyria: a syndrome of severe photosensitivity and liver failure. *QJM* 1995; **88**: 541-9.

107. Whatley SD, Mason NG, Holme SA *et al*. Molecular epidemiology of erythropoietic protoporphyria in the U.K. *Br J Dermatol* 2010; **162**: 642-6.

108. Minder EI, Schneider-Yin X, Mamet R *et al*. A homoallelic FECH mutation in a patient with both erythropoietic protoporphyria and palmar keratoderma. *J Eur Acad Dermatol Venereol* 2010; **24**: 1349-53.

109. Holme SA, Whatley SD, Roberts AG *et al*. Seasonal palmar keratoderma in erythropoietic protoporphyria indicates autosomal recessive inheritance. *J Invest Dermatol* 2009; **129**: 599-605.

110. Norris PG, Nunn AV, Hawk JL *et al*. Genetic heterogeneity in erythropoietic protoporphyria: a study of the enzymatic defect in nine affected families. *J Invest Dermatol* 1990; **95**: 260-3.

111. Morais P, Mota A, Baudrier T *et al*. Erythropoietic protoporphyria: a family study and report of a novel mutation in the FECH gene. *Eur J Dermatol* 2011; **21**: 479-83.

112. Aplin C, Whatley SD, Thompson P *et al*. Late-onset erythropoietic porphyria caused by a chromosome 18q deletion in erythroid cells. *J Invest Dermatol* 2001; **117**: 1647-9.

113. Sassa S, Akagi R, Nishitani C *et al*. Late-onset porphyrias: what are they? *Cell Mol Biol (Noisy -le-grand)* 2002; **48**: 97-101.

114. Bharati A, Badminton MN, Whatley SD *et al*. Late-onset erythropoietic protoporphyria in association with haematological malignancy. *Clin Exp Dermatol* 2006; **31**: 668-70.

115. Goodwin RG, Kell WJ, Laidler P *et al*. Photosensitivity and acute liver injury in myeloproliferative disorder secondary to late-onset protoporphyria caused by deletion of a ferrochelatase gene in hematopoietic cells. *Blood* 2006; **107**: 60-2.

116. Berroeta L, Man I, Goudie DR *et al*. Late presentation of erythropoietic protoporphyria: case report and genetic analysis of family members. *Br J Dermatol* 2007; **157**: 1030-1.

117. Frank J, Poblete-Gutierrez P, Neumann NJ. Photosensitivity in the elderly-think of late-onset protoporphyria. *J Invest Dermatol* 2013; **133**: 1467-71.

118. Azad J, Brennan P, Carmichael AJ. New mutation identified in two sisters with adult-onset erythropoietic protoporphyria. *Clin Exp Dermatol* 2013; **38**: 601-5.

119. Went LN, Klasen EC. Genetic aspects of erythropoietic protoporphyria. *Ann Hum Genet* 1984; **48**: 105-17.

120. Gouya L, Deybach JC, Lamoril J *et al*. Modulation of the phenotype in dominant erythropoietic protoporphyria by a low expression of the normal ferrochelatase allele. *Am J Hum Genet* 1996; **58**: 292-9.

121. Henriksson M, Timonen K, Mustajoki P *et al*. Four novel mutations in the ferrochelatase gene among erythropoietic protoporphyria patients. *J Invest Dermatol* 1996; **106**: 346-50.

122. Schneider-Yin X, Gouya L, Meier-Weinand A *et al*. New insights into the pathogenesis of erythropoietic protoporphyria and their impact on patient care. *Eur J Pediatr* 2000; **159**: 719-25.

123. Gouya L, Martin-Schmitt C, Robreau AM *et al*. Contribution of a common single-nucleotide polymorphism to the genetic predisposition for erythropoietic protoporphyria. *Am J Hum Genet* 2006; **78**: 2-14.

124. Wiman A, Floderus Y, Harper P. Novel mutations and phenotypic effect of the splice site modulator IVS3-48C in nine Swedish families with erythropoietic protoporphyria. *J Hum Genet* 2003; **48**: 70-6.

125. Whatley SD, Mason NG, Khan M *et al*. Autosomal recessive erythropoietic protoporphyria in the United Kingdom: prevalence and relationship to liver disease. *J Med Genet* 2004; **41**: e105.

126. Schneider-Yin X, Mamet R, Minder EI *et al*. Biochemical and molecular diagnosis of erythropoietic protoporphyria in an Ashkenazi Jewish family. *J Inherit Metab Dis* 2008; **31 Suppl 2**: S363-S367.

127. Aurizi C, Schneider-Yin X, Sorge F *et al*. Heterogeneity of mutations in the ferrochelatase gene in Italian patients with erythropoietic protoporphyria. *Mol Genet Metab* 2007; **90**: 402-7.

128. McGuire BM, Bonkovsky HL, Carithers RL, Jr. *et al*. Liver transplantation for erythropoietic protoporphyria liver disease. *Liver Transpl* 2005; **11**: 1590-6.

129. Kansky A, Bercic M. Erythropoietic protoporphyria in Slovenia. Epidemiologic study. *Dermatologica* 1981; **163**: 232-8.

130. Marko PB, Miljkovic J, Gorenjak M *et al*. Erythropoietic protoporphyria patients in Slovenia. *Acta Dermatovenerol Alp Panonica Adriat* 2007; **16**: 99-102, 104.

131. Todd DJ, Nevin NC, Burrows D. Prevalence of gallstones in patient with erythropoietic protoporphyria in Northern Ireland. *J Eur Acad Dermatol Venereol* 1992; **1**: 109-12.

132. Holme SA, Anstey AV, Finlay AY *et al*. Erythropoietic protoporphyria in the U.K.: clinical features and effect on quality of life. *Br J Dermatol* 2006; **155**: 574-81.

133. Parker M, Corrigall AV, Hift RJ *et al*. Molecular characterization of erythropoietic protoporphyria in South Africa. *Br J Dermatol* 2008; **159**: 182-91.

134. Lamola AA, Piomelli S, Poh-Fitzpatrick MG *et al*. Erythropoietic protoporphyria and lead intoxication: the molecular basis for difference in cutaneous photosensitivity. II. Different binding of erythrocyte protoporphyrin to hemoglobin. *J Clin Invest* 1975; **56**: 1528-35.

135. Schnait FG, Wolff K, Konrad K. Erythropoietic protoprophyria--submicroscopic events during the acute photosensitivity flare. *Br J Dermatol* 1975; **92**: 545-57.

136. Brun A, Sandberg S. Mechanisms of photosensitivity in porphyric patients with special emphasis on erythropoietic protoporphyria. *J Photochem Photobiol B* 1991; **10**: 285-302.

137. Shehade SA, Chalmers RJ, Prescott RJ. Predictable and unpredictable hazards of erythropoietic protoporphyria. *Clin Exp Dermatol* 1991; **16**: 185-7.

138. Fenton L, Ferguson J, Ibbotson S *et al*. Energy-saving lamps and their impact on photosensitive and normal individuals. *Br J Dermatol* 2013; **169**: 910-5.

139. Graham-Brown MP, Ilchyshyn A. Development of acute phototoxic reaction during surgery in a patient with erythropoietic protoporphyria. *Clin Exp Dermatol* 2013; **38**: 566-8.

140. Herbert A, Corbin D, Williams A *et al*. Erythropoietic protoporphyria: unusual skin and neurological problems after liver transplantation. *Gastroenterology* 1991; **100**: 1753-7.

141. Anstey AV, Hift RJ. Liver disease in erythropoietic protoporphyria: insights and implications for management. *Postgrad Med J* 2007; **83**: 739-48.

142. Casanova-Gonzalez MJ, Trapero-Marugan M, Jones EA *et al*. Liver disease and erythropoietic protoporphyria: a concise review. *World J Gastroenterol* 2010; **16**: 4526-31.

143. Barnes HD, Hurworth E, Millar JH. Erythropoietic porphyrin hepatitis. *J Clin Pathol* 1968; **21**: 157-9.

144. Bentley DP, Meek EM. Clinical and biochemical improvement following low-dose intravenous iron therapy in a patient with erythropoietic protoporphyria. *Br J Haematol* 2013; **163**: 289-91.

145. Todd DJ. Gallstones in children. *Am J Dis Child* 1991; **145**: 971-2.

146. Lecluse AL, Kuck-Koot VC, van WH *et al*. Erythropoietic protoporphyria without skin symptoms-you do not always see what they feel. *Eur J Pediatr* 2008; **167**: 703-6.

147. Poh-Fitzpatrick MB. The "priming phenomenon" in the acute phototoxicity of erythropoietic protoporphyria. *J Am Acad Dermatol* 1989; **21**: 311.

148. Doss MO, Frank M. Hepatobiliary implications and complications in protoporphyria, a 20-year study. *Clin Biochem* 1989; **22**: 223-9.

149. Minder EI, Haldemann AR, Schneider-Yin X. Exacerbation of erythropoietic protoporphyria by hyperthyroidism. *J Inherit Metab Dis* 2010; **33 Suppl 3**: S465-S469.

150. Schmidt H, Snitker G, Thomsen K *et al*. Erythropoietic protoporphyria. A clinical study based on 29 cases in 14 families. *Arch Dermatol* 1974; **110**: 58-64.

151. Poh-Fitzpatrick MB. Human protoporphyria: reduced cutaneous photosensitivity and lower erythrocyte porphyrin levels during pregnancy. *J Am Acad Dermatol* 1997; **36**: 40-3.

152. Bewley AP, Keefe M, White JE. Erythropoietic protoporphyria improving during pregnancy. *Br J Dermatol* 1998; **139**: 145-7.

153. Madu AE, Whittaker SJ. Erythropoietic protoporphyria in pregnancy. *J Obstet Gynaecol* 2006; **26**: 687-8.

154. Granick S. The structural and functional relationships between heme and chlorophyll. *Harvey Lect* 1948; **Series 44**: 220-45.

155. Bachem A, Reed CI. The penetration of light through human skin. *Am J Physiol* 1931; **97**: 86-91.

156. Anderson RR, Parrish JA. The optics of human skin. *J Invest Dermatol* 1981; **77**: 13-9.

157. Rimington C, Cripps DJ. Biochemical and Fluorescence-Mycroscopy Screening-Tests for Erythropoeietic Protoporphyria. *Lancet* 1965; **1**: 624-6.

158. Lau KC, Lam CW. Automated imaging of circulating fluorocytes for the diagnosis of erythropoietic protoporphyria: a pilot study for population screening. *J Med Screen* 2008; **15**: 199-203.

159. Castano AP, Demodiva TN, Hamblin MR. Mechanisms in photodynamic therapy: part one - photosenstizers, photochemistry and cellular localization. *Photodiagnosis Photodyn Ther* 2004; **1**: 279-93.

160. Schneider-Yin X, Minder EI. Erythropoietic Protoporphyria and X-Linked Dominant Protoporphyria . Ferreira, G. C. (29), 299-328. 2013. Singapure, World Scientific Publishing Company . Kadish, K. M., Simth, K. M., and Guilard, R.

161. Sarkany RP, Alexander GJ, Cox TM. Recessive inheritance of erythropoietic protoporphyria with liver failure. *Lancet* 1994; **344**: 958-9.

162. Mendez M, Poblete-Gutierrez P, Moran-Jimenez MJ *et al*. A homozygous mutation in the ferrochelatase gene underlies erythropoietic protoporphyria associated with palmar keratoderma. *Br J Dermatol* 2009; **160**: 1330-4.

163. Holme SA, Anstey AV, Badminton MN *et al*. Serum 25-hydroxyvitamin D in erythropoietic protoporphyria. *Br J Dermatol* 2008; **159**: 211-3.

164. Spelt JM, de Rooij FW, Wilson JH *et al*. Vitamin D deficiency in patients with erythropoietic protoporphyria. *J Inherit Metab Dis* 2010; **33 Suppl 3**: S1-S4.

165. Allo G, Garrido-Astrin M, de Salamanca RE *et al*. Bone mineral density and vitamin D levels in erythropoietic protoporphyria. *Endocrine* 2013; **44**: 803-7.

166. Gross U, Frank M, Doss MO. Hepatic complications of erythropoietic protoporphyria. *Photodermatol Photoimmunol Photomed* 1998; **14**: 52-7.

167. Bonkovsky HL, Schned AR. Fatal liver failure in protoporphyria. Synergism between ethanol excess and the genetic defect. *Gastroenterology* 1986; **90**: 191-201.

168. Bloomer JR. Pathogenesis and therapy of liver disease in protoporphyria. *Yale J Biol Med* 1979; **52**: 39-48.

169. Bloomer JR. The liver in protoporphyria. *Hepatology* 1988; **8**: 402-7.

170. Wahlin S, Stal P, Adam R *et al*. Liver transplantation for erythropoietic protoporphyria in Europe. *Liver Transpl* 2011; **17**: 1021-6.

171. Holme SA, Thomas CL, Whatley SD *et al*. Symptomatic response of erythropoietic protoporphyria to iron supplementation. *J Am Acad Dermatol* 2007; **56**: 1070-2.

172. Baker H. Erythropoietic protoporphyria provoked by iron therapy. *Proc R Soc Med* 1971; **64**: 610-1.

173. Milligan A, Graham-Brown RA, Sarkany I *et al*. Erythropoietic protoporphyria exacerbated by oral iron therapy. *Br J Dermatol* 1988; **119**: 63-6.

174. McClements BM, Bingham A, Callender ME *et al*. Erythropoietic protoporphyria and iron therapy. *Br J Dermatol* 1990; **122**: 423-4.

175. Lyoumi S, Abitbol M, Andrieu V *et al*. Increased plasma transferrin, altered body iron distribution, and microcytic hypochromic anemia in ferrochelatase-deficient mice. *Blood* 2007; **109**: 811-8.

176. Beguin Y. Soluble transferrin receptor for the evaluation of erythropoiesis and iron status. *Clin Chim Acta* 2003; **329**: 9-22.

177. Rufener EA. Erythropoietic protoporphyria: a study of its psychosocial aspects. *Br J Dermatol* 1987; **116**: 703-8.

178. Van den Keybus C, Laperre J, Roelandts R. Protection from visible light by commonly used textiles is not predicted by ultraviolet protection. *J Am Acad Dermatol* 2006; **54**: 86-93.

179. Frank J, Poblete-Gutierrez P. Delayed diagnosis and diminished quality of life in erythropoietic protoporphyria: results of a cross-sectional study in Sweden. *J Intern Med* 2011; **269**: 270-4.

180. Cox AM. Porphyria and vampirism: another myth in the making. *Postgrad Med J* 1995; **71**: 643-4.

181. Löffler G, Petrides P, Heinrich P. *Biochemie und Pathobochemie*, 8. edn. Springer, Berlin, 2007.

182. Weber U, Goerz G, Baseler H *et al*. [Canthaxanthin retinopathy. Follow-up of over 6 years]. *Klin Monatsbl Augenheilkd* 1992; **201**: 174-7.

183. Minder EI, Schneider-Yin X, Steuer J *et al*. A systematic review of treatment options for dermal photosensitivity in erythropoietic protoporphyria. *Cell Mol Biol (Noisy-le-grand)* 2009; **55**: 84-97.

184. Virtamo J, Taylor PR, Kontto J *et al*. Effects of alpha-tocopherol and beta-carotene supplementation on cancer incidence and mortality: 18-year postintervention follow-up of the Alpha-tocopherol, Beta-carotene Cancer Prevention Study. *Int J Cancer* 2014; **135**: 178-85.

185. Mathews-Roth MM, Rosner B. Long-term treatment of erythropoietic protoporphyria with cysteine. *Photodermatol Photoimmunol Photomed* 2002; **18**: 307-9.

186. Norris PG, Baker CS, Roberts JE *et al*. Treatment of erythropoietic protoporphyria with N-acetylcysteine. *Arch Dermatol* 1995; **131**: 354-5.

187. Bijlmer-Iest JC, Baart dlF, Van Asbeck BS *et al*. Protoporphyrin photosensitivity cannot be attenuated by oral N-acetylcysteine. *Photodermatol Photoimmunol Photomed* 1992; **9**: 245-9.

188. Warren LJ, George S. Erythropoietic protoporphyria treated with narrow-band (TL-01) UVB phototherapy. *Australas J Dermatol* 1998; **39**: 179-82.

189. Garcia-Martin P, De AD, To-Figueras J *et al*. Phototolerance induced by narrow-band UVB phototherapy in severe erythropoietic protoporphyria. *Photodermatol Photoimmunol Photomed* 2012; **28**: 261-3.

190. Harms J, Lautenschlager S, Minder CE *et al*. An alpha-melanocyte-stimulating hormone analogue in erythropoietic protoporphyria. *N Engl J Med* 2009; **360**: 306-7.

191. Key NS, Rank JM, Freese D *et al*. Hemolytic anemia in protoporphyria: possible precipitating role of liver failure and photic stress. *Am J Hematol* 1992; **39**: 202-7.

192. Wahlin S, Srikanthan N, Hamre B *et al*. Protection from phototoxic injury during surgery and endoscopy in erythropoietic protoporphyria. *Liver Transpl* 2008; **14**: 1340-6.

193. Bischoff-Ferrari HA, Can U, Staehelin HB *et al*. Severe vitamin D deficiency in Swiss hip fracture patients. *Bone* 2008; **42**: 597-602.

194. Rand EB, Bunin N, Cochran W *et al*. Sequential liver and bone marrow transplantation for treatment of erythropoietic protoporphyria. *Pediatrics* 2006; **118**: e1896-e1899.

195. Wahlin S, Aschan J, Bjornstedt M *et al*. Curative bone marrow transplantation in erythropoietic protoporphyria after reversal of severe cholestasis. *J Hepatol* 2007; **46**: 174-9.

196. Dowman JK, Gunson BK, Mirza DF *et al*. UK experience of liver transplantation for erythropoietic protoporphyria. *J Inherit Metab Dis* 2011; **34**: 539-45.

197. Eichbaum QG, Dzik WH, Chung RT *et al*. Red blood cell exchange transfusion in two patients with advanced erythropoietic protoporphyria. *Transfusion* 2005; **45**: 208-13.

198. Eefsen M, Rasmussen A, Wulf HC *et al*. Erythropoietic protoporphyria and pretransplantation treatment with nonbiological liver assist devices. *Liver Transpl* 2007; **13**: 655-7.

199. Wahlin S, Harper P. Pretransplant albumin dialysis in erythropoietic protoporphyria: a costly detour. *Liver Transpl* 2007; **13**: 1614-5.

200. Tewari A, Marsden J, Naik H *et al*. Oral cholestyramine is not an effective treatment for uncomplicated erythropoietic protoporphyria. *J Am Acad Dermatol* 2012; **67**: 1383-4.

201. Sperl J, Prochazkova J, Martasek P *et al*. N-acetyl cysteine averted liver transplantation in a patient with liver failure caused by erythropoietic protoporphyria. *Liver Transpl* 2009; **15**: 352-4.

202. Richard E, Robert-Richard E, Ged C *et al*. Erythropoietic porphyrias: animal models and update in gene-based therapies. *Curr Gene Ther* 2008; **8**: 176-86.

203. Oustric V, Manceau H, Ducamp S *et al*. Antisense oligonucleotide-based therapy in human erythropoietic protoporphyria. *Am J Hum Genet* 2014; **94**: 611-7.

204. Ejima Y, Yang L, Sasaki MS. Aberrant splicing of the ATM gene associated with shortening of the intronic mononucleotide tract in human colon tumor cell lines: a novel mutation target of microsatellite instability. *Int J Cancer* 2000; **86**: 262-8.

205. Ottini L, Falchetti M, Saieva C *et al*. MRE11 expression is impaired in gastric cancer with microsatellite instability. *Carcinogenesis* 2004; **25**: 2337-43.

206. Shi H, Bencze KZ, Stemmler TL *et al*. A cytosolic iron chaperone that delivers iron to ferritin. *Science* 2008; **320**: 1207-10.

207. Kashi Y, King DG. Simple sequence repeats as advantageous mutators in evolution. *Trends Genet* 2006; **22**: 253-9.

208. Zhou Y, Bizzaro JW, Marx KA. Homopolymer tract length dependent enrichments in functional regions of 27 eukaryotes and their novel dependence on the organism DNA (G+C)% composition. *BMC Genomics* 2004; **5**: 95.

209. Kniffen J. Protoporphyrin removal in intrahepatic porphyrastasis. *Gastroenterology* 1970; **58**: 1027.

210. Gordeuk VR, Brittenham GM, Hawkins CW *et al*. Iron therapy for hepatic dysfunction in erythropoietic protoporphyria. *Ann Intern Med* 1986; **105**: 27-31.

211. Kumar S, Bandyopadhyay U. Free heme toxicity and its detoxification systems in human. *Toxicol Lett* 2005; **157**: 175-88.

212. Lewis BP, Green RE, Brenner SE. Evidence for the widespread coupling of alternative splicing and nonsense-mediated mRNA decay in humans. *Proc Natl Acad Sci U S A* 2003; **100**: 189-92.

213. Webby CJ, Wolf A, Gromak N *et al*. Jmjd6 catalyses lysyl-hydroxylation of U2AF65, a protein associated with RNA splicing. *Science* 2009; **325**: 90-3.

214. Boeckel JN, Guarani V, Koyanagi M *et al*. Jumonji domain-containing protein 6 (Jmjd6) is required for angiogenic sprouting and regulates splicing of VEGF-receptor 1. *Proc Natl Acad Sci U S A* 2011; **108**: 3276-81.

VIII. ORIGINAL PUBLICATIONS

I. Variations in the length of poly-C and poly-T tracts in intron 3 of the human ferrochelatase gene.
Barman J, Schneider-Yin X, Mamet R, Schoenfeld N, Minder EI.
Cellular and molecular biology (Noisy-le-Grand, France) 55.2 (2009): 102-110.

II. Iron availability modulates aberrant splicing of ferrochelatase through the iron-and 2-oxoglutarate dependent dioxygenase Jmjd6 and U2AF^{65}.
Barman-Aksözen J, Béguin C, Dogar A.M, Schneider-Yin X, Minder EI.
Blood Cells, Molecules, and Diseases 51.3 (2013): 151-161.

IV. In ferrochelatase-deficient protoporphyria patients, ALAS2 expression is enhanced and erythrocytic protoporphyrin-concentration correlates with iron availability.
Barman-Aksözen J, Minder EI, Schubiger C, Biolcati G, Schneider-Yin X.
Blood Cells, Molecules, and Diseases 54.1 (2015): 71-77.

Cellular and Molecular Biology ™ **55**, N°2, 102-110
DOI 10.1170/T859

ISSN 1165-158X
2009 Cell. Mol. Biol.™

VARIATIONS IN THE LENGTH OF POLY-C AND POLY-T TRACTS IN INTRON 3 OF THE HUMAN FERROCHELATASE GENE

J. BARMAN[1], X. SCHNEIDER-YIN[1], R. MAMET[2], N. SCHOENFELD [2,3], E. I. MINDER[1]

[1]Zentrallabor, Stadtspital Triemli, Birmensdorferstrasse 497, 8063 Zurich, Switzerland
Fax: +41 44 466 2744; E-mail: elisabeth.minder@triemli.stzh.ch
[2] National Laboratory for the Biochemical Diagnoses of Porphyrias, Rabin Medical Center, Beilinson Hospital, Petah-Tikva, Israel
[3] Department of Human Molecular Genetics and Biochemistry, The Sackler Faculty of Medicine, Tel Aviv University, Tel Aviv, Israel
E.L. Minder : Zentrallabor, Stadtspital Triemli, Birmensdorferstrasse 497, 8063 Zurich, Switzerland Fax: +41 44 466 2744; Email:elisabeth.minder@triemli.stzh.ch

Received, March 30th 2009; Accepted May 5th, 2009; Published July 1st, 2009

Abstract – The third intron of human ferrochelatase (FECH) gene contains according to NCBI, a poly-C (11) and a poly-T (24) tracts which are located approximately 900 bp upstream from the known splice modulating SNP IVS3-48 c/t. Ferrochelatase catalyses the last step in heme biosynthesis and a deficiency of this enzyme results in the hereditary disorder of erythropoietic protopoprhyria (EPP). During the course of mutation analysis in the *FECH* gene among EPP patients, we observed variations in the length of the poly-C and poly-T tracts. To study these variations, we analyzed a total of 54 individuals of Swiss and Israeli origins. Among them, 37 were control subjects (23 individuals with the genotype t/t and 14 with the genotype c/t), 10 were unrelated EPP patients (genotype c/M) and 7 were unrelated asymptomatic mutation carriers (genotype t/M). The length of poly-C tract varied from 10 to 16, that of poly-T tract from 22 to 24 in the study cohort. Statistic analysis showed that the low-expressed FECH allele (IVS3-48c) is associated with poly-C12, C13 and C15 and poly-T22. In addition, the segregation of poly-C and poly-T tracts was studied in two Israeli EPP families. Instabilities, as seen by both insertion and deletion of one nucleotide between two generations, were observed only in the poly-T tract. The function of the poly-C and poly-T tracts are yet to be explored.

Key words:

INTRODUCTION

Erythropoietic protoporphyria (EPP, OMIM#177000) is a hereditary disorder of the heme biosynthetic pathway. The affected enzyme ferrochelatase (FECH, EC 4.99.1.1) catalyzes the insertion of iron into protoporphyrin IX to form heme. As the result of ferrochelatase deficiency, a large amount of protoporphyrin accumulates in the body and is responsible for the clinical symptoms of cutaneous photosensitivity in EPP patients (1). In approximately 93% of the cases, EPP patients carry a c/M genotype i.e., a mutated FECH allele (M) *in trans* to a low-expressed allele. This low allele is characterized by a c-variant (c) at a polymorphic site in intron 3 (IVS3-48 c/t). The resulting enzyme activity in patients is ~35% of that of normal individuals. Individuals with a t/M genotype i.e., a combination of a normal IVS3-48t allele (t) with an M allele, show a 50% reduction in the enzyme activity, without clinical symptoms of EPP. Both t/t and c/t genotypes present neither biochemical nor clinical signs of EPP (4). About 4% of the EPP cases are recessive with one mutation on each of the two FECH alleles. Another 3% of the cases are the so called variant EPP in which deletions in the 5-aminolevulinate synthase 2 (ALAS2) gene were found (11).

The third intron of human ferrochelatase (FECH) gene contains a poly-C and a poly-T tract which are located approximately 900 bp upstream from IVS3-48. According to the sequence data from NCBI, the length of these tracts are 11 for poly-C and 24 for poly-T (accession number NT025028). During the course of mutation analysis in the *FECH* gene

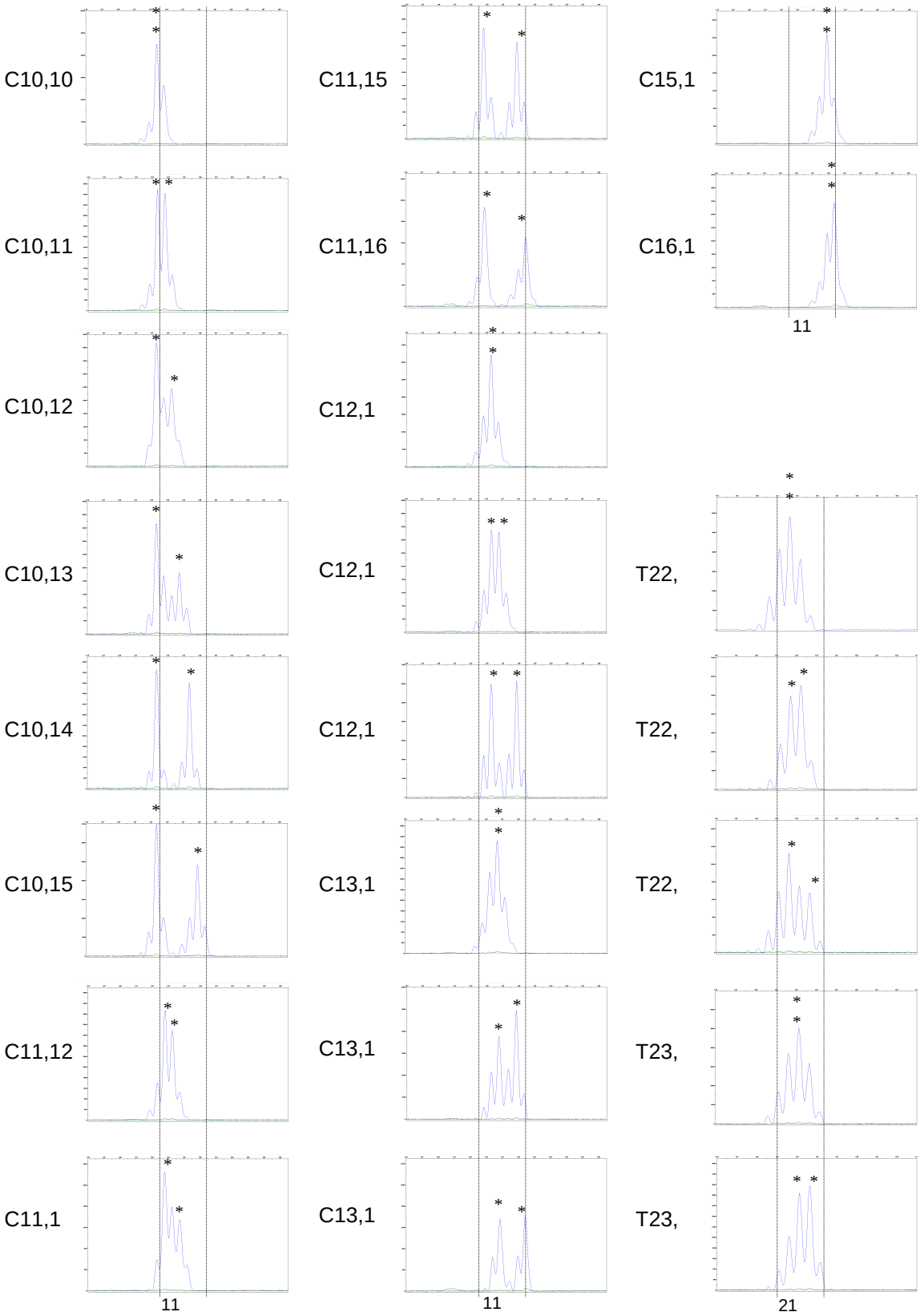

Figure 1. Examples of electropherograms showing various poly-C and poly-T alleles. The alleles are indicated by asterisks (*). The vertical lines align identical peaks among different electropherograms.

Table 1 Information on the study cohort of 54 unrelated individuals

Origin	Genotype t/t	t/M	c/t	c/M
Swiss	**9** (unrelated controls)	**5** (from unrelated EPP families)*	**5** (unrelated controls)	**10** (from unrelated EPP families)*
Israeli	**10** (unrelated controls) **4** (unrelated family members: individual 3 and 4 from *Family 1*; individual 3 and 7 from *Family 2*; see Fig.2)	**2** (unrelated family members: individual 2 from *Family 1*; individual 2 from *Family 2*)	**8** (unrelated controls) **1** (individual 1 from *Family* 1)	-
total	**23**	**7**	**14**	**10**

* The individuals are not related to each other.

Table 2 Distribution of poly-C alleles among EPP patients, carriers and control subjects (n= 54)

Length	Genotype t/t and t/M			Genotype c/t and c/M			calculated frequency (%)*	
of polyC	t/t	t/M	t/t & t/M	c/t	c/M	c/t & c/M	t	Diff c-t
C10	11	3	14	1	0	1	23.3	-21.3
C11	7	1	8	0	0	0	13.3	-13.3
C12	9	5	14	14	12	26	23.3	30.8
C13	7	2	9	6	6	12	15.0	10.0
C14	2	1	3	0	0	0	5.0	-5.0
C15	9	1	10	7	2	9	16.7	2.1
C16	1	1	2	0	0	0	3.3	-3.3
sum	**46**	**14**	**60**	**28**	**20**	**48**	**100**	**0**

* The frequency of t-associated alleles was based on the frequency observed in the combined M/t and t/t genotypes; the difference c-t was calculated from the observed frequency in the c/t and M/c genotype after subtraction of the frequency of the (t/t and M/t) genotype. For example, for the C10 allele, the calculated t allele frequency equals 14/60 x 100% = 23.3; Diff c-t = (1/48 x 100%) – 23.3 = -21.3. Positive numbers indicate over-representation and negative under representation of these alleles in the c/t genotype assuming an identical distribution of poly-C alleles in the t/t and c/t genotype.

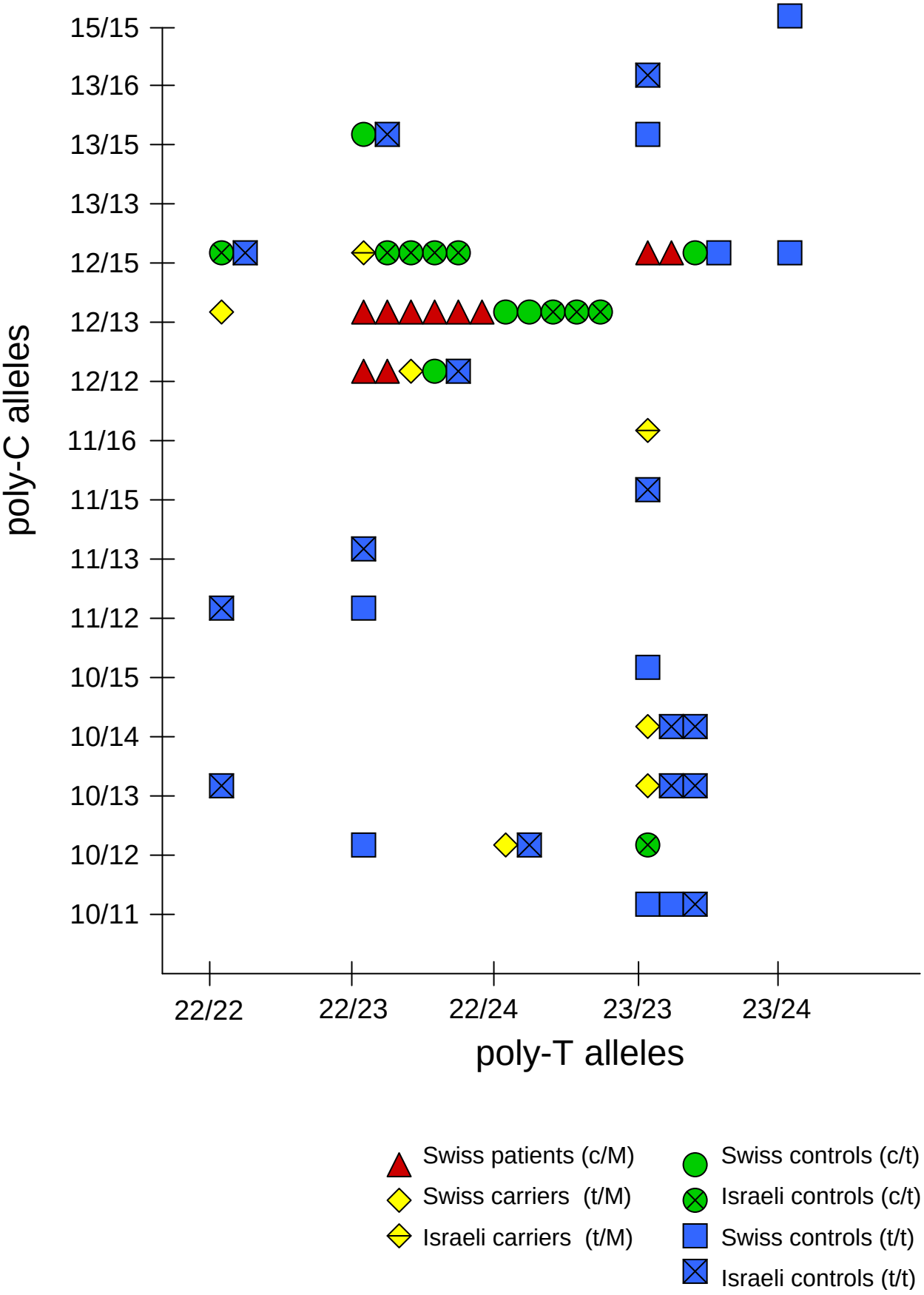

Figure 2. Genotypes of poly-C and poly-T tracts from 54 unrelated individuals of EPP patients, carriers and of control subjects.

among EPP patients, we observed variations in the length of the poly-C and poly-T tracts. In this study, we analyzed these variations among individuals with the four above-mentioned genotypes, t/t, c/t, t/M and c/M.

MATERIALS AND METHODS

Study cohort

A cohort of 54 unrelated individuals including EPP patients, carriers and control subjects was studied. The detailed information on the individuals included, of both Swiss and Israeli origins is given in Table 1. None of the individuals shared any alleles with another individual within this cohort. In addition, two previously published Israeli EPP families and 5 Swiss EPP families were analyzed (8,9, Fig.3, Table 4). All EPP patients and carriers had documented mutations in the *FECH* gene.

Analysis of poly-C and poly-T tracts

Genomic DNA from each individual was amplified by PCR using fluorescence labeled primers. For amplification of the poly-C tract, primers 5'-FAM-CCT TGC ACT CCC AGT TAT C-MGB-3' and 5'-TAC CTT CAC ATT TGT GTA ACG-3' were used. And for amplification of the poly-T tract, primers 5'-FAM-TCG TTA CAC AAA TGT GAA GGT-MGB-3' and 5'-GGA GGG ATG GCA TTA GGA-3' were used. The lengths of the PCR products were analyzed on the ABI Prism 310 genetic analyzer (Applied Biosystems, Foster City, California, USA). To determine the number of "C"s and "T"s in the poly-C and poly-T tracts, the electropherograms of probands were compared with that of "markers". These markers were generated by cloning of the non-fluorescent PCR products from a control subject into pBluescript. The number of "C"s or "T"s in individuals clones was determined by sequencing. Three poly-C clones, C10, C12 and C13, and three poly-T clones, T19, T21 and T22, were obtained. Purified plasmid DNA from the each of the six clones were amplified with fluorescence labeled primers before being analyzed on the ABI Prism 310 genetic analyzer.

Analysis of the IVS3-48c/t polymorphism was performed as previously described (9).

Statistical analysis

Non-identity of the distribution of the variable poly-C and poly-T tracts among the polymorphic IVS3-48 alleles was tested by Chi-square test including Monte Carlo simulation of the multinomial sampling distribution (http://faculty.vassar.edu/lowry/VassarStats.html).

RESULTS

Identification of different poly-C and poly-T genotypes

The analysis of the 54 unrelated individuals and members of the seven Israeli and Swiss EPP families, identified a total of 18 different poly-C and 5 different poly-T genotypes. As shown in Figure 1, the electropherogram of each genotype consists of one or two major peaks that are surrounded by a number of stutter peaks. Due to overlapping between major and stutter peaks, the assignment of individual alleles in each electropherogram was only possible with the help of "markers". As described in the Materials and Methods section, these "markers" were made from poly-C and poly-T clones with a known number of the respective nucleotides.

Distribution of poly-C and poly-T among genotypes t/t, M/t, c/t and c/M

The 54 unrelated individuals carried different genotypes with respect to IVS-48 i.e., 23 individuals with the t/t genotype, 7 with the t/M genotype, 14 with the c/t genotype and 10 with c/M genotype (Table 1). Among them, all individuals with the M/t and c/M genotypes were selected from different EPP families.

The poly-C and poly-T genotypes of the 54 unrelated individuals were assigned according to the electropherograms shown in Figure 1. Among the 108 alleles of this cohort, seven different poly-C alleles, C10 to C16, and three different poly-T alleles, T22, T23 and T24, were identified. The allelic distribution of poly-C and poly-T among the four IVS-48 genotypes are shown in Table 2 and Table 3, respectively.

To obtain an overview on the genotype distribution among the 54 individuals, the poly-C genotype (a combination of two poly-C alleles) from each individual was plotted against the poly-T genotype (a combination of two poly-T alleles) (Figure 2). Except for C10/10 and C16/16, the remaining 16 poly-C genotypes (see Figure 1) were found among the 54 individuals. All five poly-T genotypes (see Figure 1) were observed among the 54 individuals. Variations in poly-C among EPP patients (genotype c/M, n= 10) differ significantly from the control group (genotype t/t, n=23; $p<0.001$). However, no statistically significant difference was found in poly T ($p=0.23$).

Poly-C and poly-T in the low-expressed FECH allele

To study the relationship between low-expressed *FECH* allele (IVS3-48c) and poly-C/poly-T tracts, the results in Table 2 and 3 were analyzed by chi-square test separately. Since both genotype t/M and t/t are in fact homozygous t/t at IVS3-48, the poly-C/poly-T results from these two genotypes were combined (see column "t/t & t/M" in Table 2 and 3). Likewise, c/t individuals were combined with c/M individuals (see column "c/t & c/M" in Table 2 and 3). Chi-square test was then performed in these data sets.

Table 3 Distribution of poly-T alleles among EPP patients, carriers and control subjects (n=54)

Length	Genotype t/t and t/M			Genotype c/t and c/M			calculated frequency (%)*	
of polyT	t/t	t/M	t/t & t/M	c/t	c/M	c/t & c/M	t	Diff c-t
T22	12	5	17	13	8	21	28.3	15.4
T23	31	7	38	15	12	27	63.3	-7.1
T24	3	2	5	0	0	0	8.3	-8.3
sum	**46**	**14**	**60**	**28**	**20**	**48**	**100**	**0**

*see table 2.

Table 4 Haplotypes of the IVS3-48c allele in seven Swiss and Israeli EPP families

Haplo-types	EPP families							
	A	B	C	Israeli 2(1)	Israeli 1	D	E	Israeli 2(2)
poly-C	12	12	12	13	12	12	13	13
poly-T	22	22	22	22	23	23	23	23
IVS3-48	c	c	c	c	c	c	c	c

Swiss families: A, B, C, D and E (one member of families A and E with genotype t/M are included in Table 1; one member of families B, C and D with genotype c/M are included in Table 1);
Israeli 1: *Family 1* in Figure 2;
Israeli 2 (1): the first "c" allele in individual 1 of *Family 2* (see Figure 2);
Israeli 2 (2): the second "c" allele in individual 1 of *Family 2* (see Figure 2).

The results showed that the distribution of poly-C alleles was significantly different between the t/t genotype (including M/t) and the c/t genotype (including (M/c) (p<0.0001). The calculated frequency of different poly-C alleles based on the frequency observed in the t/t genotypes showed that in the c/t genotype, C12, C13 and C15 were more frequent and the other alleles were less frequent than expected (Table 2). With the same approach, T22 was found to be associated with the IVS3-48c allele (c) (p<0.0149; Table 3).

To verify the results of chi-square test, haplotyping analysis was performed among the seven Israeli and Swiss EPP families. Eight different "poly-C/poly-T/IVS3-48c" haplotypes were resolved including two from Israeli *Family 1* (Table 4, Figure 3). Among these eight haplotypes, C12 and C13 appeared 5 and 3 times, respectively. This result is consistent with that of chi-square test. On the other hand, T22 and T23 both appeared 4 times among the eight haplotypes, although the chi-square test only indicated an association between T22 and the low-expressed allele (c).

DISCUSSION

PCR amplification of mononucleotide repeat artificially introduces insertions and/or deletions within the repeat which give rise to a mixture of products in different lengths (2). As we experienced, sequencing of such a mixture of PCR products does not produce any informative results. To overcome this analytical difficulty, we amplified the poly-C and poly-T by PCR using fluorescently labeled primers and analyzed the products by capillary electrophoresis. However, the PCR products - a mixture as they remain, appear as complex patterns in the electropherograms. Each of the electropherogram contains one or two major peaks representing homo- or heteroallele in diploids such as human. The identification of heteroalleles (major peaks) could be hampered by the presence of stutter peaks (PCR artifacts). With respect to the poly-C tract, heteroalleles can be readily recognized if the length difference between the two alleles is $\geq$ 3 nucleotides (examples are C10,13, C10,14, C10,15, C11,15, C11,16, C12,15, C13,16 in Figure 1). With the help of "markers", we were

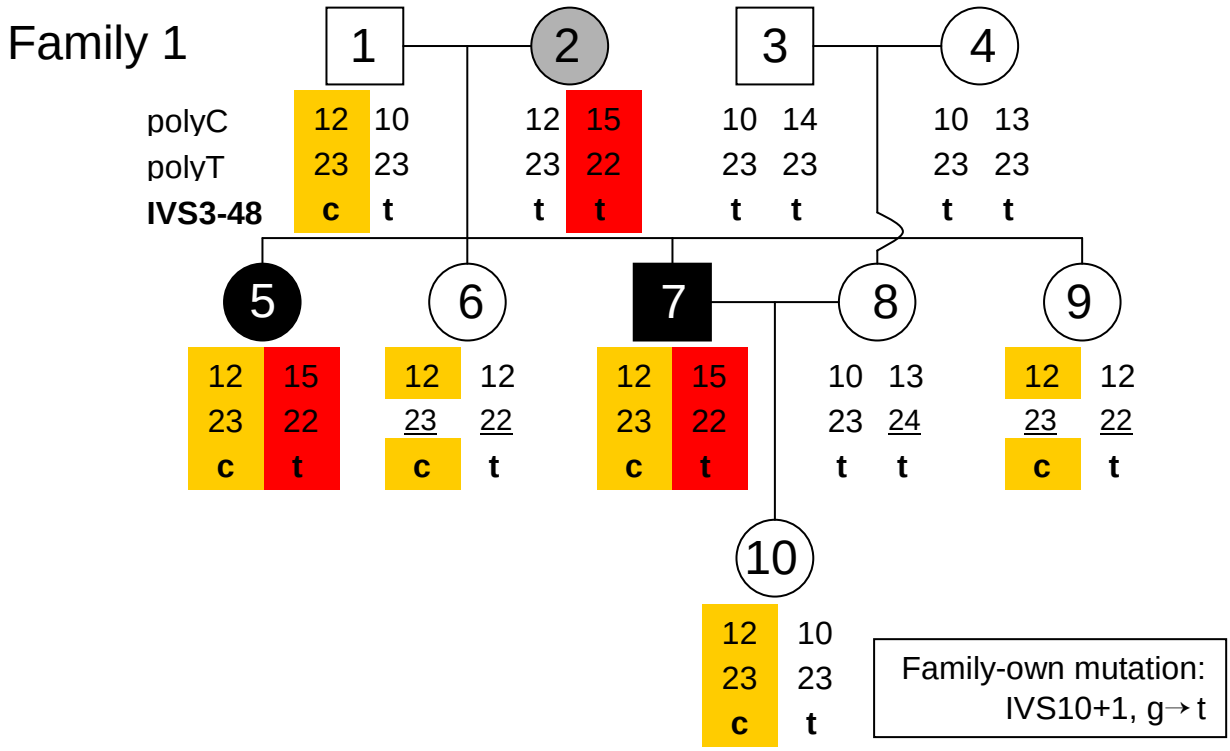

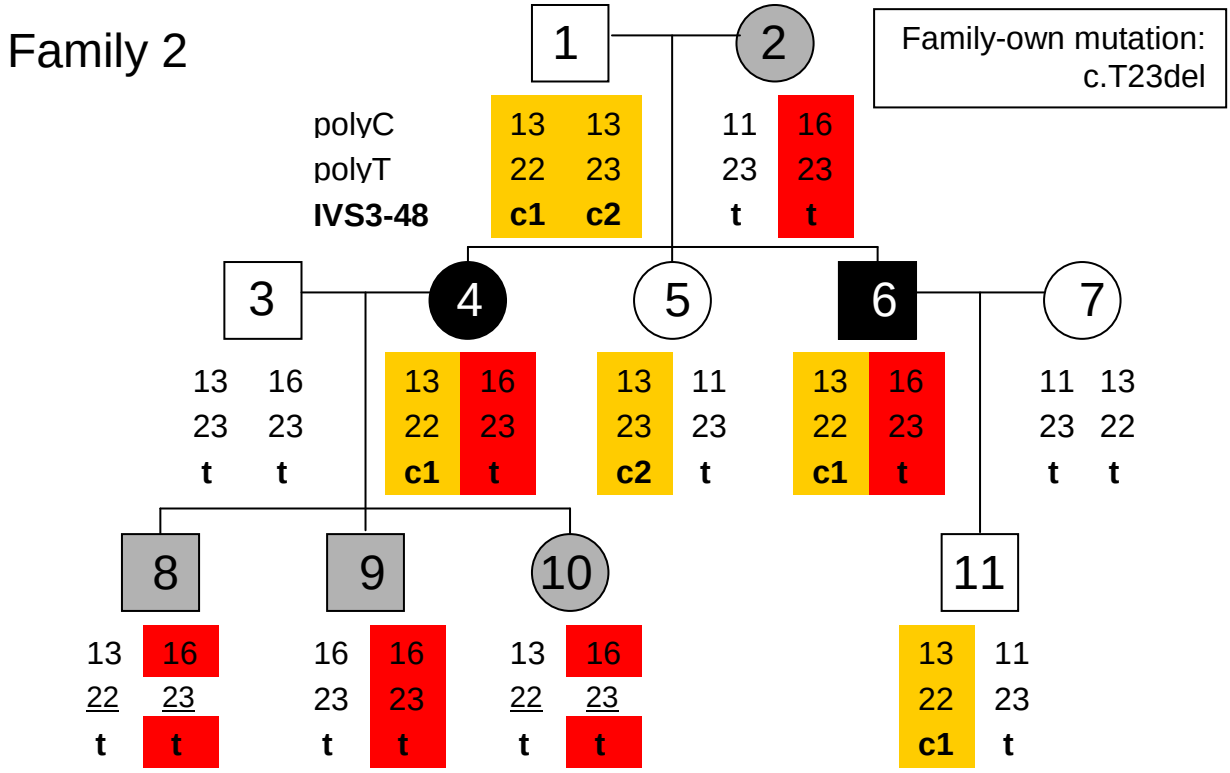

Figure 3. Segregation of poly-C, poly-T and IVS3-48c/t in two Israeli EPP families. The mutated and low-expressed FECH alleles are highlighted in *red* and *yellow*, respectively. Changes, either insertion or deletion, in the length of poly-T tract between two generations are underlined. In *Family 2*, two different IVS3-48 c alleles are represented by *c1* and *c2*, respectively.

able to assign the remaining homo- and heteroalleles.

In the poly-T tract, a difference of only one nucleotide between two alleles has been observed in the study subjects. The identification of different genotypes was made possible with the help of "markers" (Figure 1). Another observation on the poly-T tract is its instability between two generations. As shown in Figure 3, both deletion and insertion of a single T occurred in the two Israeli families (underlined numbers).

In a recent publication by Thompson and Salipante, the authors demonstrated the use of a software, named PeakSeeker, in genotyping of mononucleotide tracts (10). A computer algorithm such as PeakSeeker, could facilitate the interpretation of genotypes of mononucleotide repeats and thereby permits a more widely use of this type of highly informative markers in genetic research.

Based on both haplotypic and phylogenic analyses, Gouya et al came to a conclusion that the low-expressed IVS3-48c allele (c) arose from a single recent mutational event that occurred on the normal *FECH* allele IVS3-48t (t) some 40,000 to 60,000 years ago (4). The finding of this study supported the notion of IVS3-48c being a younger haplotype compared to IVS3-48t. As visualized in Figure 2, genotypes encompassing an IVS3-48c allele i.e., c/M and c/t shown in red and green symbols, respectively, are located closely to each other. In contrast, the blue and yellow symbols representing genotypes t/t and t/M, respectively, are more widely spread. The genotype distribution, as well as the result of the statistical analysis, suggest that the IVS3-48c haplotype is associated with fewer variations in the poly-C and poly-T tract compared to the IVS3-48t haplotype. The fewer variations were compatible with less meiotic or replicative modifications due to the younger age. The fewer variations could be further interpreted by the fact that the poly-C and poly-T tracts are located in a close vicinity to IVS3-48. According to a study of Gouya et al, the IVS3-48c variant is located within an extended haplotype [GGTA] spanning from the 5' noncoding region (-3670A/G) to intron 4 (IVS4-1197C/A) (5). The finding of the associated poly-C and poly-T alleles fit within this haplotype.

Deletions in the poly-T tract resulting in aberrant splicing, have been observed in cancer related genes such as *ATM* and *MRE 11* (3,7). The instability of poly-T tract has therefore been suggested to play a role in the development of cancer. In general, homopolymer tracts are significantly over-represented and more widely spread in the genome than simply by chance (6,12). However, any possible functions of the poly-C and poly-T tracts of the *FECH* gene in the low expression mechanism remain to be studied.

REFERENCES

1. Anderson K.E., Sassa S., Bishop D., Desnick R.J., Disorders of heme biosynthesis: X-linked sideroblastic anemia and the porphyrias. In Scriver CR, Beaudet AL, Sly WS, Valle D, eds. *The Metabolic and Molecular Basis of Inherited Disease* Ed 8, McGraw-Hill, New York, NY, 2991-3062, 2001.

2. Clarke L.A., Rebelo C.S., Gonçalves J., Boavida M.G., Jordan P., PCR amplification introduces errors into mononucleotide and dinucleotide repeat sequences. *Mol. Pathol*. 2001, **54**: 351-353.

3. Ejima Y., Yang L., Sasaki M.S., Aberrant splicing of the ATM gene associated with shortening of the intronic mononucleotide tract in human colon tumor cell lines: a novel mutation target of microsatellite instability. *Int. J. Cancer* 2000, **86**: 262-268.

4. Gouya L., Martin-Schmitt C., Robreau A.M., Austerlitz F., Da Silva V., Brun P., Simonin S., Lyoumi S., Grandchamp B., Beaumont C., Puy H., Deybach J.C., Contribution of a common single-nucleotide polymorphism to the genetic predisposition for erythropoietic protoporphyria. *Am. J. Hum. Genet.* 2006, **78**: 2-14.

5. Gouya L., Puy H., Robreau A.M., Bourgeois M., Lamoril J., Da Silva V., Grandchamp B., Deybach J.C., The penetrance of dominant erythropoietic protoporphyria is modulated by expression of wildtype FECH. *Nat, Genet*. 2002, **30**: 27-28.

6. Kashi Y., King D.G., Simple sequence repeats as advantageous mutators in evolution. *Trends Genet*. 2006, **22**: 253-259.

7. Ottini L., Falchetti M., Saieva C., De Marco M., Masala G., Zanna I., Paglierani M., Giannini G., Gulino A., Nesi G., Mariani Costantini R., Palli D., MRE11 expression is impaired in gastric cancer with microsatellite instability. *Carcinogenesis*. 2004, **25**: 2337-2343.

8. Schneider-Yin X., Mamet R., Minder E.I., Schoenfeld N., Biochemical and molecular diagnosis of erythropoietic protoporphyria in an Ashkenazi Jewish family. *J. Inherit. Metab. Dis.* 2008 Aug 31. [Epub ahead of print]

9. Schoenfeld N., Mamet R., Minder E.I., Schneider-Yin X., A "null allele" mutation is responsible for erythropoietic protoporphyria in an Israeli patient who underwent liver transplantation: relationships among biochemical, clinical, and genetic parameters. *Blood Cells Mol. Dis.* 2003, **30**: 298-301.

10. Thompson J.M., Salipante S.J., PeakSeeker: a program for interpreting genotypes of mononucleotide repeats. *BMC Res. Notes*. 2009, Feb 3;2(1):17. [Epub ahead of print]

11. Whatley SD, Ducamp S, Gouya L, Grandchamp B, Beaumont C, Badminton MN, Elder GH, Holme SA, Anstey AV, Parker M, Corrigall AV, Meissner PN, Hift RJ, Marsden JT, Ma Y, Mieli-Vergani G, Deybach JC, Puy H, C-terminal deletions in the ALAS2 gene lead to gain of function and cause X-linked dominant protoporphyria without anemia or iron overload. *Am. J. Hum. Genet.* 2008, **83**: 408-14.

12. Zhou Y., Bizzaro J.W., Marx K.A., Homopolymer tract length dependent enrichments in functional regions of 27 eukaryotes and their novel dependence on the organism DNA (G+C)% composition. *BMC Genomics*. 2004, **5**: 95.

Blood Cells, Molecules and Diseases 51 (2013) 151–161

Contents lists available at ScienceDirect

Blood Cells, Molecules and Diseases

journal homepage: www.elsevier.com/locate/bcmd

Iron availability modulates aberrant splicing of ferrochelatase through the iron- and 2-oxoglutarate dependent dioxygenase Jmjd6 and U2AF^{65}

Jasmin Barman-Aksözen [a,b], Chantal Béguin [a], Afzal M. Dogar [c], Xiaoye Schneider-Yin [a], Elisabeth I. Minder [a,*]

[a] Institute of Laboratory Medicine, Stadtspital Triemli, Zurich, Switzerland
[b] Institute of Laboratory Animal Science, University of Zurich, Zurich, Switzerland
[c] Department of Chemistry and Applied Biosciences, Institute of Pharmaceutical Sciences, The Swiss Federal Institute of Technology, Zurich, Switzerland

ARTICLE INFO

Article history:
Submitted 19 December 2012
Revised 20 March 2013
Available online 18 June 2013

(Communicated by J.T. Prchal, M.D., 12 May 2013)

Keywords:
Aberrant splicing
Ferrochelatase
Iron
Jmjd6
U2AF^{65}

ABSTRACT

Erythropoietic protoporphyria (EPP) results from partial deficiency of ferrochelatase (FECH). Genetically, EPP patients differ from asymptomatic mutation carriers at the unmutated FECH allele, the expression of which is modulated by single nucleotide polymorphism IVS3-48C/T. The IVS3-48C genotype, which is present among patients, leads to correct splicing of 60% of the pre-mRNA and to alternative splicing of 40%, the latter mRNA-product being destroyed by nonsense-mediated decay. An IVS3-48T genotype generates 80% correct and 20% aberrant products. Our study demonstrated that under iron deficient conditions, the aberrant splice product was increased to 56% and 50% of total FECH mRNA in erythroleukemic K562 and lymphoblastoid cell lines, respectively, both being homozygous for IVS3-48T. Concomitantly, FECH protein was decreased. Iron deficiency had less effect on the FECH splice ratio in an IVS3-48C/C lymphoblastoid cell line. Effects similar to iron deficiency were generated by siRNA knockdown of either splicing factor U2AF^{65} or Fe(II)- and 2-oxoglutarate-dependent dioxygenase Jumonji domain-containing protein 6 (Jmjd6), which interacts with U2AF^{65} by lysyl-hydroxylation. Based on these results, we propose that the availability of iron, a co-factor of Jmjd6, modulates U2AF^{65}-lysyl-hydroxylation. This in turn, influences the relative amounts of correct and aberrant FECH mRNA splice products and thus, regulates the FECH enzyme activity.

Introduction

Ferrochelatase (FECH), the last enzyme of the heme biosynthesis pathway, catalyzes the insertion of ferrous iron into the heme precursor, protoporphyrin IX (PPIX). A partial deficiency of ferrochelatase causes erythropoietic protoporphyria (EPP, OMIM 177000), an inherited disorder which is characterized by painful photosensitivity due to the accumulation of PPIX in the skin. Intron 3 of the ferrochelatase pre-mRNA can be either correctly spliced or alternatively spliced at an aberrant site located 63 bp upstream from the correct splice site (IVS3-63). The aberrant splicing results in an mRNA product which contains an additional 63 bp intronic sequence. Due to the presence of a premature termination codon (PTC) within this insertion, the aberrant splice product is subjected to nonsense mediated decay (NMD) and does not serve as a template for protein synthesis. In a minigene assay, it was found that a single nucleotide polymorphism (SNP) at position −48 of intron 3 determines the relative amount of normal and aberrant splice products [13]. If a T is present at the −48 position (IVS3-48T), the more frequent genotype in the general population, 10 to 20% of the FECH pre-mRNA is aberrantly spliced. In an IVS3-48C genotype, however, the amount of aberrant splice product is increased to 30–40% of the total transcripts. The combination of IVS3-48C *in trans* to a deleterious mutation in the *FECH* gene causes EPP, whereas individuals having an IVS3-48T allele *in trans* to a mutated ferrochelatase allele are asymptomatic [12].

The promoter region of human *FECH* gene contains sequences for recognition of both ubiquitous Sp1 family of transcription factors, as well as for erythroid-specific *trans*-acting factors NF-E2 and GATA-1 [43]. Regulation of ferrochelatase occurs at the transcriptional level, in that the Sp1-driven promoter with a minimal size of 150-bp directs expression of the *FECH* gene in all types of cells, and the erythroid-specific promoter (approximately 4 kb in size) controls upregulation of ferrochelatase during erythropoiesis [31]. The C-terminus of ferrochelatase contains 4 cysteine residues arranged in a sequence (C-X_7-C-X_2-C-X_4-C), which is a fingerprint for a [2Fe–2S] binding motif [6]. Mutations in these cysteine residues were associated with EPP [38]. However, the exact role of this Fe–S cluster in the enzyme reaction remains unclear [2].

Cellular iron storage and uptake are coordinately regulated post-transcriptionally by iron-regulatory proteins 1 and 2 (IRP-1 and IRP-2). When iron supply is limited, IRP blocks the translation of ferritin mRNA and stabilizes the mRNA of transferrin receptor by binding to iron-responsive elements in these mRNAs. The regulatory mechanism ensures an adequate supply of iron for the synthesis of hemoproteins and other

* Corresponding author at: Stadtspital Triemli, Institute of Laboratory Medicine, Birmensdorferstrasse 497, CH-8063 Zürich, Switzerland. Fax: +41 44 466 2709.
E-mail address: elisabeth.minder@triemli.zuerich.ch (E.I. Minder).

1079-9796/$ – see front matter © 2013 Elsevier Inc. All rights reserved.
http://dx.doi.org/10.1016/j.bcmd.2013.05.008

iron-containing molecules and at same time, prevents iron overload which is hazardous for the organism [34].

A regulatory function of alternative splicing with a PTC, termed regulated unproductive splicing and translation (RUST), has been described in a number of other genes [27]. The biosynthesis of heme is tightly regulated since its intermediary porphyrins as well as the end product heme are toxic to the organism if present in excess (reviewed in references [2,24,25]). Is the alternative splicing of intron 3 of the *FECH* gene, and therefore the amount of ferrochelatase enzyme, regulated? To study this possibility, we conducted *in vitro* experiments in cultured cells and demonstrated that iron, a substrate of ferrochelatase, has an influence on the amounts of correct and aberrant transcripts of the *FECH* gene as well as on the level of ferrochelatase protein. We also explored the mechanism by which iron regulates splicing of intron 3 of the *FECH* gene.

Experimental procedures

Mutational analysis and genotyping among EPP patients and healthy donors

Mutational analysis in the *FECH* gene and genotyping of IV3-48C/T were performed among eight EPP patients in connection with the porphyria diagnosis to which all patients gave their informed consent. Informed consent was also obtained from eight healthy donors with regard to the testing of IVS3-48C/T. Peripheral blood samples were obtained from all individuals. DNA isolation, PCR amplification and sequence analysis were performed as previously described [37].

Seven of the EPP patients were heterozygous for one of following mutations, *p*.Q59X, 212–213 ins T, 580–584delTACAG and *p*.S151P. No mutation was found in the coding exons and exon–intron boundaries of the *FECH* gene of one EPP patient although both clinical and biochemical evidences were sufficient to support the EPP diagnosis in this patient (Supplementary Table). All EPP patients were heterozygous for IVS3-48C/T, whereas all healthy donors were homozygous for IVS3-48T/T.

Establishing lymphoblastoid cell lines

Additional blood samples were collected from one of the EPP patients, who carried the p.Q59X mutation *in trans* to IVS3-48C (genotype M/C) and from one of the healthy donors (genotype T/T). *p*.Q59X is the most frequent mutation in Switzerland [39]. This null-allele mutation is located in exon 2 of the *FECH* gene. A blood sample was also collected from another individual who was homozygous for IVS3-48C/C (genotype C/C) after informed consent. Lymphoblastoid cell lines were established from these three individuals by transformation of the mononuclear cells with EBV according to a standard procedure [8].

All studies involving human subjects were approved by our local ethics committee.

Cell culture

EBV-immortalized human lymphoblastoid cell lines and the human erythroleukemic K562 cell line (American Type Culture Collection) were cultured in RPMI 1640 medium (Gibco, Invitrogen, Carlsbad, California, USA) supplemented with 10% fetal calf serum (Bioconcepts Amimed, Allschwil, Switzerland) and streptomycin/penicillin (Gibco, Invitrogen) at 37 °C under 5% CO_2. The cells were split 1:5 every third day to maintain an exponential growth phase. In each experiment, one million cells were seeded in 6-well cluster plates. Upon addition of different chemical substances, the cells were incubated for 24 h, 48 h or 60 h.

Chemicals

Both deferoxamine mesylate salt (DFO) and ferric ammonium citrate (FAC; ammonium iron (III) citrate) were purchased from Sigma-Aldrich (St. Louis, Missouri, USA); dimethyloxalylglycine (DMOG) from Bio-Science Products (Buchs, Switzerland) and 1,2-dimethyl-3-hydroxy-4-pyridone (deferiprone) from ACROS Organics, Thermo Fisher Scientific (Waltham, MA, USA). All chemicals were dissolved in ddH_20 and sterile filtered (Millipore, 22 μm filters) to obtain stock solutions. The stock solutions were directly applied to the cell culture medium. Ready-made cycloheximide (CHX) solution (100 mg/ml in DMSO) was purchased from Sigma-Aldrich. In cell culture experiments, the CHX solution was further diluted with DMSO to obtain desired concentrations. The concentration of DMSO in all cell culture media was 0.2%.

RNA isolation and real-time PCR

Total RNA was extracted by using the RNeasy Mini Kit according to the manufacture's protocol (Qiagen, Hilden, Germany). The protocol includes an on-column digestion of genomic DNA. Nuclear and cytoplasmic RNA was separated by using the SurePrep Nuclear or Cytoplasmatic RNA Purification Kit (Thermo Fisher BioReagents, Waltham, MA, USA). The quality of RNA was evaluated using RNA Nano chips on Agilent 2001 bioanalyzer (Agilent Technologies, Santa Clara, California, USA). RNA was then quantified on Nanodrop 2000c Spectrophotometer (Thermo Fisher Scientific). One-thousand nanograms of total RNA from each isolation was reverse transcribed into cDNA by using the Transcriptor First Strand cDNA Synthesis Kit and anchored-oligo(dT)18 primer (Roche Diagnostics Inc., Basel, Switzerland).

For quantification of cDNA, real-time PCR was performed on ABI PRISM 7000 using gene specific primers and TaqMan probes (Applied Biosystems, Life Technologies, Carlsbad, California, USA). One-twentieth of the resulting cDNA was used in each reaction. All measurements were done in triplicate. To differentiate between normally and aberrantly spliced FECH mRNAs, two separate real-time PCR TaqMan assays were employed. The amount of normally spliced product was measured by using a commercial TaqMan primer-probe set which is localized on the exon 3-exon 4 boundary (Hs01555261_m1, Applied Biosystems, Life Technologies). Quantification of the aberrant splice product was carried out by using a self-designed primer–probe set (see below). Transcripts of $U2AF^{65}$, Jmjd6 and TFRC (transferrin receptor 1) were quantified by using commercially available TaqMan real-time PCR primer-probe sets (Hs00200737_m1, Hs00397095_m1 and HS00951083_m1) from Applied Biosystems, Life Technologies. Beta-actin (Hs99999903_m1) was used as an endogenous control to calculate the amount of each transcript. Specifically, the threshold cycle (Ct) value from a particular transcript was subtracted by that of β-actin to obtain a delta-Ct value. Arbitrary unit (a.u.) was defined as $2^{-\Delta Ct} \times 10^3$.

Real-time PCR quantification of aberrantly spliced FECH mRNA

To quantify the amount of aberrantly spliced FECH mRNA, a set of TaqMan primer–probe was designed to detect specifically a region of FECH mRNA containing both exons 3 and 4 as well as the 63 bp insertion between the two exons. Primer ferroins2f: 5′-AGA CCT CAT GAC ACT TCC TAT TCA GA-3′. Primer ferroins2r: 5′-CGA TGA ATG GTG CCA GCT T′-3′. Probe ferroins2: 6-FAM-TAA GCT GGA ATA AAA TCC ACT-MGB. The efficiency of the real-time PCR reaction was proven to be closed to 100% (slope ≈ 3.3). No signals were detected when amplifying genomic DNA samples. All mRNAs, unless otherwise indicated, were detected at the steady state levels without inhibition of the nonsense mediated decay.

siRNA transfection assays

For transfection of cells with siRNA, 300 000 K562 cells were plated in 6-well plates containing 2 ml RPMI 1640 medium supplemented with 10% fetal calf serum without antibiotics. Stocks (40 μM) of pre-annealed siRNA against Upf1, $U2AF^{65}$ and Jmjd6 mRNA were diluted in Oligofectamine reagent and OptiMem (Invitrogen) according to the

manufacture's protocol. Five-hundred microliters of the mix was added drop wise to the cells. Incubation time was between 48 h and 72 h.

The sequence of siRNAs are as follows: Upf1_1s: 5′-GAG AAU CGC CUA CUU CAC UTT-3′ [33]; Jmjd6_1: 5′-GAGGGAACCAGCAAGACGA-3′ [5]; U2AF2 (U2AF^{65}): 5′-GCA CGG UGG ACU GAU UCG U-3′ [32].

Western blot

The cytosolic and membrane fractions of the cells were separated by using the QProteome Cell Compartment Kit (Qiagen). The protein concentrations in these fractions were quantified by the benzethonium chloride method on a clinical chemistry analyzer, Cobas 501 (TPUC3; Roche Diagnostics Inc., Rotkreuz, Switzerland) [16,29]. Equal amount of protein from each fraction was dissolved in lysis buffer in a final volume of 15 μl and was then mixed with 5 μl of loading buffer (NuPage LDS 4× LDS Sample Buffer). The sample (15 μl) was loaded onto a precast NuPage gel containing 4–12% BisTris (1.5 mm, 15 wells). The gel was run at a constant voltage of 100 V in an X Cell II Chamber (Invitrogen). Magic Mark XP Western Blot protein standard was used as a weight marker (Invitrogen). Gels were blotted on 0.45 μm Nitrocellulose using X Cell II Blot Module (Invitrogen). The membrane was then blocked with TBS Blotto A Blocking Reagent (Santa Cruz Biotechnology Inc., Santa Cruz, USA.) for 40 min. Membranes were first incubated with primary antibodies over night at 4 °C, then washed twice with PBS-Tween and finally incubated with the secondary antibody for 1 h at room temperature. The following antibodies were used: ferrochelatase primary antibody (sc-49663; in 1:200 dilution) and secondary antibody donkey anti goat IgG-HRP (sc-2020; in 1:2000 dilution; Santa Cruz Biotechnology Inc.). Beta-actin primary antibody: monoclonal anti beta-actin (A5316; in 1:5000 dilution) and secondary antibody: anti-mouse IgG peroxidase antibody produced in goat (A9917; in 1:2000 dilution; Sigma-Aldrich). Bands were visualized by staining the membranes with Sigma FAST DAB horse radish peroxidase substrate (Sigma-Aldrich). Membranes were photographed with Quantity One device (Bio-Rad laboratories, INC., Hercules, California, USA). The intensities of the bands were densitometrically quantified with Image J-software (http://rsbweb.nih.gov/ij/download.html) [1].

Statistical analysis

Data were analyzed by either *t*-test or one-way ANOVA followed by Bonferroni post hoc correction using SPSS version 19, IBM-SPSS, Chicago, IL. A two-sided $p \leq 0.05$ was considered to be statistically significant.

Sequence comparison

A partial sequence of the human *FECH* gene containing intron 3 and exon 4 was imported into the UCSC Genome Browser (http://genome.ucsc.edu/) [11,19–21,36] in order to search for the corresponding sequences among other species. The following sequences were obtained from the USCS Genome Browser: Chimp: Oct. 2010 (CGSC 2.1.3/panTro3); Gorilla: May 2011 (gorGor3.1/gorGor3); Orangutan: July 2007(WUGSC 2.0.2/ponAbe2). In addition, the sequence of Homo sapiens (NT025028) was obtained from NCBI (http://www.ncbi.nlm.nih.gov/gene/?term=FECH). The extracted sequences were aligned by the software CLUSTAL W (http://www.ch.embnet.org/software/ClustalW.html) [26,41].

Results

The amounts of correctly and aberrantly spliced FECH mRNA are determined by the genotype with regard to IVS3-48C/T

First, we tested whether the results from the minigene assay are reproducible *in vivo*. To this aim, the IVS3-48 genotypes of eight healthy donors and eight EPP patients were determined by sequencing of the *FECH* gene as previously described [37]. All EPP patients were heterozygous for IVS3-48C/T, whereas all healthy donors were homozygous for IVS3-48T/T. To measure the amount of aberrantly spliced FECH mRNA in the peripheral blood cells of these individuals, a quantitative TaqMan real-time PCR assay was developed. In addition, a commercially available TaqMan assay was employed to quantify the amount of correctly spliced FECH mRNA (the primers and probe are located at the exon 3–exon 4 boundary). The results showed a clear genotype dependency. In the control subjects of T/T genotype, the amount of aberrantly spliced mRNA comprised 21.5% (SD = 7.5%) of the total FECH mRNA, as opposed to 34.5% (SD = 5.1%) in EPP patients (an IVS3-48C allele *in trans* to a mutated *FECH* allele; $p < 0.005$; Fig. 1A). The clear genotype dependency confirmed previous findings in mini-gene models and lymphoblastoid cells by Gouya et al. [13].

Next, we measured the levels of two FECH transcripts in lymphoblastoid cell lines generated from individuals with genotypes T/T, C/C and M/C (M stands for mutated allele). The lymphoblastoid cell line with the T/T genotype showed the highest amount of correctly spliced FECH mRNA *i.e.*, 88.3% (SD = 1.9%, n = 7) of the total amount of transcripts at the steady state level. The aberrant FECH mRNA accounted therefore for 11.7% of the total amount of transcripts in this cell line. In the C/C cell line, the ratio between normal and aberrant splice products was 84.0% to 16.0% (SD = 3.9%, n = 5). A slightly higher amount of aberrant splice product *i.e.* 18.9% (SD = 4.3%, n = 3) of the total transcripts was observed in the M/C cell line (Fig. 1B).

Because the metabolic defect of EPP mainly manifests in late erythropoiesis, a human erythroleukemic cell line (K562) displaying most of the features of erythropoiesis was investigated [3,23,28]. The K562 cell line, also having a T/T genotype with respect to IVS3-48 as determined by sequence analysis, showed 18.6% aberrantly spliced FECH mRNA (SD = 3.9%, n = 4; Fig. 1B).

As stated above, the aberrantly spliced FECH mRNA contains a PTC in its additional 63 bp intronic sequence and is therefore subjected to nonsense mediated decay (NMD) [13]. To further characterize this process, we conducted a series of experiments using two different approaches to inhibit NMD in the K562 cells. In both experiments, we were able to demonstrate a dose-dependent accumulation of the aberrant splice product.

In the first experiment, cycloheximide (CHX) was used, a compound that blocks protein synthesis and therefore inhibits NMD in eukaryotic organisms. The experimental conditions *i.e.*, concentrations (from 50 to 100 μM) and incubation time (6 h) had been previously optimized for the K562 cells in our laboratory. Fig. S1A in Appendix A shows the results of CHX treatment of K562 cells. An increase of 5.6 fold in the amount of aberrant splice FECH was observed in cells treated with 100 μM CHX compared to untreated cells (DMSO alone). Interestingly, under the same condition, the amount of normal FECH transcript was also increased by 1.7 fold, which indicated that the half-life of normal FECH mRNA was extended. This could be explained by the fact that CHX blocks protein translation and therefore slows down the decay of normal FECH mRNA, which occurs after several rounds of translation [9].

Up-frameshift protein 1 (UPF1) is an evolutionarily conserved protein with RNA/DNA-dependent ATPase and RNA helicase activity. It plays an essential role in NMD which eliminates aberrant mRNAs harboring PTC [15]. In our second experiment, Upf1 was selectively knocked down by siRNA. The conditions (30 and 60 nM, 72 h) used in the siRNA experiments had also been optimized previously. As shown in Fig. S1B (the left panel), transfection of K562 cells with siRNA against Upf1 resulted in a maximum of 54.9% reduction in its mRNA level (from 20.48 arbitrary units, SD = 8.27 mocked condition to 11.25 arbitrary units, SD = 3.21 under 30 nM siRNA treatment). With respect to the FECH transcripts, the aberrantly spliced mRNA increased from 3.4 arbitrary units (SD = 0.9) in UPF1-mocked transfection to 7.4 arbitrary units (SD = 1.4) under 60 nM siRNA against UPF1.

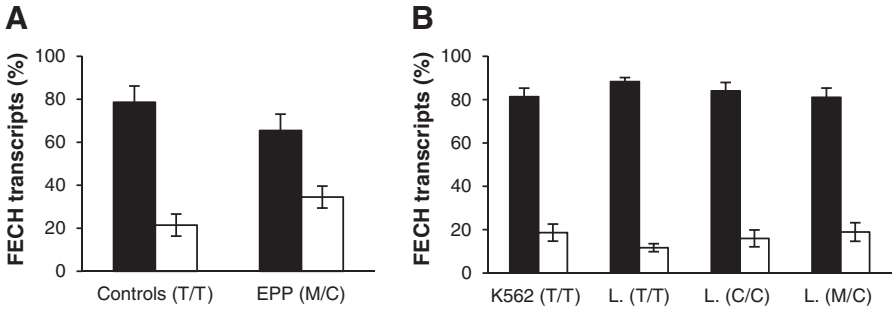

Fig. 1. Association between SNP IVS3-48 C/T and the amount of FECH transcripts measured by real-time PCR. (A) Percentage of correct and aberrant FECH splice variants in whole blood samples of eight healthy controls with the genotype IVS3-48T/T and eight EPP patients with the genotype IVS3-48C/M (mutation *in trans* to IVS3-48C). (B) Percentage of correct and aberrant FECH splice variants in K562 cell line (genotype IVS3-48T/T) and in three lymphoblastoid cell lines with the genotypes IVS3-48T/T, C/C and M/C, respectively. In all figures, the correct and aberrant splice variants are represented by solid and empty bars, respectively.

The amount of aberrantly spliced mRNA was significantly different among the three conditions ($p < 0.005$). Thereby, the post hoc test showed that the effect of 60 nM siRNA differed significantly from that of both 0 and 30 nM siRNA. The levels of correctly spliced FECH transcript were not affected, which lay between 14.8 (SD = 4.1; mock) and 15.3 arbitrary units (SD = 4.0; 30 nM siRNA) (n = 3; Fig. S1B, the right panel).

Iron depletion by DFO down-regulates the amount of normally spliced FECH mRNA and enhances aberrant intron 3 splicing in K562 and lymphoblastoid cell lines

To test whether iron availability alters the amount of correctly spliced FECH mRNA, we treated the erythroleukemic cell line K562 (genotype T/T) and lymphoblastoid cell lines of different genetic backgrounds (genotype T/T, C/C and M/C) with an iron-chelating agent, deferoxamine (DFO) and measured the amounts of correctly and aberrantly spliced products by quantitative real-time PCR.

As shown in Fig. 2A, during treatment of K562 cells with DFO at different concentrations (50, 100 and 200 μM) for 60 h, the proportion of correctly spliced mRNA decreased from 83.3% (SD = 1.2%; 0 μM) to 43.7% (SD = 5.9%; 200 μM) of the total FECH mRNA, and concurrently, the aberrantly spliced mRNA increased from 16.7% (0 μM) to 56.3% (200 μM) of the total FECH mRNA. The difference between 0 μM and 100 μM or 200 μM was statistically significant, $p < 0.0001$ (n = 4). Similar dose-dependent changes in both the correct and aberrant products occurred under a concentration range from 0 μM to 100 μM in lymphoblastoid cell line of the T/T genotype after 24 h of incubation as shown in Fig. 2B. The correctly spliced mRNA decreased from 90.4% (SD = 1.1%; 0 μM) to 50.1% (SD = 3.6%; 100 μM) and the aberrantly spliced mRNA increased from 9.6% (0 μM) to 49.9% (100 μM) of the total. A higher concentration of DFO (200 μM) did not result in any further changes in the splice ratio (correct *vs.* aberrant products remained approximately 50%:50%). The difference between 0 μM and 100 μM or 200 μM was statistically significant, $p < 0.0001$ (n = 3).

Only marginal changes were found in lymphoblastoid cell lines of both the C/C and M/C genotypes (Figs. 2C and D). After treatment of the C/C lymphoblastoid cell line with DFO for 48 h, the correctly spliced product dropped only slightly, from 84.4% (SD = 3.1%; 0 μM) to 71.3% (SD = 3.1%; 100 μM) of the total, whereas the aberrantly splice product increased from 15.6% (0 μM) to 28.7% (100 μM) of the total. The difference between 0 μM and 100 μM or 200 μM was statistically significant $p < 0.005$ (n = 3; Fig. 2C). In the M/C lymphoblastoid cell line, the corresponding changes were 81.4% (SD = 3.7%, n = 3) to 64.8% (SD = 7.8%) and 18.6% to 35.2%. The difference between 0 μM and 100 μM or 200 μM was statistically significant, $p < 0.05$ (n = 3; Fig. 2D). Similar to the T/T cells, a higher concentration of DFO (200 μM) did not cause any further changes in the splice ratio in both the C/C and M/C cell lines.

To test whether the DFO concentrations we used were physiologically relevant, we measured the expression level of transferrin receptor 1 (TFRC), a gene known to be regulated by iron, in the K562 cell line under the same conditions. The amount of TFRC mRNA increased significantly in response to DFO-induced iron depletion (data not shown).

To verify the observed effect of DFO on the FECH splice products, a second iron chelator, deferiprone was tested in the K562 cells (Fig. 3A). Since three molecules of deferiprone are needed to chelate one molecule of iron, the concentrations of deferiprone used were three times higher than that of DFO *i.e.*, 0 μM, 150 μM, 300 μM and 600 μM (the incubation time remained at 60 h). The results were similar to that of DFO treated K562 cells.

Products of ferrochelatase, zinc protoporphyrin IX or heme, did not have any effects on the ratio between the two splice products. We were unable to test the effect of one of the substrates of ferrochelatase, protoporphyrin IX, as it was difficult to handle experimentally due to its poor solubility in aqueous medium (data not shown).

Neutralization of the DFO effect by iron supplementation in vitro

To test whether the decrease in FECH mRNA and the increase in aberrant splice product were indeed caused by iron depletion rather than nonspecific interaction of DFO with cells, a stoichiometric amount of iron (ferric ammonium citrate as iron source; FAC), together with DFO, was added to the culture media.

The four middle panels of Fig. 2 show the results of this experiment in K562 cells, T/T, C/C and M/C lymphoblastoid cell lines, respectively. In both K562 and T/T lymphoblastoid cells, the strong effects of DFO as seen in the left panels, are prevented after treating the cells with DFO and iron at equimolar concentrations (50 μM, 100 μM and 200 μM) for the same amount of time as described for DFO alone. More precisely, under these concentrations, the proportions of the correctly spliced product were between 76.4% (SD = 2.5%) and 82.5% (SD = 4.8%) of the total, close to the baseline value (0 μM of both DFO and iron) of 84.5% (SD = 4.3%; K562 cells) and 88.7% (SD = 1.4%; T/T cells). Concomitantly, the proportions of aberrantly spliced product remained near the baseline value. In both the C/C and M/C cell lines, neutralizations of the effects of DFO were also observed, although the effects of DFO were much weaker than that in the K562 and T/T cell lines as shown above. Treatment of iron alone had no effects on splicing in any of the cell lines as shown in the four right panels of Fig. 2.

In a separate experiment on the K562 cells, a slightly different protocol was used. Instead of adding DFO and iron simultaneously as described in the experiment above, DFO and iron were added sequentially to the culture media. As depicted in Fig. 3B, the K562 cells were first grown in media containing 100 μM of DFO for 24 h. An equimolar concentration of iron was then added to the culture. The cells continued to grow in the media containing both DFO and iron for an additional of 24 h before

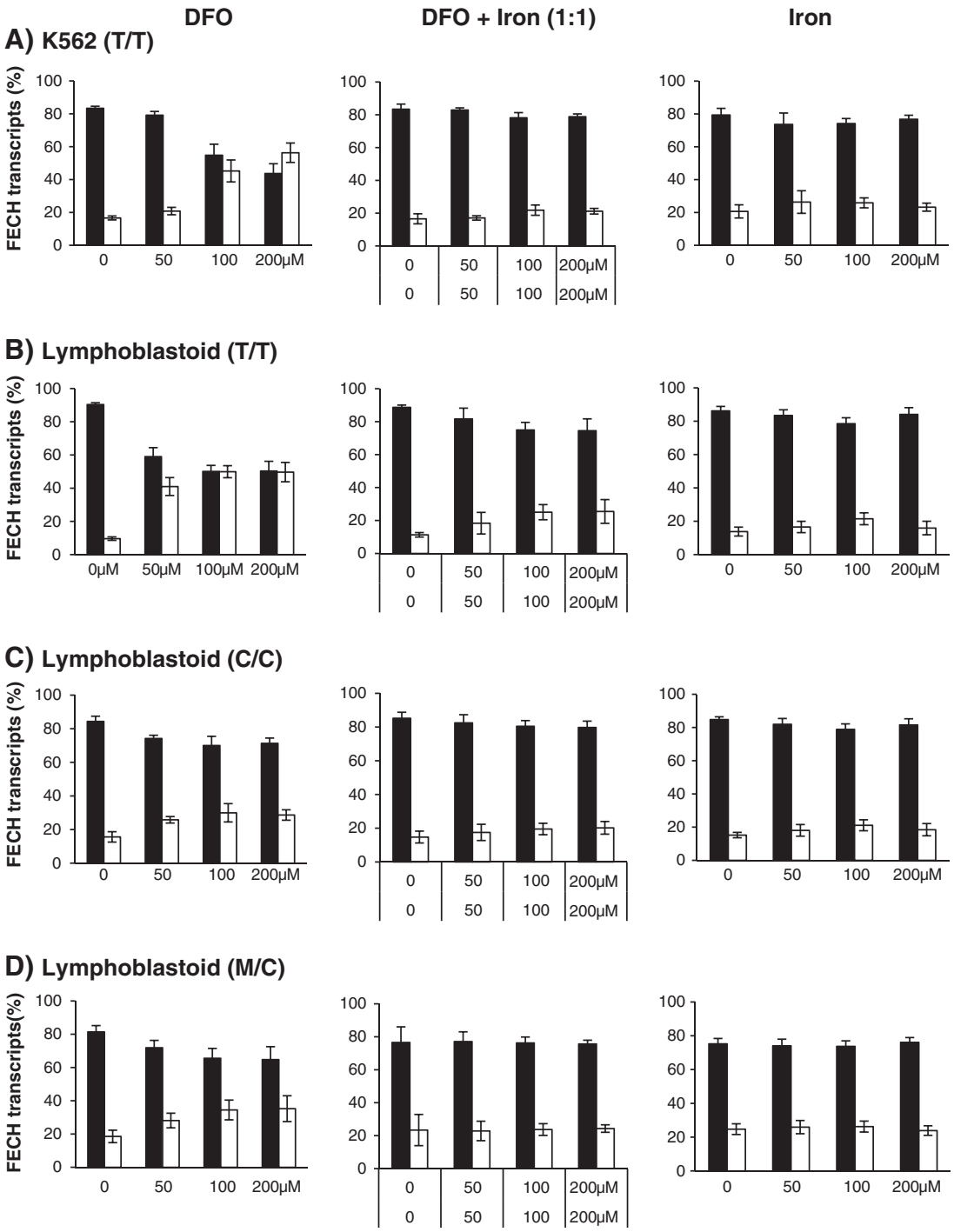

Fig. 2. Effects of iron availability on FECH splicing. The percentage of correct and aberrant FECH transcripts in K562 cell line, and T/T, C/C and M/C lymphoblastoid cell lines are displayed in rows A, B, C and D, respectively. Four left panels: Dose-dependent changes after treatment of the cells with different concentrations of iron chelator deferoxamine (DFO); four middle panels: The effect of DFO is reversed by addition of equimolar amounts of iron (ferric ammonium citrate); four right panels: Treatment of cells with iron alone does not have an effect on the splice ratio. The time of exposure is indicated in the text.

harvesting. As controls, cells grown in media containing either DFO alone for 48 h or iron alone for 24 h were used, in addition to the no-treatment control. The result showed a complete reversal of the DFO effect as the amounts of both correctly and aberrantly spliced products returned to the baseline value *i.e.*, to that of the untreated cells ($n = 3$). The overall significance was $p < 0.003$, whereby the post-hoc test found only a significance between the DFO-only treatment and the other three conditions, but not among the three.

DFO-induced change in FECH mRNA ratio occurs predominantly in the nucleus

Since splicing of nascent mRNA occurs in the nucleus of the cell, an effect of DFO on splicing efficiency should lead to an increase of aberrantly spliced mRNA predominantly in the nucleus. To test this hypothesis, we treated the K562 cells with 100 μM of DFO for 48 h and isolated RNA from cytoplasm and nucleus separately. As shown in Fig. 3C, in the

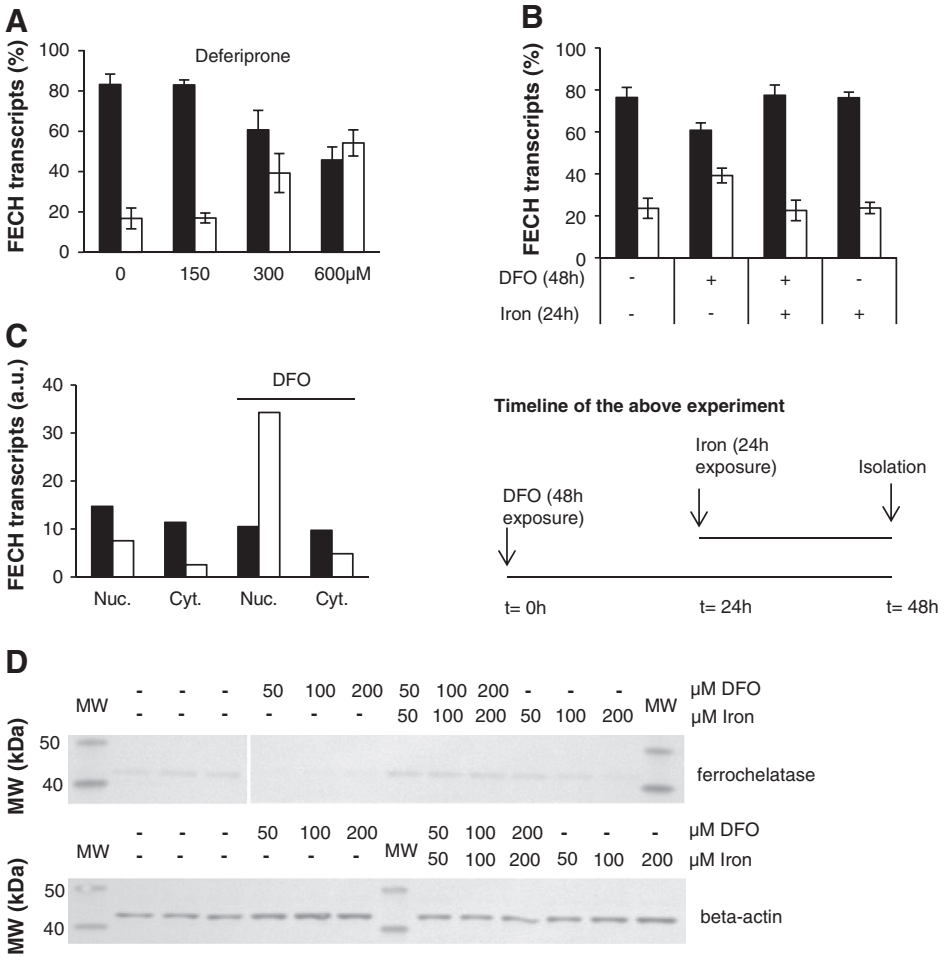

Fig. 3. Effects of iron chelators DFO and deferiprone on FECH splicing in K562 cells. (A) Effect of deferiprone on splice ratio (percentage of correct and aberrant splice variants); (B) Effect of a sequential application of DFO followed by iron (as shown in the bottom of diagram B) on the percentage of correct and aberrant splicing. Changes in splice ratio after treatment of cells by DFO for 24 h and then iron for additional 24 h (the fifth and sixth bars from the left) are shown. As controls, no treatment (the first and second bars from the left), DFO alone for 48 h (the third and fourth bars from the left) and iron alone for the last 24 h (the seventh and eight bars from the left) were used. (C) Effect of DFO on splice ratio in the nuclear (Nuc.) and the cytoplasmic (Cyt.) fractions of cell lysate (four right bars) compared to untreated controls (four left bars). The correct and aberrant transcripts are expressed in arbitrary units (a.u.; see the Experimental procedures section). One representative experiment is shown. (C) Effect of 50 to 200 μM DFO on the amount of ferrochelatase protein in the Western-blot analysis (lanes 5–7). As controls, no treatment (lanes 2–4), equimolar amounts of iron and DFO (lanes 8–10) and iron (lanes 11–13) are displayed. Beta-actin (the lower part) is used for standardization. MW, molecular weight marker.

nucleus, the amount of aberrant FECH mRNA in DFO-treated cells was 4.5 times higher than that in untreated cells. In the cytoplasm, the DFO-induced difference was only 1.9 fold. The result was confirmed in two additional experiments. This finding indicated that DFO treatment enhances aberrant splicing of newly synthesized FECH mRNA.

Decrease of the amount of FECH protein after iron chelation

Next, we tested if the down regulation of correctly spliced FECH mRNA under iron depletion is reflected by a decrease in the amount of FECH protein. Again, we treated K562 cells with DFO (50, 100 and 200 μM), iron or a stoichiometric amount of both iron and DFO for 60 h and isolated proteins from the cytosolic and membrane fractions separately. Equal amounts of protein from the membrane fraction, where ferrochelatase is located, and from the cytosolic fraction, where β-actin is located, were analyzed on Western-blot (Fig. 3D). The result showed a strong decrease of FECH protein under the iron deficient condition, whereas FECH protein levels remained unchanged in samples treated with either iron alone or with stoichiometric amounts of both iron and DFO.

As the next step, we explored possible mechanism(s) by which iron regulates the alternative splicing of FECH intron 3.

siRNA mediated silencing of splice factor U2AF^{65} leads to a decrease of correctly spliced and an increase in aberrantly spliced FECH mRNA

Splicing of precursor mRNAs requires accurate recognition of splice sites by the spliceosome, an assembly of small nuclear ribonucleoprotein particles (snRNPs) and extrinsic (non-snRNP) protein splicing factors [18]. The U2 snRNP auxiliary factor (U2AF) is an essential splicing factor composed of two subunits. The large subunit of 65-kDa (U2AF^{65}) binds to the polypyrimidine tract (PY-tract) upstream from the 3′ splice site and promotes U2 snRNP binding to the pre-mRNA [32,45]. Although the small subunit U2AF^{35} is important for the splicing of introns that contain short or weak PY-tracts, the recognition of a weak 3′ binding site requires the interaction between the two subunits [14,32].

In intron 3 of the *FECH* gene, both the constitutive and aberrant splicings contain an AG dinucleotide at their 3′ splice sites. However, they differ in the strength of the Py-tract that precedes the 3′ splice sites. As shown in Fig. 4, the aberrant splice site is preceded by a 23-nucleotide polypyrimidine-rich sequence including a stretch of 15 cytosines/thymines (Cs/Ts). In contrast, the Py-tract of the constitutive splice site contains mostly short sequences of 3 or less Cs/Ts. Apparently, enough correct FECH mRNA is generated, which indicates a sufficient recognition of the weak Py-tract, as reflected in the splice ratio between normal and aberrant products.

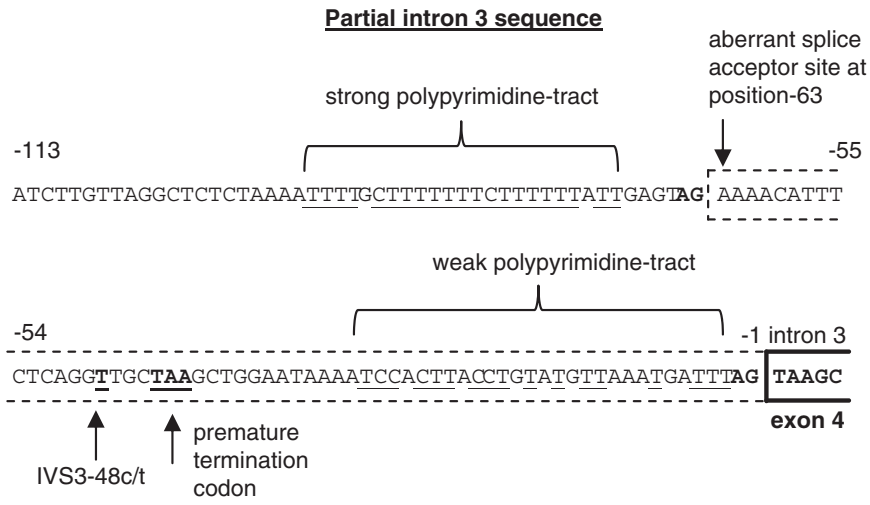

Fig. 4. A partial sequence showing the intron 3–exon 4 boundary of the *FECH* gene. The AG dinucleotides from both the constitutive splice site and an aberrant splice site at position −63 are in *bold*. Position −48 and a premature termination codon TAA at position −44 are in *bold* and *underlined*. T and C nucleotides within polypyrimidine tracts in front of both correct and aberrant splice acceptor sites are *underlined*. The alternative splice site is preceded by a strong PY-tract containing 21 pyrimidines and two interspersing purines. The constitutive splice site, on the other hand, is preceded by a weaker PY-tract which consists of mostly short sequences of three or less pyrimidines.

To study the action of splice factor U2AF^{65} on splicing of FECH intron 3, we targeted U2AF^{65} by siRNA and measured the splice ratio between normal and aberrant products. As shown in the left panel of Fig. 5A, transfection of K562 cells with different concentrations of siRNA against U2AF^{65} resulted in 35.5% (10 nM siRNA) to 48.7% (50 nM siRNA) reduction in its mRNA level. The difference between 0 nM (mock) and 50 nM or 100 nM was statistically significant, $p < 0.05$ (n = 3; the left panel of Fig. 5A). With respect to the FECH transcripts, the correctly spliced mRNA decreased from 72.2% (SD = 4.7%; mock) to 57.4% (SD = 8.3%; 100 nM siRNA) of the total (the right panel of Fig. 5A). The difference between 0 nM and 100 nM was statistically significant, $p < 0.05$ (n = 3). In parallel, the aberrant product increased from 27.8% (SD = 4.7%; mock) to 42.6% (SD = 8.3%; 100 nM siRNA) of the total.

These data indicated that U2AF^{65} down regulation mimics the effect of iron deprivation. Webby et al. recently reported that splice factor U2AF^{65} is hydroxylated by the iron-, oxoglutarate (2OG)- and oxygen-dependent dioxygenase Jumonji domain-containing protein 6 (Jmjd6) [44]. Being iron-dependent, Jmjd6 could act as a sensor for iron availability and therefore might be the link between iron-deprivation and splicing regulation. As a next step, we tested the putative involvement of Jmjd6 in splicing of FECH intron 3.

siRNA mediated silencing of dioxygenase Jmjd6 decreases the correctly spliced and increases the aberrantly spliced FECH mRNAs

Treatment of K562 cells with different concentrations of siRNA against Jmjd6 led to 20.8% (SD = 3.5%; 10 nM siRNA) to 40.4% (SD = 7.5%; 30 nM siRNA) reduction in Jmjd6 mRNA ($p < 0.01$; Fig. 5B, the left panel). Under these treatment conditions, the proportions of the correctly spliced FECH mRNA decreased from 81.2% (SD = 2.2%; mocked) to 73.7% (SD = 1.3%; 50 nM siRNA) of the total FECH transcripts and the aberrant variant increased from 18.8% (mocked) to 26.3% (50 nM siRNA) of the total transcripts ($p < 0.001$; n = 3; Fig. 5B, the right panel).

Although targeting the synthesis of a particular transcript by siRNA is a highly specific approach, this technique only achieved an approximately 40% reduction in mRNA of both U2AF^{65} and Jmjd6. Since Jmjd6 does not directly influence FECH splicing, rather it exerts its action *via* U2AF^{65}, targeting Jmjd6 resulted in a small change in the amount of correctly spliced product i.e., from 81.2% to 73.7% (difference = 7.5%) of the total, as compared to a larger change from 76.8% to 62.6% (difference = 14.2%) when targeting U2AF^{65} directly. To maximize the effect of Jmjd6 on FECH splicing, we conducted additional experiments using less specific but more effective inhibitors of Jmjd6.

Inhibition of Jmjd6 by cobalt chloride ($CoCl_2$) and by dimethyloxallyl glycine (DMOG), an analogue of oxoglutarate

The activity of iron- and oxoglutarate dependent dioxygenases can be inhibited by iron deprivation using chelators such as DFO or by other divalent metal ions such as cobalt, which can compete with iron. Alternatively, analogues of oxoglutarate such as DMOG, can block the substrate binding site of the enzyme *via* competitive inhibition (For review see: [35]).

Treatment of K562 cells with $CoCl_2$ (concentrations ranging from 50 to 200 μM) for 24 h resulted in a strong and dose-dependent decrease of FECH mRNA and a concomitant increase in aberrant splice product to 44.8% (SD = 8.8%; at 200 μM) of the total transcripts ($p < 0.05$; Fig. 5C).

In the experiments with DMOG, we tested the levels of FECH transcripts as well as ferrochelatase protein. Like with cobalt chloride, treatment of K562 cells with DMOG (concentrations 2.5 mM and 5 mM) for 24 h resulted in a strong and dose-dependent decrease of FECH mRNA and an increase in aberrant splice product to 51.8% (SD = 5.4%; at 5 mM) of the total ($p < 0.001$; Fig. 5D). In the Western blot analysis of ferrochelatase from the membrane fraction of the cell lysate, the intensity of bands decreased as the concentration of DMOG increased (Fig. 5E).

Discussion

The present study demonstrated an association between the availability of iron and regulation of alternative splicing of FECH intron 3. Based on our results, we put forward the following hypothesis to explain the underlying mode of action/mechanism (Fig. 6, upper panel): In cells with a normal iron status, ferrous iron together with substrates oxygen and 2-OG bind to Jmjd6. The dioxygenase Jmjd6 catalyzes the posttranslational lysyl-5-hydroxylation of U2AF^{65} [44]. The tandem RNA recognition motif domains (RRM) of U2AF^{65} exhibit a broad range of conformations [17]. The RRM adopt two remarkably distinct arrangements, *i.e.* closed and open ones, in the absence or presence of a high affinity PY-tract, respectively. The equilibrium between the two conformations functions as a molecular control unit

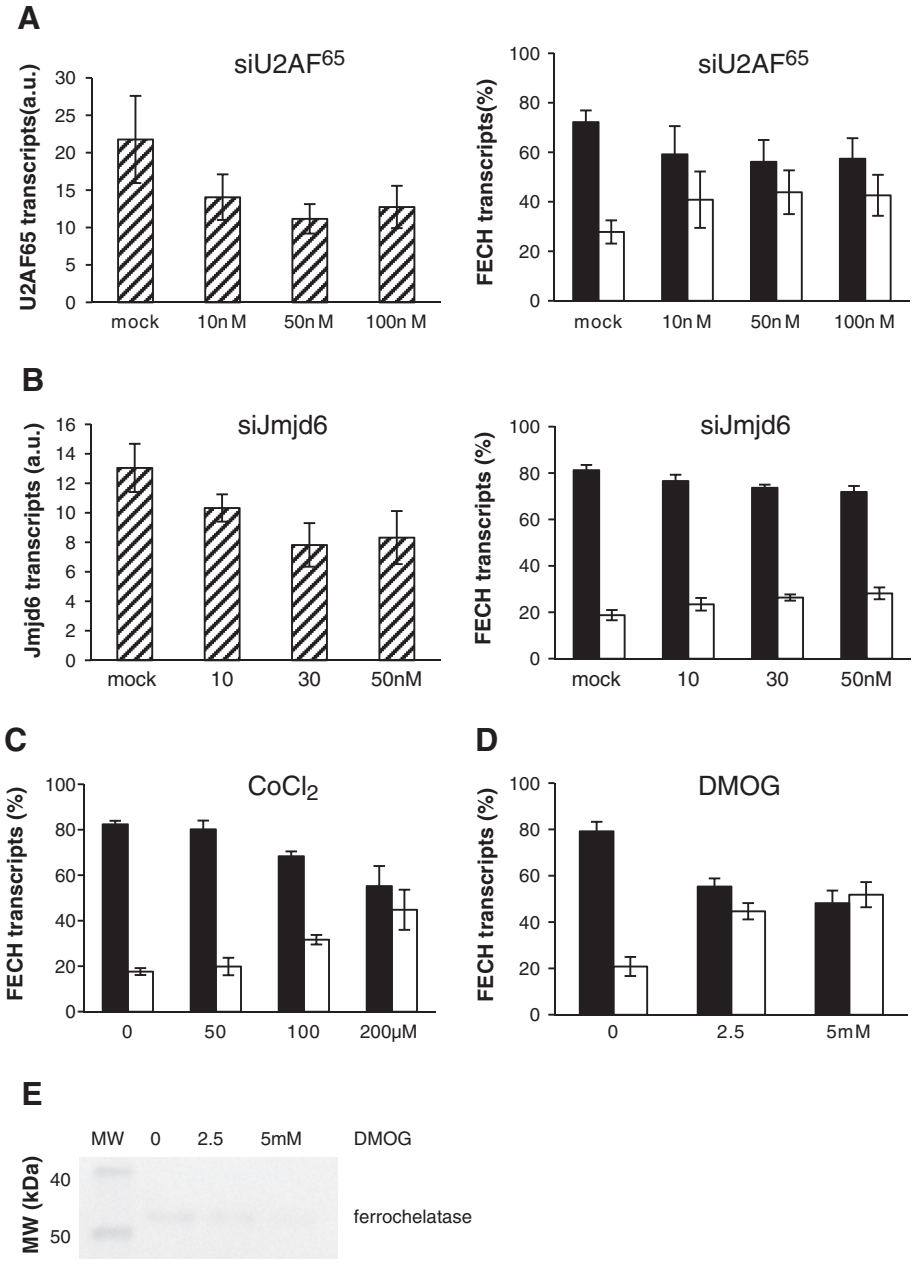

Fig. 5. Effects of down regulation of splice regulators U2AF^{65} and Jmjd6 on FECH splicing. Row A: Inhibition of U2AF^{65} by siRNA at variable concentrations as indicated in the abscissa. Expression of the U2AF^{65} transcripts (left panel) and the effect on the splice ratio (right panel). Row B: Inhibition of Jmjd6 by siRNA at variable concentrations as indicated in the abscissa. Expression of Jmjd6 transcripts (left panel) and the effect on the splice ratio (right panel). The transcripts of both U2AF^{65} and Jmjd6 are expressed in arbitrary units (a.u.). Inhibition of Jmjd6 with both $CoCl_2$ (panel C) and DMOG (panel D) at variable concentrations as indicated in the abscissa, and their effects on the splice ratio. Changes in the amount of ferrochelatase protein by Western-blot analysis after inhibition of Jmjd6 with 2.5 and 5 mM DMOG (panel E). Equal amount of protein from the membrane fraction was loaded on the gel (see the Experimental procedures section).

that translates the natural variations in PY-tract nucleotide composition, length and functional strength into the efficiency of U2AF^{65} to recruit U2snRNP to the spliceosome [30]. The conserved α-helical surface of RRM 2 of U2AF^{65} that is only accessible in the open configuration contains the lysyl residue K276, as it has been demonstrated by Webby et al., is hydroxylated by Jmjd6 and upon hydroxylation, it alters the splicing of certain genes [44]. Our study demonstrates that both inhibition of Jmjd6 and siRNA mediated down-regulation of U2AF^{65} induce a shift from correct to aberrant splicing of the FECH intron 3 (Fig. 6, lower panel).

Jmjd6 belongs to a large family of iron- and 2OG-dependent dioxygenase enzymes that are involved in numerous metabolic activities including collagen biosynthesis, fatty acid metabolism, DNA repair, RNA and chromatin modifications, and hypoxic sensing [35]. Our study establishes a link between one of the dioxygenases and heme biosynthesis which by itself is closely associated with oxygen metabolism, as heme is directly involved in oxygen transport and acts as a prosthetic group of cytochromes.

Prior to Webby et al. who established for the first time the connection between alternative splicing and oxygen and iron sensing *via* Jmjd6, Kim et al. observed that under iron-deprived condition a splice variant of spermidine/spermine N(1)-acetyltransferase mRNA increased in several cell lines [22]. More recently, Boeckel et al. described that treatment with siRNA against Jmjd6 resulted in an increase in the

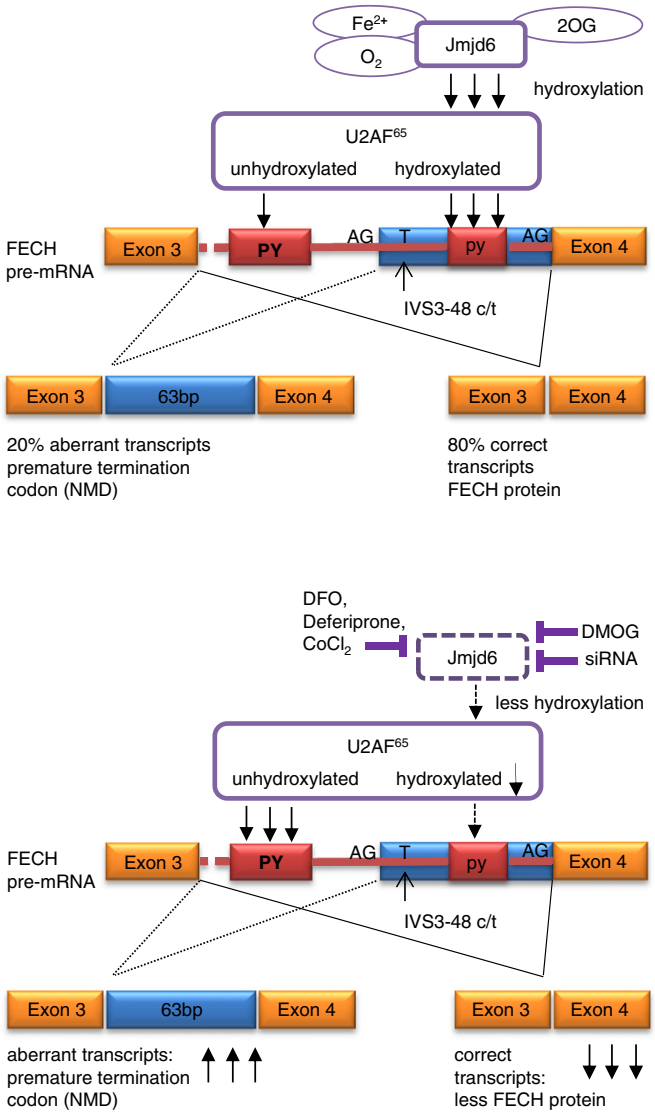

Fig. 6. A proposed model to explain the iron-mediated splice regulation of FECH intron 3. The upper panel: Under physiological conditions, upon binding with iron, oxygen and 2-oxoglutarate dioxygenase Jmjd6 hydroxylates lysine residues in the splice factor U2AF^{65}, which in turn binds preferably to the weak polypyrimidine tract in front of the constitutive splice site and directs splicing to generate predominantly the correct transcript, 80% of the total. The lower panel: Inhibition of Jmjd6 activity can be achieved by iron deprivation with either DFO or deferiprone, by competitive inhibition of iron binding with $CoCl_2$, by competitive inhibition of 2-oxoglutarate binding with DMOG, and by suppression of transcription with specific siRNA against Jmjd6. Inhibition of U2AF^{65} can be achieved by siRNA. Upon inhibition of either Jmjd6 or U2AF^{65}, the splice ratio shifts toward the aberrant product, leading to fewer amounts of both FECH mRNA and protein.

soluble form of Flt1, a product of alternative splicing, and a subsequent inhibition of angiogenesis [5]. All three above-mentioned studies, together with ours, demonstrated that the regulation of alternative splicing by both iron deprivation and inhibition of Jmjd6 is involved in a broad range of metabolic processes.

As stated before, iron deprivation caused an increase in aberrant splicing and decreases of both FECH mRNA and protein. However, this result was not in a total agreement with that of Taketani et al. [40], who reported a decrease of only FECH protein and activity, but not of FECH mRNA in K562 cells treated with 50–150 μM DFO for 16 h. More recently, Crooks et al. reported that iron deprivation diminished the stability of newly formed FECH protein without altering the level of FECH mRNA or the mature protein [7]. FECH is an iron–sulphur cluster containing protein and an intact iron sulphur cluster is required for enzymatic activity [10]. Crooks et al. assumed that under iron-deprivation the newly formed FECH lacks the iron–sulphur cluster which explains the instability and rapid degradation. They concluded that the effect of iron deprivation is similar to the disease ISCU-myopathy, an inborn defective biosynthesis of iron sulphur clusters with reduced FECH activity (OMIM 255125). In both studies, however, the failure in detecting any reduction in FECH mRNA under iron deprivation could be explained by the use of northern blot analysis for the quantitative FECH mRNA determination which most likely is unable to discriminate between the normal and aberrant splice products since these two mRNA species differ only by 63 bp in size.

The influence of iron chelation by DFO on alternative splicing depended on the genotype in the lymphoblastoid cell lines: The cell line bearing the SNP type IVS3-48T/T which is the most frequent in Caucasians showed the strongest increase in the amount of aberrantly spliced mRNA under iron-deprived conditions. By contrast, a much smaller increase in the amount of aberrant FECH transcript by iron deprivation was observed in the cell lines with both the C/C and M/C genotypes. Assuming that the described effect of iron deprivation on splicing in the T/T genotype is a regulatory feature, the observed loss in sensitivity in the IVS3-48C background constitutes a loss of potential for regulation. Taking both together, the increase in aberrant splicing under baseline condition and the lack of that increase under iron deprivation indicate that even if there is enough iron available, the C/C genotype behaves in a manner as if iron is deficient.

The 3′ end of intron 3 of the *FECH* gene including the aberrant splice site at position −63 and both PY tracts, is highly conserved among hominids (Fig. 7). Among the available sequences of chimp, gorilla and orangutan, only the T-variant at position −48 is documented, even if we cannot exclude the possibility of the C-variant present at a low frequency among the non-human species of hominids. However, this is unlikely as Gouya et al. demonstrated that the C-variant appeared in the human population about 60'000 years ago as a de-novo mutation in humans and was not present in the original human *FECH* [12].

Based on the fact that the frequency of IVS3-48C varies considerably among different populations, one might speculate that this large variation may be related to the availability of dietary iron. In a population that is under chronic iron-deficient conditions, regulation of iron might be of less importance than in populations with sufficient iron supply. The Japanese population, for example, has a high prevalence of the IVS3-48C genotype [12]. On the other hand, the dietary habits of Japanese *i.e.*, a relatively low intake of iron and high intake of iron-absorption inhibitors such as green tea and soybeans make them more vulnerable to iron deficiency compared to the Caucasian population [4,42]. Therefore, the regulation of transcription of ferrochelatase among Japanese might be less important compared to that in Caucasians.

Based on the results of this study, we propose that availability of iron regulates the activity of ferrochelatase by alternative splicing and RUST. Iron-signaling involves Jmjd6, which modulates U2AF^{65}-lysyl-hydroxylation. This in turn, influences the relative amounts of correct and aberrant FECH mRNA splice products and consecutively the amount of FECH protein.

Conflict of interest statement

All authors declare that they have no conflict of interest.

Acknowledgments

This work was support by the Velux Foundation (480) and the Hartmann Müller Stiftung (1187). We thank Prof. Daniel Schümperli, University of Bern; Prof. Jonathan Hall, Swiss Federal Institute of Technology, Zurich; Prof. Konrad Basler and Prof Kurt Bürki, University of Zurich, Switzerland; and Prof. Jiuyong Xie, University of Manitoba, Canada for the fruitful discussion of this work. We also thank Dr. Markus

Fig. 7. Comparison of partial *FECH* intron 3–exon 4 sequences among hominids. The exon 4 sequence is in *bold*, the polypyrimidine tracts are *underlined* and sequence elements related to *FECH* intron 3 splicing are highlighted in *gray*. Conserved nucleotides are indicated by asterisk, among which are both constitutive and aberrant splice sites, both weak and strong polypyrimidine tracts and the stop codon at position −44. At position −48 all hominids carry a T.

Dorner, The Rockefeller University, New York, USA and Prof. David Nadal, Children's Hospital, Zürich Switzerland for their help in establishing lymphoblastoid cell lines.

Appendix A. Supplementary data

Supplementary data to this article can be found online at http://dx.doi.org/10.1016/j.bcmd.2013.05.008.

References

[1] M.D. Abràmoff, P.J. Magalhaes, S.J. Ram, Image processing with ImageJ, Biophotonics Int. 11 (2004) 36–42.
[2] K. Anderson, S. Sassa, D.F. Bishop, R.J. Desnick, Disorders of heme biosynthesis: X-linked sideroblastic anemia and the porphyrias, in: C.R. Scriver, M. Beaugrand, W.S. Sly, D. Valle (Eds.), The Metabolic and Molecular Basis of Inherited Disease, McGraw-Hill, New York, 2001, pp. 2991–3062.
[3] L.C. Andersson, K. Nilsson, C.G. Gahmberg, K562—a human erythroleukemic cell line, Int. J. Cancer 23 (1979) 143–147.
[4] K. Asakura, S. Sasaki, K. Murakami, et al., Iron intake does not significantly correlate with iron deficiency among young Japanese women: a cross-sectional study, Public Health Nutr. 12 (2009) 1373–1383.
[5] J.N. Boeckel, V. Guarani, M. Koyanagi, et al., Jumonji domain-containing protein 6 (Jmjd6) is required for angiogenic sprouting and regulates splicing of VEGF-receptor 1, Proc. Natl. Acad. Sci. U. S. A. 108 (2011) 3276–3281.
[6] A.E. Burden, C. Wu, T.A. Dailey, et al., Human ferrochelatase: crystallization, characterization of the [2Fe–2S] cluster and determination that the enzyme is a homodimer, Biochim. Biophys. Acta 1435 (1999) 191–197.
[7] D.R. Crooks, M.C. Ghosh, R.G. Haller, et al., Posttranslational stability of the heme biosynthetic enzyme ferrochelatase is dependent on iron availability and intact iron–sulfur cluster assembly machinery, Blood 115 (2010) 860–869.
[8] M. Dorner, F. Zucol, C. Berger, et al., Distinct ex vivo susceptibility of B-cell subsets to epstein–barr virus infection according to differentiation status and tissue origin, J. Virol. 82 (2008) 4400–4412.
[9] H.L. Ennis, M. Lubin, Cycloheximide: aspects of inhibition of protein synthesis in mammalian cells, Science 146 (1964) 1474–1476.
[10] G.C. Ferreira, R. Franco, S.G. Lloyd, et al., Mammalian ferrochelatase, a new addition to the metalloenzyme family, J. Biol. Chem. 269 (1994) 7062–7065.
[11] P.A. Fujita, B. Rhead, A.S. Zweig, et al., The UCSC Genome Browser database: update 2011, Nucleic Acids Res. 39 (2011) D876–D882.
[12] L. Gouya, C. Martin-Schmitt, A.M. Robreau, et al., Contribution of a common single-nucleotide polymorphism to the genetic predisposition for erythropoietic protoporphyria, Am. J. Hum. Genet. 78 (2006) 2–14.
[13] L. Gouya, H. Puy, A.M. Robreau, et al., The penetrance of dominant erythropoietic protoporphyria is modulated by expression of wildtype FECH, Nat. Genet. 30 (2002) 27–28.
[14] S. Guth, C. Martinez, R.K. Gaur, J. Valcarcel, Evidence for substrate-specific requirement of the splicing factor U2AF(35) and for its function after polypyrimidine tract recognition by U2AF(65), Mol. Cell. Biol. 19 (1999) 8263–8271.
[15] N. Imamachi, H. Tani, N. Akimitsu, Up-frameshift protein 1 (UPF1): multitalented entertainer in RNA decay, Drug Discov. Ther. 6 (2012) 55–61.
[16] J. Iwata, O. Nishikaze, New micro-turbidimetric method for determination of protein in cerebrospinal fluid and urine, Clin. Chem. 25 (1979) 1317–1319.
[17] J.L. Jenkins, K.M. Laird, C.L. Kielkopf, A broad range of conformations contribute to the solution ensemble of the essential splicing factor U2AF(65), Biochemistry 51 (2012) 5223–5225.
[18] M.S. Jurica, M.J. Moore, Pre-mRNA splicing: awash in a sea of proteins, Mol. Cell 12 (2003) 5–14.
[19] D. Karolchik, A.S. Hinrichs, T.S. Furey, et al., The UCSC table browser data retrieval tool, Nucleic Acids Res. 32 (2004) D493–D496.
[20] W.J. Kent, BLAT—the BLAST-like alignment tool, Genome Res. 12 (2002) 656–664.
[21] W.J. Kent, C.W. Sugnet, T.S. Furey, et al., The human genome browser at UCSC, Genome Res. 12 (2002) 996–1006.
[22] K. Kim, J.H. Ryu, J.W. Park, et al., Induction of a SSAT isoform in response to hypoxia or iron deficiency and its protective effects on cell death, Biochem. Biophys. Res. Commun. 331 (2005) 78–85.
[23] H.P. Koeffler, D.W. Golde, Human myeloid leukemia cell lines: a review, Blood 56 (1980) 344–350.
[24] Y. Kohgo, K. Ikuta, T. Ohtake, et al., Body iron metabolism and pathophysiology of iron overload, Int. J. Hematol. 88 (2008) 7–15.
[25] S. Kumar, U. Bandyopadhyay, Free heme toxicity and its detoxification systems in human, Toxicol. Lett. 157 (2005) 175–188.
[26] M.A. Larkin, G. Blackshields, N.P. Brown, et al., Clustal W and Clustal X version 2.0, Bioinformatics 23 (2007) 2947–2948.
[27] B.P. Lewis, R.E. Green, S.E. Brenner, Evidence for the widespread coupling of alternative splicing and nonsense-mediated mRNA decay in humans, Proc. Natl. Acad. Sci. U. S. A. 100 (2003) 189–192.
[28] C.B. Lozzio, B.B. Lozzio, Human chronic myelogenous leukemia cell-line with positive Philadelphia chromosome, Blood 45 (1975) 321–334.
[29] R.W. Luxton, P. Patel, G. Keir, E.J. Thompson, A micro-method for measuring total protein in cerebrospinal fluid by using benzethonium chloride in microtiter plate wells, Clin. Chem. 35 (1989) 1731–1734.
[30] C.D. Mackereth, T. Madl, S. Bonnal, et al., Multi-domain conformational selection underlies pre-mRNA splicing regulation by U2AF, Nature 475 (2011) 408–411.
[31] S.T. Magness, A. Tugores, E.S. Diala, D.A. Brenner, Analysis of the human ferrochelatase promoter in transgenic mice, Blood 92 (1998) 320–328.
[32] T.R. Pacheco, M.B. Coelho, J.M. Desterro, et al., In vivo requirement of the small subunit of U2AF for recognition of a weak 3′ splice site, Mol. Cell. Biol. 26 (2006) 8183–8190.
[33] A. Paillusson, N. Hirschi, C. Vallan, et al., A GFP-based reporter system to monitor nonsense-mediated mRNA decay, Nucleic Acids Res. 33 (2005) e54.
[34] P. Ponka, Cellular iron metabolism, Kidney Int. Suppl. 69 (1999) S2–S11.
[35] N.R. Rose, M.A. McDonough, O.N. King, et al., Inhibition of 2-oxoglutarate dependent oxygenases, Chem. Soc. Rev. 40 (2011) 4364–4397.
[36] K.R. Rosenbloom, T.R. Dreszer, M. Pheasant, et al., ENCODE whole-genome data in the UCSC Genome Browser, Nucleic Acids Res. 38 (2010) D620–D625.

[37] U.B. Rufenacht, L. Gouya, X. Schneider-Yin, et al., Systematic analysis of molecular defects in the ferrochelatase gene from patients with erythropoietic protoporphyria, Am. J. Hum. Genet. 62 (1998) 1341–1352.
[38] X. Schneider-Yin, L. Gouya, M. Dorsey, et al., Mutations in the iron–sulfur cluster ligands of the human ferrochelatase lead to erythropoietic protoporphyria, Blood 96 (2000) 1545–1549.
[39] X. Schneider-Yin, J. Harms, E.I. Minder, Porphyria in Switzerland, 15 years experience, Swiss Med. Wkly. 139 (2009) 198–206.
[40] S. Taketani, Y. Adachi, Y. Nakahashi, Regulation of the expression of human ferrochelatase by intracellular iron levels, Eur. J. Biochem. 267 (2000) 4685–4692.
[41] J.D. Thompson, D.G. Higgins, T.J. Gibson, CLUSTAL W: improving the sensitivity of progressive multiple sequence alignment through sequence weighting, position-specific gap penalties and weight matrix choice, Nucleic Acids Res. 22 (1994) 4673–4680.
[42] S. Tsugane, S. Sasaki, M. Kobayashi, et al., Dietary habits among the JPHC study participants at baseline survey. Japan Public Health Center-based Prospective Study on Cancer and Cardiovascular Diseases, J. Epidemiol. 11 (2001) S30–S43.
[43] A. Tugores, S.T. Magness, D.A. Brenner, A single promoter directs both housekeeping and erythroid preferential expression of the human ferrochelatase gene, J. Biol. Chem. 269 (1994) 30789–30797.
[44] C.J. Webby, A. Wolf, N. Gromak, et al., Jmjd6 catalyses lysyl-hydroxylation of U2AF65, a protein associated with RNA splicing, Science 325 (2009) 90–93.
[45] P.D. Zamore, M.R. Green, Identification, purification, and biochemical characterization of U2 small nuclear ribonucleoprotein auxiliary factor, Proc. Natl. Acad. Sci. U. S. A. 86 (1989) 9243–9247.

Blood Cells, Molecules and Diseases 54 (2015) 71–77

Contents lists available at ScienceDirect

Blood Cells, Molecules and Diseases

journal homepage: www.elsevier.com/locate/bcmd

In ferrochelatase-deficient protoporphyria patients, ALAS2 expression is enhanced and erythrocytic protoporphyrin concentration correlates with iron availability

Jasmin Barman-Aksözen [a], Elisabeth I. Minder [a], Carina Schubiger [a], Gianfranco Biolcati [b], Xiaoye Schneider-Yin [a,*]

[a] Institute of Laboratory Medicine, Triemli Hospital, Zürich, Switzerland
[b] Porphyria Center, San Gallicano Dermatologic Institute IRCCS, Rome, Italy

ARTICLE INFO

Article history:
Submitted 22 April 2014
Accepted 25 July 2014
Available online 30 August 2014

(Communicated by Dr. M. Narla, DSc, 25 July 2014)

Keywords:
Ferrochelatase
5-Aminolevulinic acid synthase
Cutaneous porphyria
Iron
Protoporphyria

ABSTRACT

The activity of the erythroid-specific isoenzyme of 5-aminolevulinic acid synthase (ALAS2), the first and rate-limiting enzyme in heme biosynthesis, is down-regulated during iron-deficiency. Ferrochelatase (FECH), the last enzyme of this pathway, inserts iron into protoporphyrin IX (PPIX) to form heme. Patients with erythropoietic protoporphyria (EPP), an inherited deficiency in FECH, often show signs of iron deficiency in addition to phototoxicity which is caused by PPIX accumulation. However, iron supplementation often leads to exacerbation of phototoxicity. We report three EPP patients who had reduced erythrocytic PPIX concentrations when they were iron-deficient and their microcytic and hypochromic anemia deteriorated. Additionally, we found a significant increase in the amount of ALAS2 mRNA and protein among EPP patients. To verify the connection between FECH deficiency and ALAS2 over-expression, we inhibited FECH in cultured cells and found a subsequent increase in ALAS2 mRNA. We conclude that the primary deficiency in ferrochelatase leads to a secondary increase in ALAS2 expression. The combined action of these two enzymes within the heme biosynthetic pathway contributes to the accumulation of PPIX. Furthermore, we hypothesize that EPP patients may benefit from a mild iron deficiency since it would limit PPIX production by restricting ALAS2 over-expression.

Introduction

The heme biosynthetic pathway consists of eight enzymes that sequentially convert glycine and succinyl CoA to heme [35]. This pathway is tightly regulated in order to prevent any accumulation of noxious intermediates under physiological conditions [1,23]. The regulation is achieved by the first and rate-limiting enzyme in the pathway, 5-aminolevulinic acid synthase (ALAS). This enzyme has two isozymes, the housekeeping form ALAS1 and the erythroid-specific form ALAS2 [7,10,21,38]. The activity of ALAS1 in the liver is controlled by the end-product heme via a negative feedback mechanism, whereas ALAS2 is not regulated by heme [17,26,34]. Instead, iron is involved in the regulation of ALAS2 activity at the translational level. The 5′-untranslated region of ALAS2 mRNA contains an iron-responsive element (IRE) that acts as a binding site for the IRE-binding proteins (IRPs) 1 and 2. A low intracellular free iron-pool leads to the binding of IRP1 or 2 to IRE which then blocks the translation of ALAS2 mRNA and in turn reduces the amount of active enzyme formed [6,30,33].

Ferrochelatase (FECH) catalyzes the last step in the heme biosynthetic pathway, the insertion of ferrous iron (Fe^{2+}) into protoporphyrin IX (PPIX) to form heme. In the case of a partial FECH deficiency, which causes the hereditary disorder of erythropoietic protoporphyria (EPP, OMIM #177000), the substrate PPIX, but not the cosubstrate iron, accumulates in the body and causes symptoms of cutaneous phototoxic reactions in these patients [12,24]. A similar accumulation of PPIX can be the result of inherited ALAS2 hyperactivity, which is the underlying cause of X-linked dominant protoporphyria (XLDPP, OMIM #300752) with a clinical presentation indistinguishable from that of EPP [38]. The clinical observation of XLDPP indicates that when ALAS2, the rate-limiting enzyme in erythroid heme biosynthesis, is overly active, the FECH reaction becomes rate-limiting and as a result, PPIX accumulates.

In addition to PPIX accumulation, iron metabolism is disturbed in EPP, as a significant proportion of the patients show signs of iron deficiency including a low serum iron and ferritin concentration and microcytic and hypochromic anemia [14,19,36,40]. However, iron supplementation has been seen to exacerbate the skin symptoms in a number of patients — a paradox that could not be explained so far [5,25,29]. In a minority of patients with protoporphyria, a beneficial effect of iron supplementation has been reported [18,22]. Since all case reports but one, were published prior to the discovery of XLDPP, the possibility

* Corresponding author at: Stadtspital Triemli, Institute of Laboratory Medicine, Birmensdorferstrasse 497, CH-8063 Zürich, Switzerland. Fax: +41 44 466 2709.
E-mail address: xiaoye.schneider@triemli.zuerich.ch (X. Schneider-Yin).

http://dx.doi.org/10.1016/j.bcmd.2014.07.017
1079-9796/

that some of the described subjects suffered from XLDPP instead of EPP, exists. As different pathophysiologies are involved in these two disorders, XLDPP and EPP patients might react differently to iron supplementation.

In this study, we present clinical observations on exacerbation of a microcytic, hypochromic anemia (a biological expression of iron deficiency) and a concomitant decrease of protoporphyrin levels in three EPP patients, which indicates that iron may have a regulatory effect on protoporphyrin accumulation in EPP. Because ALAS2 activity is regulated by iron, we quantified the amount of both ALAS2 mRNA and ALAS2 protein in peripheral blood samples from EPP patients and compared their levels with those from control subjects. In addition, we conducted in vitro experiments to measure the level of ALAS2 mRNA after inhibition of FECH. By putting all three elements together, FECH deficiency, ALAS2 expression and iron availability, we propose an extended model to explain the pathophysiology of EPP.

Materials and methods

Subjects

Three EPP patients from our outpatient clinic are described in detail with respect to their clinical presentation and laboratory findings. In addition, we studied 17 clinically and genetically diagnosed EPP patients and twenty non-porphyric subjects. This study was approved by the local ethics committee and was conducted in concordance with the Helsinki declaration. Written informed consent was obtained from all subjects. Peripheral blood samples were collected in PAXgene Blood RNA tubes and DB Vacutainer® CPT™ tubes from these individuals for isolation of total RNA and protein, respectively. Reticulocyte count and hydroxymethylbilane synthase (HMBS) activity were measured in EDTA- and heparin-anticoagulated blood samples, respectively.

Laboratory analyses

Erythrocyte indices, serum iron, transferrin saturation and soluble transferrin receptor (sTfR), reticulocyte count, and erythrocyte PPIX concentration were performed as routine analyses either at the Institute of Laboratory Medicine, Triemli Hospital or at the Institute of Clinical Chemistry, University Hospital of Zürich, Switzerland. HMBS activity measurements were conducted at the Institute of Laboratory Medicine, Triemli Hospital according to a published protocol [32].

Chemicals and reagents

N-methyl protoporphyrin (NMPP) was purchased from Sigma-Aldrich (St. Louis, Missouri, USA). A 1 mM stock solution of NMPP was prepared by dissolving the substance in a 20 mM NH_4OH (Sigma--Aldrich) solution containing 2% Tween 20 (Sigma-Aldrich). The same solvent (20 mM NH_4OH and 2% Tween 20) was used for preparation of different working solutions with concentrations ranging from 2.5 to 10 μM in a final volume of 60 μl. Butylated hydroxytoluene (BHT) was purchased from Sigma-Aldrich and resolved in ethanol (96–100%) to a concentration of 100 μg/ml (stock solution) and was used in the cell culture at a final concentration of 0.5 μg/ml.

Cell culture

The human erythroleukemic K562 cell line (American Type Culture Collection) was cultured in RPMI 1640 medium (Gibco, Invitrogen, Carlsbad, California, USA) supplemented with 10% fetal calf serum (Bioconcepts Amimed, Allschwil, Switzerland) and streptomycin/penicillin (Gibco, Invitrogen) at 37 °C under 5% CO_2. The cells were split 1:5 every third day to maintain an exponential growth phase. For each experiment, 100,000 cells were washed with medium without antibiotics and seeded in a 6-well cluster plate containing 6 ml fresh medium. The cells were treated with different concentrations (0, 2.5, 5 and 10 μM) of NMPP and incubated for eight days [3,20]. As controls, non-treated cells, cells treated with solvent, BHT (antioxidant) or ethanol only and cells treated with both solvent and BHT were used. After four days, the medium was refreshed. All measurements were conducted in duplicates. The experiment was repeated three times.

RNA isolation and RT-PCR

Total RNA was extracted from peripheral blood samples by the PAXgene Blood RNA Kit (PreAnalytiX GmbH, Hombrechtikon, Switzerland) according to the manufacturer's protocol. Total RNA was isolated from cultured cells by using the RNeasy Mini Kit (Qiagen, Hilden, Germany) according to the manufacturer's protocol including the optional on-column DNase digestion step. The quality of RNA was evaluated using RNA Nano chips on an Agilent 2001 bioanalyzer (Agilent Technologies, Santa Clara, California, USA). RNA was then quantified on a Nanodrop 2000c Spectrophotometer (Thermo Fisher Scientific, Waltham, Massachusetts, USA). One-thousand nanograms of total RNA from each isolation were reverse transcribed into cDNA by using the Transcriptor First Strand cDNA Synthesis Kit and anchored-oligo(dT)18 primer (Roche Diagnostics Inc., Basel, Switzerland).

For quantification of cDNA, real-time PCR was performed on an ABI PRISM 7000 using gene specific primers and TaqMan probes (ALAS2, Hs01085694_m1; FECH, Hs01555261_m1 and beta-actin, Hs99999903_m1; Applied Biosystems, Life Technologies, Carlsbad, California, USA). One-twentieth of the resulting cDNA was used in each reaction. All measurements were done in triplicates. To obtain the relative concentration of either FECH or ALAS2, the threshold cycle (Ct) value of these transcripts was subtracted by that of β-actin (ΔCt). The concentration was expressed in arbitrary unit (a.u.) as $2^{-\Delta Ct} \times 10^3$.

Western blot analysis

Peripheral blood samples (8 ml) were collected into BD Vacutainer® CPT™ tubes containing 2 ml Ficoll and 1 ml 0.1 M sodium citrate (Becton, Dickinson and Company, Franklin Lakes, NJ, USA). The tube was centrifuged within 2 h after blood collection at 3000 rpm for 25 min which separates mononuclear cells, granulocytes and erythrocytes based on their density. After centrifugation, 200 μl of the upper layer of the red blood cell fraction which contains mainly reticulocytes and young erythrocytes, were carefully collected. In addition, 200 μl of the mononuclear cell fraction was collected. Both cell fractions were washed twice with PBS and used for protein isolation.

For isolation of the cytosolic and membrane protein fractions of the cells Qproteome Cell Compartment Kit (Qiagen) was used according to the manufacturer's protocol. Western blot analysis was conducted according to a previously described protocol with slight modifications [5]. The protein concentration in the fractions was determined by the benzethonium chloride method on a clinical chemistry analyzer, Cobas 501 (TPUC3; Roche Diagnostics Inc., Rotkreuz, Switzerland). In the Western blot analysis, an equal amount of protein from each sample was loaded on the gel. For the detection of ALAS2 protein, ALAS2 primary antibody (D4 sc166739 in 1:200 dilution) and secondary antibody goat anti mouse IgG-HRP (sc2005 in 1:2000 dilution; Santa Cruz Biotechnology Inc., Santa Cruz, CA, USA) were used. The ALAS2 protein was visualized by staining the membranes with Sigma FAST DAB horse radish peroxidase substrate as previously described [5]. The intensity of ALAS2 bands was densitometrically quantified with the Image J-software (http://rsbweb.nih.gov/ij/download.html) which gives numerical readings (arbitrary units, a.u.).

Table 1
Erythrocyte indices and iron status in three EPP patients.

	HGB (♀12.0–15.4 g/dL; ♂14.0–18.0 g/dL)	HCT (36–45%)	RBC (♀3.9–5.15 × 10^{12}/L; ♂4.5–5.9 × 10^{12}/L)	MCV (♀80–99 fL; ♂82–89 fL)	MCH (♀27–34 pg/RBC; ♂28–32 pg/RBC)	Soluble TfR (patients 1 and 3: 0.76–1.76 mg/L) (patient 2: 1.9–4.4 mg/L)	Free PPIX (<0.20 μmol/L RBC)	Iron (6.6–26.0 μmol/L)	Transferrin saturation (23–46%)	ferritin (13–150 μg/L)
Patient 1										
02.10.2012	**11.9**	38	4.47	84	27	n.a.	**21.1**	n.a.	n.a.	n.a.
11.01.2013	12.2	39	5.04	**78**	**24**	n.a.	**21.0**	n.a.	n.a.	n.a.
15.03.2013	**9.5**	**32**	4.62	**70**	**21**	n.a.	**5.5**	n.a.	n.a.	n.a.
09.04.2013	**9.9**	**33**	4.89	**67**	**20**	**4.43**	n.a.	n.a.	n.a.	n.a.
Patient 2										
08.08.2007	n.a.	n.a.	n.a.	n.a.	n.a.	n.a.	**26.6**	n.a.	n.a.	n.a.
02.05.2011	**11.2**	**34**	4.8	**72**	**23**	**9.5**	**37.0**	**3.1**	**3**	**10**
19.06.2012	**11.0**	**33**	4.66	**70**	**24**	n.a.	**49.3**	n.a.	n.a.	n.a.
18.09.2012	**10.8**	**34**	4.88	**69**	**22**	n.a.	**29.6**	n.a.	n.a.	n.a.
04.03.2013	**10.6**	**33**	4.73	**69**	**22**	n.a.	**29.9**	**2.2**	**3**	**3**
17.04.2013	**10.2**	**31**	4.56	**69**	**22**	n.a.	**21.8**	**3.0**	**3**	**5**
27.06.2013	**9.2**	38	4.24	**67**	**22**	**11.45**	**22.8**	**3.0**	**8**	**3**
02.07.2013	**10.1**	**31**	4.67	**67**	**22**	**10.79**	**24.0**	**56.5**	**64**	**6**
09.07.2013	**10.7**	**34**	5.08	**67**	**21**	**11.63**	**18.0**	**5.5**	**6**	**5**
19.07.2013	**9.5**	**30**	4.4	**67**	**22**	**10.9**	**22.1**	**2.2**	**3**	**4**
Patient 3										
28.06.2000	**13.9**	n.a.	n.a.	n.a.	n.a.	n.a.	**28.2**	n.a.	n.a.	n.a.
24.11.2009	**13.6**	n.a.	n.a.	n.a.	n.a.	1.22	**27.1**	n.a.	n.a.	n.a.
30.05.2012	**12.5**	n.a.	n.a.	n.a.	n.a.	n.a.	**11.0**	n.a.	n.a.	n.a.
05.06.2013	**13.1**	n.a.	5.22	**76**	**25**	n.a.	**16.8**	n.a.	n.a.	n.a.

Reference ranges are given in *parentheses*. Abnormal values are in **bold**.
HGB, hemoglobin; HCT, hematocrit; RBC, red blood cell count; MCV, mean corpuscular volume; MCH, mean corpuscular hemoglobin; sTfR, soluble transferrin receptor; PPIX, protoporphyrin IX.
n.a., not available.

Statistical analysis

Data were analyzed by either Mann–Whitney U test or Pearson product–moment correlation coefficient (VassarStats, Richard Lowry, www.vassarstats.net). A one-sided $p \leq 0.05$ was considered to be statistically significant.

Results

Case reports

Patient 1

An 18-year-old female EPP patient suffered from photosensitivity since early childhood. In addition, she intermittently showed clinical symptoms of iron deficiency including fatigue and dizziness that were accompanied by a drop in hemoglobin levels. She had no increased menstrual bleeding or any additional blood loss. However, her regular diet was low on iron. In the late summer of 2012, she received intravenous iron supplementation from her family physician. Shortly thereafter, she complained about worsening of the skin symptoms and visited our outpatient clinic in October.

Because of the exacerbation of EPP symptoms, we advised her to stop iron supplementation. In the spring of 2013, the symptoms of fatigue and dizziness returned. At this time, erythrocyte indices showed microcytosis and hypochromia with a hemoglobin concentration of 9.5 g/dL. In addition, her soluble transferrin receptor (sTfR) was increased, indicating an iron deficiency during formation of new erythrocytes. The protoporphyrin concentration dropped from 21 μmol/L in January to 5.5 μmol/L in March. In April of 2013, she received another round of intravenous iron substitution from her family physician and her EPP symptoms got worse again. However, PPIX was not measured at this time (Table 1).

Patient 2

A 35-year-old female suffered from phototoxic reactions after sunlight exposure since the age of 2.5 years. The diagnosis of EPP was established at the age of 28. She began to regularly visit our outpatient clinic since 2007. Her blood test had been showing microcytic and hypochromic anemia over the years. From time to time she experienced symptoms indicating iron deficiency such as, fatigue and difficulty to concentrate on her work. In the summer of 2013, the clinical symptoms of iron deficiency intensified, likely due to frequent blood drawings for unrelated reasons. Iron deficiency was underlined by a drop in her hemoglobin concentration (9.2 g/dL) and an increase in the sTfR concentration. She was given oral iron substitution starting on June 28th, 2013 at a dosage of 105 mg per day (KENDURAL, Teofarma Inc., Lugano, Switzerland). Five days later, on July 2nd, the treatment was discontinued because of elevated liver enzymes. The patient noticed a slight increase in sunlight sensitivity after the 5-day iron supplementation. The increased sunlight sensitivity lasted one week. While PPIX concentration rose moderately from 22.8 to 24.0 μmol/L during this 5-day period, her hemoglobin level increased from 9.2 g/dL to 10.1 g/dL. Three weeks after the iron supplementation, her hemoglobin level dropped to 9.5 g/dL, which was close to the pre-treatment concentration.

Patient 3

A 51-year-old male was diagnosed with EPP at the age of 7 after severe phototoxic attacks following sunlight exposure since the age of 3. Over the past 13 years, he was tested occasionally for PPIX, hemoglobin and iron metabolism parameters (Table 1). Despite decreased hemoglobin concentrations, he never received iron supplementation.

Low iron status and correlation between iron availability and PPIX in EPP

The hemoglobin concentrations of all three patients laid either close to the lower limit of normal range or below the normal range (Table 1). The decreased hemoglobin concentrations were accompanied by microcytosis and hypochromia, as shown by low mean corpuscular volume (MCV) and low mean corpuscular hemoglobin (MCH) values. sTfR was increased during the periods of exacerbated anemia, indicating iron deficiency. In addition, patient 2 also showed low serum iron, transferrin saturation and ferritin values. Within each patient, the erythrocytic PPIX concentrations correlated significantly with that of hemoglobin, i.e. during periods of iron-deficient anemia, the erythrocytic PPIX concentration was lower than that during periods when iron was replenished (Fig. 1). The dependence of PPIX accumulation on hemoglobin level was nominally unique for each individual patient and not comparable among them.

Increase in ALAS2 expression among EPP patients

As stated in the Introduction section, ALAS2 activity is rate-limiting in the biosynthesis of erythroid heme and is regulated by iron availability. We therefore measured the amount of ALAS2 protein in the young erythrocytes from EPP patients and healthy controls by Western blot analysis. Since reticulocytes and young erythrocyts have lower specific weight than mature erythrocytes, they reside in the top layer after gradient-centrifugation of blood samples in Ficoll [8]. These young erythrocytes still contain proteins and mRNA for the heme biosynthesis enzymes. As under our experimental conditions, no beta-actin was detected in either cytosolic or membrane fractions of young erythrocytes and mononuclear cells by the Western blot analysis (data not shown), we used total protein concentration as a reference instead of beta-actin. A band corresponding to the correct size of ALAS2 was visible in the Western blot analysis of the cytosolic fraction of young erythrocytes (Fig. 2). No ALAS2 was detected by the same Western blot analysis in the membrane fraction of young erythrocytes. As in both the cytosolic and membrane fractions of mononuclear cells no ALAS2 was detected (data not shown), this result indicated that the antibody against ALAS2 does not cross-react with ALAS1 in the Western blot analysis. Subsequently, we determined the amount of ALAS2 protein in the samples from 5 EPP patients and 5 control subjects by densitometric scanning of the blot. The result showed a significant difference between patients (mean = 14,903 a.u., SD = 8288 a.u., n = 5) and control subjects (mean = 6200 a.u., SD = 5135 a.u.; $p \leq 0.05$) ie, ALAS2 protein was about two times higher in the enriched young erythrocytes from EPP patients compared to those from healthy volunteers (Fig. 3).

ALAS2 mRNA contains an IRE element and its translation is inhibited under iron-deficient conditions [6,30,33]. Since EPP patients display signs of iron deficiency, one would expect a decrease in ALAS2 protein

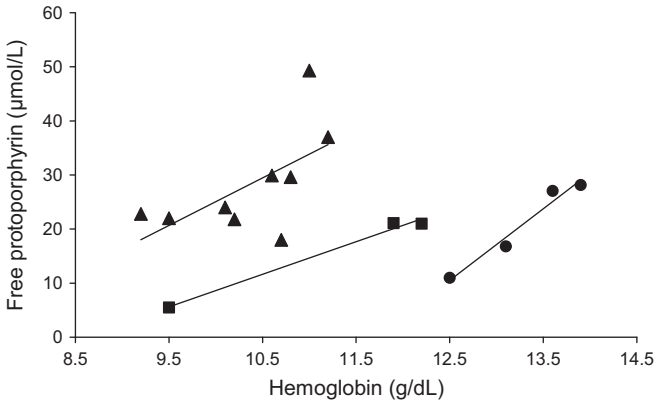

Fig. 1. Correlation between erythrocyte free protoporphyrin IX and hemoglobin concentrations in EPP. The concentration of free PPIX is plotted against that of hemoglobin from patient 1 (■), patient 2 (▲) and patient 3 (●). The numerical values are listed chronologically in Table 1. The correlation coefficients are $r = 0.99$, $p = 0.034$, n = 3 in patient 1; $r = 0.61$, $p = 0.04$, n = 9 in patient 2; and $r = 0.981$, $p = 0.0096$, n = 4 in patient 3.

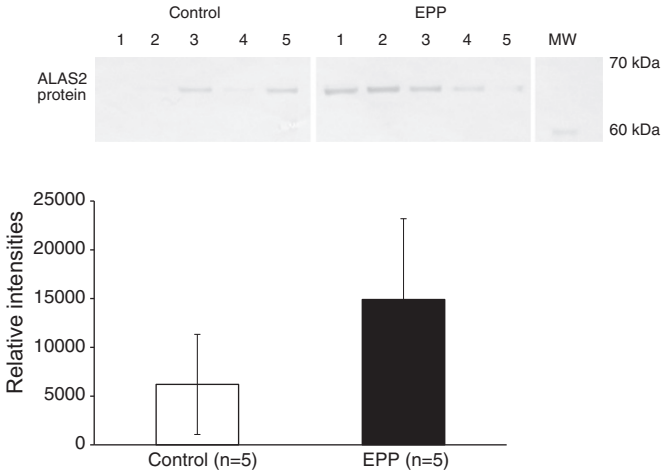

Fig. 2. Western blot analysis of the ALAS2 protein present in a cytosolic fraction from young erythrocytes. Western blot analysis of ALAS2 protein in samples from five EPP patients and five control subjects (the upper panel). The intensity of the bands was estimated by scanning the membrane with a densitometer. The result, in mean and SD of "relative intensity", is shown in the lower panel for both healthy controls (left column) and EPP patients (right column).

in these individuals compared to controls. However, an opposite effect was observed in our small cohort. To further explore this observation, we quantified the amount of ALAS2 mRNA in peripheral blood samples of 15 EPP patients and 20 healthy volunteers. As shown in Fig. 3, nine of the 15 patients had ALAS2 mRNA concentrations of ≥600 a.u. (median 782.7 a.u.; interquartile range: 329.0–948.7 a.u.). Among the 20 control subjects, 14 had ALAS2 mRNA concentrations of ≤300 a.u. (median 194.8 a.u.; interquartile range: 90.9–360.0 a.u.). The difference in ALAS2 mRNA concentration between EPP patients and control subjects was statistically highly significant ($p < 0.001$) with the median from EPP patients being about 4 times higher than that from normal controls.

No difference in the age of circulating erythrocytes between patients and controls

Erythrocyte precursors synthesize mRNA and protein during their development in the bone marrow. Before these precursors are extruded from the bone marrow into blood circulation, they lose both their nucleus and mitochondria, which renders them unable to synthesize mRNA and consequently proteins. During the first few days in circulation, they lose their residual RNA and later on, during their lifetime in circulation, the residual enzyme activities drop progressively [2]. Thus, the increase in ALAS2 protein and mRNA in the blood samples of EPP patients could either be caused by an increased expression of the enzyme during the development of erythrocytes in the bone marrow or be due to a lower mean age of erythrocytes in the blood circulation of EPP patients compared to controls. For example, an increased rate of erythropoiesis as the result of a subclinical hemolysis could be suspected. To investigate the latter possibility, we quantified the percentage of reticulocytes in the blood samples of eight EPP patients and seven healthy controls. In the case of a stimulated erythropoiesis, we would expect an increase in reticulocytes in the EPP blood samples. As shown in Fig. 4 (upper panel), the percentage of reticulocytes was 0.70%, SD = 0.30 (n = 8) in EPP patients and 0.81%, SD = 0.35 (n = 7) in healthy controls. The difference was not statistically significant.

In addition, we measured enzymatic activity of hydroxymethylbilane synthase (HMBS, another enzyme of heme biosynthesis) in washed erythrocytes from peripheral blood samples of EPP patients and healthy controls, and as an additional control, in samples from patients with acute intermittent porphyria (AIP) who have approximately half of the HMBS activity. HMBS in erythrocytes is synthesized during their development in the bone marrow only and remains active in youngerythrocytes [2]. An increased proportion of young erythrocytes in the peripheral blood would therefore lead to increased activity of HMBS [2]. As shown in Fig. 4 (lower panel), the HMBS activity (reference range: 66–126 pmol/mgHb/h) of EPP patients was 95.3, SD = 21.6 (n = 7) and that of the healthy controls 99.6, SD = 27.8 (n = 20) — the difference was not statistically significant. As expected, the HMBS activity of AIP patients was around 50% of that of control subjects i.e., 44.9, SD = 9.0 (n = 16; $p \leq 0.0001$; Fig. 4, lower panel).

These results demonstrated that the observed difference in the amount of both ALAS2 mRNA and protein between EPP patients and control subjects was not due to a difference in the age of their circulating erythrocytes.

Inhibition of FECH enzyme leads to an increase in ALAS2 mRNA in the K562 cell line

The question remained, why is ALAS2 over-expressed in young erythrocytes of EPP patients? Our hypothesis is that a deficient FECH could directly or indirectly enhance ALAS2 expression. To test this hypothesis, we incubated the erythroleukemic K562 cells with N-methyl protoporphyrin (NMPP). NMPP is a transition-state analogue of PPIX and a potent inhibitor of FECH, which has been used to induce heme deficiency in mammalian cell lines [3,37]. Treatment of K562 cells with NMPP in a concentration range of 2.5–10.0 μM did not cause significant changes in FECH mRNA. However, the amount of ALAS2 mRNA increased up to two-fold after the NMPP treatment (Fig. 5).

Discussion

About a third of EPP patients show mild anemia featuring hypochromia and microcytosis, frequently combined with low serum iron and ferritin [14,19,36,40]. In non-porphyric subjects, this type of anemia is a well-known sign of iron deficiency. On the other hand, the residual FECH activity in EPP is only 35%, which may limit heme synthesis and subsequently lead to anemia. However, other anemias due to reduced heme synthesis such as that induced by lead poisoning, are not microcytic and hypochromic. Therefore, the question arises as to which extent the anemia in EPP is due to iron deficiency or to reduced heme synthesis. In this regard, of interest is the observation that an abnormal distribution of body iron, rather than an iron deficiency, was found in an EPP mouse model [25]. This would indicate that the availability of iron for erythropoiesis could be reduced in EPP. Earlier studies in human EPP patients showed that stainable iron in bone marrow was scarce, which also indicated a lack of iron available for hemoglobin synthesis [39]. Moreover, if iron supplementation is

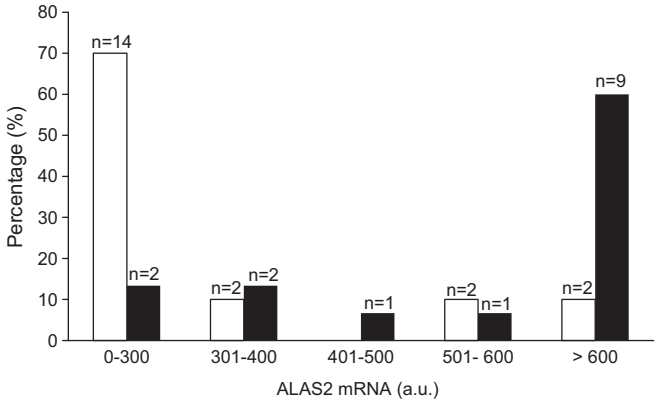

Fig. 3. Quantification of ALAS2 mRNA in EPP patients and control subjects. A histogram showing the distribution of ALAS2 mRNA concentration (in arbitrary units, a.u.) among 20 control subjects (empty column) and 15 EPP patients (solid column).

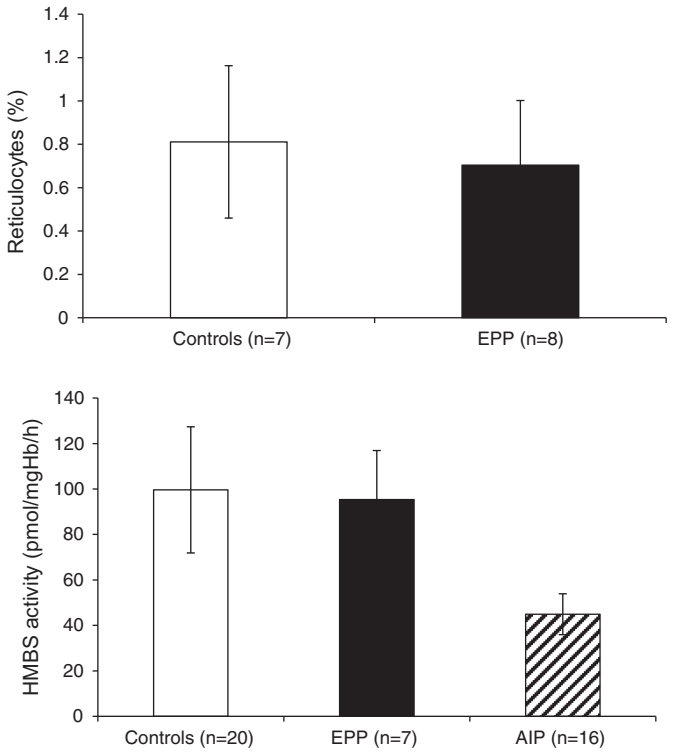

Fig. 4. Reticulocyte count in EPP patients and healthy controls (upper panel). The mean and SD of the percentage of reticulocytes in the whole blood samples of EPP patients (solid column) and healthy controls (empty column) are displayed. HMBS activity in patients and healthy controls (lower panel). Mean and SD of HMBS activity in washed erythrocytes from EPP patients (solid column) and AIP patients (hatched column), and from healthy controls (empty column) are shown.

beneficial in EPP, an iron deficit can be assumed. In the medical literature there are conflicting case reports on the effect of iron supplementation on EPP symptoms [4,18,27,31]. In our clinical experience, iron supplementation has consistently exacerbated EPP phototoxic symptoms, although it may improve the general well-being of the patients, increase their hemoglobin concentrations and thus ameliorate their anemia. In the case of an inherited deficiency of FECH activity, the lack of iron, a cosubstrate of FECH, could theoretically limit its capacity and thereby enhance the accumulation of protoporphyrin IX and in turn, aggravate the phototoxic symptoms. Iron supplementation in the case of iron deficiency should therefore improve EPP symptoms. The question is why does our clinical observation contradict the expected mechanism of enzymatic action?

Two of the three cases that we presented here underline the fact that there is a lack of biologically available iron for erythropoiesis in some EPP patients, as revealed by increased soluble transferrin receptor and low hemoglobin values. This iron deficiency measured as decreased hemoglobin concentrations correlated significantly with a reduced protoporphyrin concentration in erythrocytes. Such correlation was most obvious in patient 2, as she had low serum concentrations of iron and ferritin, decreased transferrin saturation and abnormal hematologic indices including low hemoglobin, hematocrit, MCV and MCH. All three patients showed the same tendency i.e., the lower the hemoglobin, which we assume is a marker for biologically available iron, the less PPIX accumulation in erythrocytes, and vice versa. These observations led us to conclude that iron deficiency reduces the biosynthesis of protoporphyrin through a regulated process. Our further study on ALAS2 shows that this rate-limiting enzyme of erythrocytic heme synthesis is likely involved in this process. We found a significant increase in both mRNA and protein of the erythrocytic ALAS2 in EPP patients compared to controls. An enhanced expression of ALAS2, in addition to FECH deficiency, likely contributes to the extent of elevation of erythrocytic PPIX seen in EPP patients. If iron becomes scarce, iron responsive proteins 1 and 2 (IRP1, IRP2) bind to the iron response element (IRE) in the mRNA of ALAS2 [9,11,13,16]. This binding is thought to reversibly prevent the translation of ALAS2 mRNA [6,30]. Instead of the expected reduction in translation, we found an increase in ALAS2 protein in EPP blood samples. However, the increase in ALAS2 protein was less pronounced than that in mRNA, which indicates that the translational block due to the low iron is partially in place. This theory can be used to explain the clinical observation on worsening of light sensitivity under iron therapy as seen in many patients: The increased availability of iron by supplementation releases the translational block on the elevated ALAS2 mRNA, and the newly formed enzyme further increases PPIX production. For ethical reasons, especially because of the risk of liver damage, iron cannot be given to patients experimentally in order to observe the full magnitude of PPIX increase. However, the available data from the three patients presented here did show a parallel increase/decrease in PPIX concentration and hemoglobin value, which we assume, is an indirect measure for iron availability.

As mentioned above, the increases in ALAS2 mRNA and especially ALAS2 protein could not be explained by the known mechanism of iron regulation. This led us to further speculate that ALAS2 expression may be influenced directly or indirectly by FECH. To test this hypothesis, we conducted in vitro experiments in the erythroleukemic K562 cell line using NMPP to interfere with FECH activity in order to mimic the in vivo situation in EPP patients. Indeed, ALAS2 mRNA increased significantly during NMPP-induced inhibition, whereas FECH mRNA did not change. Our in vitro results are in concordance with earlier findings by Inafuku et al. [19], who induced an experimental EPP in mice by feeding the animals with griseofulvin, a substance which is converted to NMPP in the liver. The authors found a two-fold increase in the ALAS2 mRNA but no change in the FECH mRNA in these mice after eight days of feeding.

Our current model for the regulation of heme biosynthesis in EPP during erythropoiesis is the following: the inherited deficiency of FECH leads to an over-expression of ALAS2 in developing erythrocytes. This overactive enzyme will contribute to PPIX accumulation in addition to that caused by FECH deficiency. The frequently observed iron deficiency in EPP patients limits ALAS2 over-expression and thereby restricts the amount of PPIX accumulation. The extent of PPIX accumulation not only influences the severity of phototoxic symptoms, but may also affect the risk of complicating liver damage [15,28,29]. In this respect a slight shortage in iron could be beneficial to EPP patients and therefore, iron should be supplemented only when the symptoms of iron deficiency becomes incapacitating.

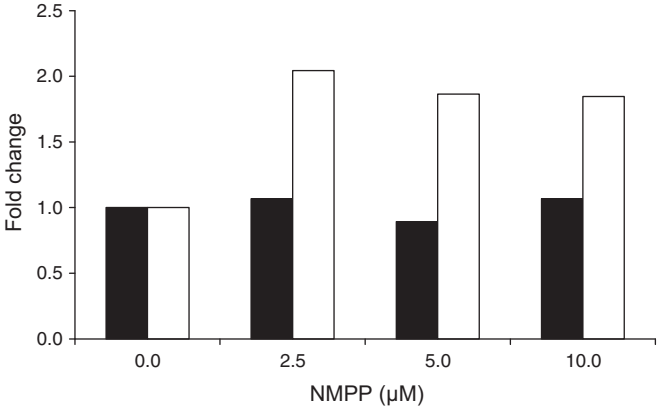

Fig. 5. Quantification of FECH and ALAS2 mRNA from K562 cells treated with N-methyl protoporphyrin (NMPP). Fold change compared to controls in mRNA of FECH (solid columns) and ALAS2 (empty columns) under treatment with NMPP after eight days of incubation.

Acknowledgments

We would like to thank Mirjam Balimann and Janina Mondgenast for their technical assistance, Sarah Ducamp and Hana Manceau for the exchange of recombinant ALAS2 proteins and discussions, Antoinette Monn for supervising the hematological analyses, Jonathan Hall, Kazumichi Furuyama and Rocco Falchetto, chairman of the Swiss Society for Porphyria, for their fruitful discussions and all patients and participants for taking part in the study.

References

[1] K. Anderson, S. Sassa, D.F. Bishop, R.J. Desnick, Disorders of heme biosynthesis: X-linked sideroblastic anemia and the porphyrias, in: C.R. Scriver, M. Beaugrand, W. S. Sly, D. Valle (Eds.), The Metabolic and Molecular Basis of Inherited Disease, McGraw-Hill, New York, 2001, pp. 2991–3062.
[2] K.E. Anderson, S. Sassa, C.M. Peterson, A. Kappas, Increased erythrocyte uroporphyrinogen-I-synthetase, delta-aminolevulinic acid dehydratase and protoporphyrin in hemolytic anemias, Am. J. Med. 63 (1977) 359–364.
[3] H. Atamna, J. Liu, B.N. Ames, Heme deficiency selectively interrupts assembly of mitochondrial complex IV in human fibroblasts: revelance to aging, J. Biol. Chem. 276 (2001) 48410–48416.
[4] H. Baker, Erythropoietic protoporphyria provoked by iron therapy, Proc. R. Soc. Med. 64 (1971) 610–611.
[5] J. Barman-Aksozen, C. Beguin, A.M. Dogar, et al., Iron availability modulates aberrant splicing of ferrochelatase through the iron- and 2-oxoglutarate dependent dioxygenase Jmjd6 and U2AF(65), Blood Cells Mol. Dis. 51 (2013) 151–161.
[6] C.R. Bhasker, G. Burgiel, B. Neupert, et al., The putative iron-responsive element in the human erythroid 5-aminolevulinate synthase mRNA mediates translational control, J. Biol. Chem. 268 (1993) 12699–12705.
[7] D.F. Bishop, A.S. Henderson, K.H. Astrin, Human delta-aminolevulinate synthase: assignment of the housekeeping gene to 3p21 and the erythroid-specific gene to the X chromosome, Genomics 7 (1990) 207–214.
[8] K.G. Clark, D.C. Nicholson, Erythrocyte protoporphyrin and iron uptake in erythropoietic protoporphyria, Clin. Sci. 41 (1971) 363–370.
[9] A. Constable, S. Quick, N.K. Gray, M.W. Hentze, Modulation of the RNA-binding activity of a regulatory protein by iron in vitro: switching between enzymatic and genetic function? Proc. Natl. Acad. Sci. U.S.A. 89 (1992) 4554–4558.
[10] T.C. Cox, M.J. Bawden, N.G. Abraham, et al., Erythroid 5-aminolevulinate synthase is located on the X chromosome, Am. J. Hum. Genet. 46 (1990) 107–111.
[11] T.C. Cox, M.J. Bawden, A. Martin, B.K. May, Human erythroid 5-aminolevulinate synthase: promoter analysis and identification of an iron-responsive element in the mRNA, EMBO J. 10 (1991) 1891–1902.
[12] H.A. Dailey, P.N. Meissner, Erythroid heme biosynthesis and its disorders, Cold Spring Harb. Perspect. Med. 3 (2013) a011676.
[13] T. Dandekar, R. Stripecke, N.K. Gray, et al., Identification of a novel iron-responsive element in murine and human erythroid delta-aminolevulinic acid synthase mRNA, EMBO J. 10 (1991) 1903–1909.
[14] C. Delaby, S. Lyoumi, S. Ducamp, et al., Excessive erythrocyte PPIX influences the hematologic status and iron metabolism in patients with dominant erythropoietic protoporphyria, Cell Mol. Biol. (Noisy-le-grand) 55 (2009) 45–52.
[15] M.O. Doss, M. Frank, Hepatobiliary implications and complications in protoporphyria, a 20-year study, Clin. Biochem. 22 (1989) 223–229.
[16] B. Goossen, M.W. Hentze, Position is the critical determinant for function of iron-responsive elements as translational regulators, Mol. Cell. Biol. 12 (1992) 1959–1966.
[17] S. Granick, P. Sinclair, S. Sassa, G. Grieninger, Effects by heme, insulin, and serum albumin on heme and protein synthesis in chick embryo liver cells cultured in a chemically defined medium, and a spectrofluorometric assay for porphyrin composition, J. Biol. Chem. 250 (1975) 9215–9225.
[18] S.A. Holme, C.L. Thomas, S.D. Whatley, et al., Symptomatic response of erythropoietic protoporphyria to iron supplementation, J. Am. Acad. Dermatol. 56 (2007) 1070–1072.
[19] S.A. Holme, M. Worwood, A.V. Anstey, et al., Erythropoiesis and iron metabolism in dominant erythropoietic protoporphyria, Blood 110 (2007) 4108–4110.
[20] H. Horiguchi, B.H. Franklin, Erythropoietin induction in Hep3B cells is not affected by inhibition of heme biosynthesis, Biochim. Biophys. Acta 1495 (2000) 231–236.
[21] G.A. Hunter, G.C. Ferreira, Molecular enzymology of 5-aminolevulinate synthase, the gatekeeper of heme biosynthesis, Biochim. Biophys. Acta 1814 (2011) 1467–1473.
[22] J. Kniffen, Protoporphyrin removal in intrahepatic porphyrastasis, Gastroenterology 58 (1970) 1027.
[23] Y. Kohgo, K. Ikuta, T. Ohtake, et al., Body iron metabolism and pathophysiology of iron overload, Int. J. Hematol. 88 (2008) 7–15.
[24] M. Lecha, H. Puy, J.C. Deybach, Erythropoietic protoporphyria, Orphanet J. Rare Dis. 4 (2009) 19.
[25] S. Lyoumi, M. Abitbol, V. Andrieu, et al., Increased plasma transferrin, altered body iron distribution, and microcytic hypochromic anemia in ferrochelatase-deficient mice, Blood 109 (2007) 811–818.
[26] B.K. May, S.C. Dogra, T.J. Sadlon, et al., Molecular regulation of heme biosynthesis in higher vertebrates, Prog. Nucleic Acid Res. Mol. Biol. 51 (1995) 1–51.
[27] B.M. McClements, A. Bingham, M.E. Callender, E.R. Trimble, Erythropoietic protoporphyria and iron therapy, Br. J. Dermatol. 122 (1990) 423–424.
[28] B.M. McGuire, H.L. Bonkovsky, R.L. Carithers Jr., et al., Liver transplantation for erythropoietic protoporphyria liver disease, Liver Transpl. 11 (2005) 1590–1596.
[29] L. Meerman, Erythropoietic protoporphyria. An overview with emphasis on the liver, Scand. J. Gastroenterol. (2000) 79–85 (Suppl.).
[30] O. Melefors, B. Goossen, H.E. Johansson, et al., Translational control of 5-aminolevulinate synthase mRNA by iron-responsive elements in erythroid cells, J. Biol. Chem. 268 (1993) 5974–5978.
[31] A. Milligan, R.A. Graham-Brown, I. Sarkany, H. Baker, Erythropoietic protoporphyria exacerbated by oral iron therapy, Br. J. Dermatol. 119 (1988) 63–66.
[32] E.I. Minder, X. Schneider-Yin, Porphyrins, porphobilinogen, and δ-aminolevulinic acid, in: Nenad Blau, Marinus Duran, K. Michael Gibson (Eds.), Laboratory Guide to the Methods in Biochemical Genetics, Springer, Berlin-Heidelbarg, 2008, pp. 751–780.
[33] P. Ponka, Tissue-specific regulation of iron metabolism and heme synthesis: distinct control mechanisms in erythroid cells, Blood 89 (1997) 1–25.
[34] T.J. Sadlon, T. Dell'Oso, K.H. Surinya, B.K. May, Regulation of erythroid 5-aminolevulinate synthase expression during erythropoiesis, Int. J. Biochem. Cell Biol. 31 (1999) 1153–1167.
[35] S. Sassa, Modern diagnosis and management of the porphyrias, Br. J. Haematol. 135 (2006) 281–292.
[36] X. Schneider-Yin, J. Harms, E.I. Minder, Porphyria in Switzerland, 15 years experience, Swiss Med. Wkly. 139 (2009) 198–206.
[37] Z. Shi, G.C. Ferreira, Modulation of inhibition of ferrochelatase by N-methylprotoporphyrin, Biochem. J. 399 (2006) 21–28.
[38] G.R. Sutherland, E. Baker, D.F. Callen, et al., 5-Aminolevulinate synthase is at 3p21 and thus not the primary defect in X-linked sideroblastic anemia, Am. J. Hum. Genet. 43 (1988) 331–335.
[39] A. Turnbull, H. Baker, B. Vernon-Roberts, I.A. Magnus, Iron metabolism in porphyria cutanea tarda and in erythropoietic protoporphyria, Q. J. Med. 42 (1973) 341–355.
[40] S. Wahlin, Y. Floderus, P. Stal, P. Harper, Erythropoietic protoporphyria in Sweden: demographic, clinical, biochemical and genetic characteristics, J. Intern. Med. 269 (2011) 278–288.

IX. Acknowledgements

My sincere gratitude to all who made this thesis possible. I want to especially express my gratitude to

Elisabeth Minder
Thank you very much for the great and intellectually inspiring times in your lab. I highly enjoyed to discuss and develop new ideas together and appreciated your constant support in realizing research ideas. In you, I found the academic mentor a student hopes for.

Xiaoye Schneider-Yin
You are a great supervisor, motivator and friend. Thank you so much for all the enthusiasm you put into our projects. I especially appreciate the independence you allow me and, at the same time, that you are always present when I reach my borders.

Kurt Bürki, Konrad Basler, Paolo Cinelli, Pawel Pelcar, Thomas Lutz and Max Gassmann
The members of my thesis committee for providing a continuous supportive environment and fruitful discussions

Jon Hall and Daniel Schümperli
For exciting research cooperation during the thesis and in ongoing research projects

Sarah Ducamp and Hana Mancau
For nice discussions and the good time together in Paris

Vijay Bansode, in memoriam.
I am grateful I had the chance to get to know you.

All the people in the clinical chemistry laboratory
For technical support, helping hands and the pleasant work environment

The members of the Swiss Society for Porphyria, the Selbsthilfe EPP e.V. and the international porphyria patient community. Special thanks to the author of a certain important Wikipedia article

Rocco Falchetto
Thank you as friend and mentor for the great discussions and inputs about research, lab and life.

MK Franziska Wegmann and PCR Patrizia Contreras Reyes-Ruh
For great insights in and after the lab: Coffee contains atoms and even psychosomatic protoporphyrin peaks can be quantified!

My mother Erika Barman, thank you for teaching me the crucial ability of finding my own ways of responding to unconventional situations, and my father Arun Barman, who always and from the beginnings believed in me.

My loving husband Mehmet.